Catalyst Controlled Site-Selective C–H Functionalization

by

Amanda J. Hickman

A dissertation submitted in partial fulfillment
of the requirements for the degree of
Doctor of Philosophy
(Chemistry)
in The University of Michigan
2012

Doctoral Committee:

Professor Melanie S. Sanford, Chair
Professor Mark M. Banaszak Holl
Professor John Montgomery
Associate Professor Suljo Linic

Acknowledgements

I have had many teachers and mentors that have molded me into the scientist I am today, and I owe them all tremendous gratitude. First and foremost, I would like to think my parents for teaching me to be a critical thinker. They instilled in me a curiosity for how the world works and equipped me with the tools to find out by providing me with opportunities to explore my interests and passions. My first forays into the world of scientific discovery were creating a paper mâché stomach (complete with duodenum) on the back porch with my mom and developing an epoxy break test machine out of a cherry picker in the garage with my Dad. My parents always made time to help me with my next science fair project, listen to me practice speeches for my next contest, and brainstorm ideas for whatever pet project I had at the time. There are truly no finer parents than mine. I am blessed. I am thankful, and I owe everything I have accomplished so far to the love and support that they give freely and completely every day of my life. Thank you! I love you!

I am also very fortunate to have an incredibly supportive extended family. My sister Carla has been a wonderful role model and cheerleader throughout my life. She gave me my first lesson in hypothesis driven experimentation when she told me as a small child that she believed I could breathe out of my ears if I held my breath and nose. After our first attempt failed, she taught me the value of replicate trials. I also thank my aunts and uncles and grandparents who always encouraged and supported me in my academic and personal endeavors. In particular, I am very grateful for the many wonderful opportunities and experiences my Aunt Linda and Uncle Adrian have given to me. They showed me that the world was small and full of interesting people and places that I should explore. They have supported me with me unmatched generosity. I love you, and I appreciate all that you have done for me.

Next, I would like to think the many wonderful teachers that have contributed to my education as a scientist. Thank you, Mrs. Holmes, Mr. Lewis, Mrs. Ricketts, Mr. Gamble, Ms. Kelehear, Mr. Murray, and Mrs. Moorehouse. You are the people who introduced me to the periodic table, got me involved in science fairs, challenged me with interesting problems and conundrums, and encouraged me to pursue a career in science.

Furthermore, I am very thankful for the faculty of Harvey Mudd College where I received my bachelors in chemistry. Harvey Mudd and the faculty that make it the top notch college that it is, made me work harder than I have ever worked in

my life. I learned how to fail at Harvey Mudd, and I learned how to try again. I learned that problems that seem impossible often just need to be examined from a different reference frame. I learned that if you don't get it right the first time, you just have to "redo" it. I learned how to ask for help and how to work in teams. I am especially grateful to the Chemistry Department – a home away from home during my time in college. Thank you to Professor Bob Cave, Professor Hal Van Ryswyk, Professor William Daub, and Professor Dave Vosburg for being extraordinary teachers, great listeners, and supportive mentors. In particular I would like to thank, Professor Adam Johnson for introducing me to organometallic research. Your enthusiasm for chemistry and research were contagious. Your mentorship and guidance while I was at HMC, while I applied for graduate school, and throughout my time at Michigan has been invaluable. Thank you for caring and for being an outstanding professor, advisor, and friend.

The work presented in this thesis was conducted under the advisement of Professor Melanie Sanford. In the four years that I have worked with Melanie, I am constantly impressed by her scientific incisiveness and creativity. It has been a privilege to learn from a truly world-class scientist. Thank you, Melanie, for the opportunity to work in your lab and learn from you. I sincerely appreciate the time and effort you spent honing my presentation and communication skills and motivating me to try again.

Also, I would like to thank my thesis committee members Professor Mark Banaszak Holl, Professor John Montgomery, and Professor Suljo Linic. Thank you for serving on my committee, checking in from time to time on my progress, and for evaluating my thesis.

During my career at Michigan, I had the opportunity to collaborate with several outstanding scientists. Their work is featured and acknowledged throughout this thesis. In particular, I would like to thank Dr. Janette Villalobos for working with a young, overeager 1st year grad school student on two research projects. Thank you for the encouragement and advice. I learned a lot from you and enjoyed working together. I would also like to acknowledge Megan Cismesia, Noah Fine Nathel, and Catherine Hwang. Thank you for your hard work in the lab and for your patience as I learned how to be a better a mentor and manager. I wish all three of you the best of luck in your future endeavors. Also, thank you to Dr. Tae-Hong Park for teaching me about MOFs and the opportunity to collaborate.

Finally, I must thank the many wonderful friends that have laughed with me, cried with me, lifted me up, and got me through the last 8 years. Katie, you are my rock. You are the best, best friend anyone could ever have. I know that I am so fortunate to have you! I am so glad that we have been able to grow together and strengthen our friendship even from a distance, and I am so excited for all the exciting adventures in our future. Thank you for everything. I couldn't have done it without you. To all my pals from HMC, Michelle, Martha, Fiela, Kyle, Emily, Kyle, Devon, Drew, Erin, Brandon, Z, and really every single Mudder I have ever

met, thanks for getting me through Mudd. It was tough, but it was worth it because I met all of you.

When I first arrived in Ann Arbor, I was gripped with fear. I was sure that I had made a terrible mistake. I was wrong. Again I was blessed by an incredible support network of smart, engaging people who have filled my time here with treasured memories. Neil, I love you, and I can't live without you. Thank you for bringing balance into my life, for reminding me that there are more important things than "one more reaction." Thank you for rejoicing in my triumphs, mourning my setbacks, and for the confidence that I will never have to face life's challenges alone. We can do anything together; I can't wait to see what is in store for us next!

Joy, we did it! We made it to the end – together. Thank you for always listening and being there for me to help with science, lab politics, and career/life advice. I couldn't have made it through this last 9 months without you. I can't wait to explore Chicago together!

Matt, I am forever indebted to you for helping me hit the ground running in the Sanford lab. You were always willing to listen to me to talk about chemistry. You guided me through candidacy and my first graduate schools projects. The work in this thesis is a testament to your tremendous mentorship. I miss our chats at the bench. Me filtering for hours on end and you doing real chemistry and us discussing everything from babies to religion to relationships are some of my fondest grad school memories.

Cheryl, Erica, Jonas, Andrew, Tom, Kara, Asako, Brannon, Marion, Anna, Yingda, Chelsea, Joe, Megan, Mike, Allison, Phil, Dave, Nicki, Liz, Bean, and Adam you are the highlights of grad school. Thank you for the chemistry help. But more importantly, thanks for the beer lunches, the raspberry picking, the game nights, the dinners on Main street, the coffee runs/venting sessions, picnics, career chats, and the why are we doing this reminders. To Club Palladium – past, present, and future – Salena, Nick, Matt, Joy, Kate, Ansis, and Monica – you rock! I am so glad that I got to work with all of you. I feel like we are a family – you don't get to choose 'em, you gotta live with them (and their music choices), and you just can't help but love 'em. I wish you all the best.

Table of Contents

List of Figures

List of Tables

List of Schemes

Abstract

The development of mild and selective methods for the functionalization of arene C–H bonds remains an important challenge in organic chemistry. One strategy to achieve this goal is metal-catalyzed C–H functionalization. Significant progress has been made with substrates possessing chelating directing groups that achieve metal-catalyzed C–H functionalization at sites proximal to the directing groups. In contrast, relatively few examples of selective C–H activation of simple arenes have been reported. The goal of this dissertation was to develop catalysts that promote C–H activation and site-selective functionalization of arene C–H bonds in substrates that do not contain directing groups.

In the first half of this dissertation, we explore Pt-catalyzed H/D exchange between benzene and acidic deuterium sources as a metric for directly comparing the reactivity of different Pt C–H activation catalysts. Using this assay, we compare the reactivity of known Pt C–H activation catalysts with bi- and tridentate nitrogen ligands and elucidate trends in reactivity. In the course of these studies, *N*-aryl diimine Pt dichloride complexes with *ortho*-halogen substitution of the aryl group were identified as superior C–H activation precatalysts.

In the second half of this dissertation, we discuss our results to develop site-selective C–H functionalization reactions. Our approach is to use steric and electronic modification of ancillary ligands of the metal catalyst to both modulate reactivity and dictate the preferred site of C–H activation. *N*-aryl diimine Pd dichloride complexes were found to efficiently and site-selectively catalyze the arylation of naphthalene to afford 1-phenyl-naphthalene. Furthermore, the yield and selectivity of this reaction can be modulated by modification of the L- and X-

type ligands of the catalysts. Evidence for an unusual mechanism of C–H activation at a high oxidation state Pd^{IV} center is also presented. Additionally, this transformation was studied with a metal organic framework supported heterogeneous Pd catalyst in collaboration with Professor Adam Matzger's laboratory. Finally, the use of commercially available platinum salts under modified reaction conditions affords both a pathway to selective formation of 2-phenyl-naphthalene, as well as promising initial results for wider arene substrate scope.

Chapter 1: Introduction

One of the greatest challenges of this century is the development of low-cost and efficient methods for the conversion of chemical feedstocks, such as natural gas, directly into value added chemicals, like methanol, ethylene, propylene, etc. The selective conversion of inert C–H bonds found in alkanes and arenes into new functional groups is a powerful strategy for rapidly increasing the complexity of organic molecules.[1] Such transformations would find broad application in the preparation of alternative fuels, agrochemicals, and commodity chemicals by fundamentally changing the way chemists approach the assembly of complex molecules. Furthermore, new methods in this area have the potential to impact human health by expediting the assembly and/or late-stage modification of drug targets, natural products, imaging agents, and other biological probes.

C–H bonds are particularly strong bonds. For example benzene has a pK_a of 43 and a bond dissociation energy of 110 kcal/mol. Furthermore, these bonds are notoriously inert to both homolytic and heterolytic cleavage. C–H bonds are ubiquitous in organic molecules; therefore, any methodology must be highly selective for the target C–H bond while leaving all others intact. For example, the pharmaceutical Fluoxetine, sold as “Prozac,” shown in Figure 1, possesses multiple, unique C–H bonds, including differently substituted aromatic sp^2 C–H bonds as well as primary, secondary, and tertiary sp^3 C–H bonds. Site-selective functionalization of any one of these various sites could be desirable for structure-activity relationship studies in the pursuit of new drug derivatives or to study pharmacokinetics.

Figure 1.1. The pharmaceutical Prozac contains multiple, unique C–H bonds.

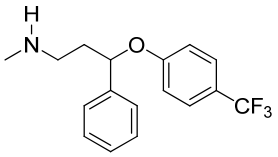

An attractive strategy for overcoming both of these challenges is the use of a transition metal catalyst. A catalyst is defined as a reagent which lowers the activation barrier of a given reaction without being consumed during that transformation. In the case of C–H functionalization, a transition metal catalyst can be used to "activate" the C–H bond by lowering the activation energy for bond scission. As shown in Scheme 1, a transition metal catalyst can coordinate to a C–H σ-bond, donating electron density into the σ* orbital (complex **A**). This in turn weakens the C–H bond and can lead to the formation of a new metal–carbon bond (Scheme 1, complex **B**). The resulting organometallic intermediate can then be further manipulated to release different carbon–X bonds, where X is halogen, oxygen, nitrogen, carbon, etc.

Scheme 1.1. Metal-catalyzed C–H activation

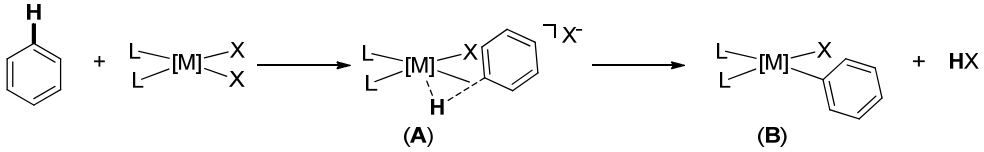

Metal-catalyzed C–H activation also provides a framework for addressing the challenge of site-selectivity. One successful approach has been the use of substrate-based control. For example one method is to use substrates that can coordinate to the metal center through the formation of a dative bond. These so-called "directing groups" (Scheme 1.2, **L**), include nitrogen heterocycles, amides, oxime ethers/esters, and imines. Upon coordination of the directing group to the

metal center, metal-mediated C–H activation occurs preferentially at a proximal C–H bond resulting in the formation of a metallocycle (Scheme 1.2)

Scheme 1.2. Ligand directed C–H activation

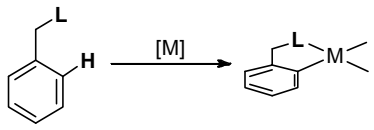

An alternative strategy is to tether an aryl halide and the C–H bond containing substrate (Scheme 1.3).[2] In this case, the aryl halide undergoes oxidative addition to the metal catalyst positioning the desired C–H bond proximal to the metal center (complex **C**). Metal-mediated C–H activation then results in the formation of a cyclometallated organometallic intermediate **D**, which can undergo further functionalization.

Scheme 1.3. Intramolecular coupling partners direct C–H activation

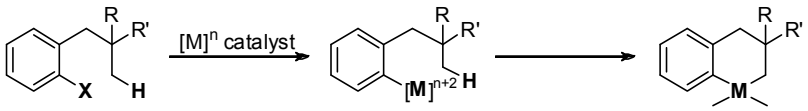

These strategies for site-selective C–H activation have led to a wide variety of new C–H functionalization reactions. In particular the last two decades have seen the development of novel Pd-catalyzed transformations for the activation and functionalization of C–H bonds[3] that are general across a wide range of directing groups. Simple Pd salts can be used to effect the selective transformation of alkane and arene C–H bonds into C–O, C–OR, C–Cl, C–Br, C–I, C–F, and C–C bonds (Figure 1.2 for examples). However, the requirement for substrate-based control over selectivity inherently restricts the scope of these transformations.

Figure 1.2 Select examples of Pd-catalyzed, ligand-directed C–H functionalization

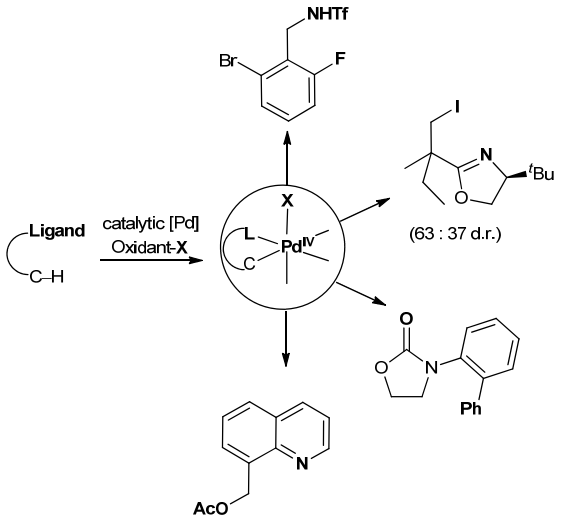

Despite this success, the ability to selectively activate and functionalize C–H bonds of simple arenes remains an important challenge in organic synthesis. In one of the most groundbreaking discoveries of the twentieth century, A. E. Shilov reported the Pt-catalyzed oxidation of alkanes and benzene.[4] A variety of simple substrates were hydroxylated using $K_2Pt^{II}Cl_4$ as the catalyst in the presence of a stoichiometric oxidant, $K_2Pt^{IV}Cl_6$ (Scheme 1.4). The proposed mechanism involved C–H bond activation at Pt^{II} (Scheme 1.4, step 1) followed by oxidation by the Pt^{IV} salt to yield a high oxidation state organometallic Pt^{IV} intermediate (step 2). Upon oxidation the Pt–carbon bond undergoes a reversal in polarity rendering the carbon electrophilic. From this high-energy, reactive intermediate a new carbon–oxygen bond is formed (step 3).[5]

Scheme 1.4. Proposed mechanism of the Shilov oxidation

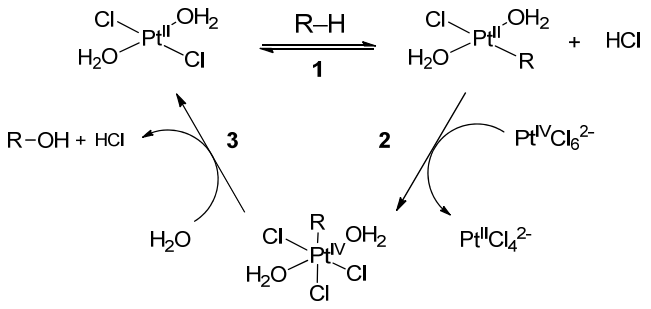

This pioneering work sparked an entire field of inquiry into new catalysts for related alkane and arene functionalization reactions.[6,7,8,9] However, there are several drawbacks to the Shilov system including use of an expensive stoichiometric Pt oxidant, low turnover numbers, the formation of undesired chlorinated side products, and catalyst deactivation via platinum metal deposition. Initial efforts to improve this transformation were focused on studying the three individual steps of the proposed mechanism.

In particular, considerable effort has aimed to design ligands for Pt-catalyzed C–H activation. Since the 1980's many Pt^{II} complexes containing diverse bi- and tridentate nitrogen donor ligands have been synthesized and their reactivity toward C–H bond scission has been evaluated by both stoichiometric formation of organo-Pt intermediates and by H/D exchange assays. Although these studies have provided valuable insights into reactivity, mechanism, and selectivity, [6] the inconsistency in reaction conditions and catalyst design makes it impossible to compare the reactivity of different catalysts or decipher trends. In the case of stoichiometric investigations, the platinum complexes that were probed are considerably different in structure than the catalytically active platinum chloride complex used in the Shilov system calling in to question the applicability of the observed results to a catalytic reaction. Although H/D exchange assays do probe catalytically relevant intermediates, there are no standard conditions in the literature; therefore, it is impossible to directly compare the results of one catalyst to another.

In the first half of this dissertation, we explore Pt-catalyzed H/D exchange between benzene and acidic deuterium sources as a metric for directly comparing the reactivity of different Pt C–H activation catalysts. In chapter 2, we present the development of a systematic H/D exchange assay including rigorous evaluation of background uncatalyzed exchange and the impact of common additives.[10] Using this quick, first-pass assay, we can directly compare the reactivity of known Pt C–H activation catalysts to elucidate trends in reactivity. We also examined the impact of temperature. Additionally, we demonstrated that this assay is a valuable tool to probe a new class of quaternized nitrogen ligands for Pt-catalyzed C–H activation.[11]

In the course of these studies, a diimine Pt dichloride catalyst was identified as a superior C–H activation catalyst under all conditions examined. In chapter 3, we further investigate this class of catalyst by studying the initial rates of C–H activation using our catalytic H/D exchange assay. A series of diimine ligands were synthesized to probe the effects of sterics, electronics, and halogen substitution. The analogous Pt dichloride complexes were then subjected to the H/D exchange conditions. The results of these catalytic studies are directly compared to previously reported trends observed for the stoichiometric C–H activation of benzene by related cationic diimine Pt methyl complexes.

In the second half of this dissertation, we discuss our results to develop site-selective C–H functionalization reactions. Compared to the H/D exchange reactions discussed above, Shilov-type functionalization reactions involve two additional steps in the catalytic cycle – oxidation and reductive elimination. There has been extensive investigation of the stoichiometric reactivity of Pt^{IV} organometallic species implicated in the putative Shilov catalytic cycle.[12,13,14,15] Detailed study of the parameters governing the mechanism and chemoselectivity of C–C, C–halogen, and C–O bond forming reductive elimination at Pt^{IV} has been of great interest. Modulation of reactivity and chemoselectivity has been shown to depend on oxidant,[16] supporting ligands,[17,18] and the presence of nucleophilic additives.[19] These stoichiometric studies also revealed that platinum complexes

typically exhibit slow rates of reductive elimination and ligand exchange. These factors can result in low overall turnover numbers (TONs) and small turnover frequencies (TOFs) for catalytic functionalization reactions.

One way to circumvent this problem is to instead use Pd catalysts. Although more difficult to oxidize,[20] Pd catalysts should exhibit faster rates of reductive elimination. Over the past eight years, numerous exciting advances have demonstrated the viability of high oxidation state Pd^{IV} and Pd^{III} species analogous to those invoked in the Shilov cycle. These intermediates have been implicated in catalytic ligand-directed Pd-catalyzed C–H functionalization reactions under oxidizing conditions.[3]

In chapters 4 and 5, we present our results on the development of a novel, site-selective catalytic C–H arylation reaction. The direct functionalization of unactivated arenes remains extremely rare, especially site-selective functionalization.[21,22,23,24,25,26,27] Our approach is to use steric and electronic modification of ancillary ligands at the metal to both modulate reactivity and dictate the preferred site of C–H activation. While catalyst control of selectivity and reactivity is common in other areas of Pd catalysis,[28,29,30,31,32,33] this approach has rarely been applied to C–H activation reactions.[34,35,36]

We chose to investigate C–H arylation since aryl–aryl bonds are ubiquitous in organic molecules including pharmaceuticals, agrochemicals, and natural products.[37] These linkages are most commonly formed via the cross-coupling of two prefunctionalized arenes (Scheme 1.5).[38] Myriad pharmaceutical and agrochemical candidates have been prepared using a Pd-catalyzed cross-coupling reaction as a key synthetic step.[39-41] Due to the broad applications of this area of catalysis, Pd-catalyzed cross-coupling was recognized by the 2010 Nobel Prize.

Scheme 1.5. Traditional Pd-catalyzed C–C coupling reactions from two prefunctionalized starting materials.

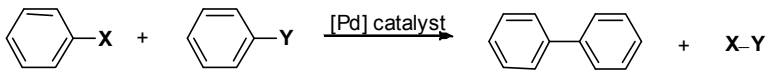

Recently, there has been tremendous progress in the development of ligand-directed, metal-catalyzed C–H arylation reactions.[42,43,44,45] In these systems, the aryl–aryl bond is formed by directly merging an arene or heteroarene with an aryl halide, aryl organometallic (*e.g.,* $ArB(OH)_2$, $ArSnBu_3$, $ArSiX_3$), or aryl iodonium salt (Scheme 1.6). Importantly, this methodology reduces the number of synthetic steps and the quantity of waste generated (since one reagent no longer must be prefunctionalized).

Scheme 1.6. Metal-catalyzed direct C–H arylation

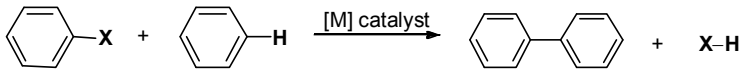

In Chapter 4, we present the first catalyst-controlled, site-selective Pd-catalyzed C–H arylation of naphthalene.[46] In this chapter, we discuss the development of our site-selective C–H arylation of naphthalene, an investigation of ligand effects on selectivity and reactivity, and evidence for an unusual mechanism of C–H activation at a high oxidation state Pd^{IV} center. Additionally, we present our collaborative work with Professor Adam Matzger's group on the development of a heterogeneous Pd catalyst for the same transformation.[47]

Finally, in chapter 5 we present preliminary results on the development of an analogous Pt-catalyzed C–H arylation reaction. Despite the exciting advances of our Pd-catalyzed methodology, two shortcomings of this system limit its synthetic applications. First, the Pd-catalyzed reaction selectively affords 1-phenyl-naphthalene; however, we were unable to develop conditions to afford 2-phenyl-naphthalene selectively with Pd catalysts. Second, the substrate scope of the Pd-catalyzed reaction was limited to naphthalene and other highly electron-rich arenes such as dimethoxybenzenes. Based on literature precedent, we hypothesized that using a Pt catalyst could result in increased reactivity for a variety of substrates and different selectivity for naphthalene C–H activation. As

presented in chapter 5, the use of commercially available platinum salts under modified reaction conditions affords both a pathway to selective formation of 2-phenyl-naphthalene, as well as promising initial results for wider arene substrate scope.

References

[1] Labinger, J. A.; Bercaw, J. E. *Nature* **2002**, *417*, 507.

[2] McGlacken, G. P.; Fairlamb, I. J. S. *Eur. J. Org. Chem.* **2009**, 4011.

[3] (a) Canty, A. J. *Dalton Trans*. **2009**, *47*, 10409. (b) Muñiz, K. *Angew. Chem. Int. Ed.* **2009**, *48*, 9412. (c) Xu, L.-M.; Li, B.-J.; Yang, Z.; Shi, Z.-J. *Chem. Soc. Rev.* **2010**, *39*, 712. (d) Sehnal, P.; Taylor, R. J. K.; Fairlamb, I. J. S. *Chem. Rev.* **2010**, *110*, 824. (e) Lyons, T. W.; Sanford, M. S. *Chem. Rev.* **2010**, *110*, 1147.

[4] Gol'dshleger, N. F.; Es'kova, V. V.; Shilov, A. E.; Shteinman, A. A. *Zh. Fiz. Khim.,* **1972**, *42*, 1979.

[5] (a) Kushch, L. A.; Lavrushko, V. V.; Misharin, Y. S.; Moravsky, A. P.; Shilov, A. E. *Nouv. J. Chim.* **1983**, *7*, 729. (b) Labinger, J. A.; Herring, A. M.; Lyon, D. K.; Luinstra, G. A.; Bercaw, J. E.; Horvath, I. T.; Eller, K. *Organometallics* **1993**, *12*, 895. (c) Luinstra, G. A.; Labinger, J. A.; Bercaw, J. E. *J. Am. Chem. Soc.* **1993**, *115*, 3004. (d) Horvath, I. T.; Cook, R. A.; Millar, J. M.; Kiss, G. *Organometallics* **1993**, *12*, 8. (e) Zamashchikov, V. V.; Popov, V. G.; Rudakov, E. S.; Mitchenko, S. A. *Dokl. Akad. Nauk SSSR* **1993**, *333*, 34. (f) Luinstra, G. A.; Wang, L. S.; Labinger, J. A.; Bercaw, J. E. *Organometallics* **1994**, *13*, 755. (g) Luinstra, G. A.; Wang, L.; Stahl, S. S.; Labinger, J. A.; Bercaw, J. E. *J. Organomet. Chem.* **1995**, *504*, 75. (h) Hutson, A. C.; Lin, M.; Basickes, N.; Sen, A. *J. Organomet. Chem.* **1995**, *504*, 69.

[6] Lersch, M.; Tilset, M. *Chem. Rev.* **2005**, *105*, 2471.

[7] Labinger, J. A.; Bercaw, J. E. *Nature* **2002**, *417*, 507.

[8] Periana, R. A.; Bhalla, G.; Tenn, W. J.; Young, K. J. H.; Liu, X. Y.; Mironov, O.; Jones, C.; Ziatdinov, V. R. *J. Mol. Catal. A* **2004**, *220*, 7.

[9] Verdernikov, A. N. "*Curr. Org. Chem.* **2007**, *11*, 1401.

[10] Hickman, A. J.; Villalobos, J. M.; Sanford, M.S *Organometallics* **2009**, *28*, 5316.

[11] Villalobos, J. M.; Hickman. A. J.; Sanford, M. S. *Organometallics* **2010**, *29*, 257.

[12] Brown, M. P.; Puddephatt, R. J.; Upton, C. E. E. *J. Chem. Soc., Dalton Trans.* **1974**, 2457.

[13] Reinartz, S.; White, P. S.; Brookhart, M.; Templeton, J. L. *J. Am. Chem. Soc.* **2001**, *123*, 6425.

[14] Kloek, S. M.; Goldberg, K. I. *J. Am. Chem. Soc.* **2007**, *129*, 3460.

[15] Luedtke, A. T.; Goldberg, K. I. *Inorg. Chem.* **2007**, *46*, 8496.

[16] Kaspi, A. W.; Goldberg. I.; Vigalok, A. *J. Am. Chem. Soc.* **2010**, *132*, 10626.

[17] Lindner, R.; Wagner, C.; Steinborn, D. *J. Am. Chem. Soc.* **2009**, *131*, 8861.

[18] Yahav-Levi, A.; Goldberg, I.; Vigalok, A.; Vedernikov, A. N. *J. Am. Chem. Soc.* **2008**, *130,* 724.

[19] Goldberg, K. I.; Yan, J.; Winter, E. L. *J. Am. Chem. Soc.* **1994**, *116*, 1573.

[20] Henry, P. M. Palladium catalyzed oxidation of hydrocarbons. Ugo, R., Ed. Reidel Publishing Company, Dordrecht: 1980.

[21.] Zhao, X.; Yeung, C. S.; Dong, V. M. *J. Am. Chem. Soc.* **2010**, *132*, 5837.

[22.] Brasche, G.; Garcia-Fortanet, J.; Buchwald, S. L. *Org. Lett.* **2008**, *10*, 2207.

[23.] Li, B. H.; Tian, S. L.; Fang, Z.; Shi, Z. J. *Angew. Chem. Int. Ed.* **2008**, *47*, 1115.

[24.] Hull, K.; Sanford, M. S. *J. Am. Chem. Soc*. **2007**, *129*, 11904.

[25] Ashenhurtst, J. A. *Chem. Soc. Rev.* **2010**, *39*, 540.

[26] You, S.; Xia, J.-B. *Top. Curr. Chem.* **2010**, *292*, 165.

[27] Lei, A.; Liu, W.; Liu, C.; Chen, M. *Dalt. Trans.* **2010**, *39*, 10352.

[28.] Slagt, v. F.; de Vries, A. H. M.; de Vries, J. G.; Kellogg, R. M. *Org. Process Res. Dev.* **2010**, *14*, 30.

[29.] Norsikian, S.; Chang, C.-W. *Curr. Org. Synth.* **2009**, *6*, 264.

[30.] Wuertz, S.; Glorius, F. *Acc. Chem. Res.* **2008**, *41*, 1523.

[31.] Hartwig, J. F. *Acc. Chem. Res.* **2008**, *41*, 1534.

[32.] Martin, R.; Buchwald, S. L. *Acc. Chem. Res.* **2008**, *41*, 1461.

[33.] Tietze, L. F.; Ila, H.; Bell, H. *Chem. Rev.* **2004**, *104*, 3453.

[34.] Catalyst-controlled selectivity in Pd-catalyzed arene olefination: Zhang, Y.-H.; Shi, B.-F.; Yu, J.-Q. *J. Am. Chem. Soc.* **2009**, *131*, 5072.

[35.] Catalyst-controlled selectivity in Pd-catalyzed arene carboxylation: Jintoku, T.; Taniguci, H.; Fujiwara, Y. *Chem. Lett.* **1987**, 1159.

[36.] Catalyst controlled selectivity/reactivity in ligand-directed C–H functionalization: Engle, K. M.; Wang, D.-H.; Yu, J.-Q *J. Am. Chem. Soc.* **2010***, 132*, 14137.

[37.] Hassan, J.; Sevignon, M.; Gozzi, C.; Schulz, E.; Lemaire, M. *Chem. Rev*. **2002**, *102*, 1359.

[38] Hassan, J.; Sevignon, M.; Gozzi, C.; Schulz, E.; Lemaire, M. *Chem. Rev*. **2002**, *102*, 1359.

[39] Magano, J.; Dunetz, J. R. *Chem. Rev.* **2011**, *111*, 2177.

[40] Torborg, C.; Beller, M. *Adv. Synth. Catal.* **2009**, *351*, 3027.

[41] Corbet, J.-P.; Mignani, G. *Chem. Rev.* **2006**, *106*, 2651.

[42.] Chiusoli, G. P.; Catellani, M.; Costa, M.; Motti, E.; Ca', N. D.; Maestri, G. *Coord. Chem. Rev*. **2010**, *254*, 456.

[43.] McGlacken, G. P.; Bateman, L. *Chem. Soc. Rev.* **2009**, *38*, 2447.

[44.] Alberico, D.; Scott, M. E.; Lautens, M. *Chem. Rev*. **2007**, *107*, 174.

[45.] Daugulis, O.; Do, H. Q.; Shabashov, D. *Acc. Chem. Res*. **2009**, *42*, 1074.

[46] Hickman, A. J.; Sanford, M. S. *ACS Catalysis*, **2011**, *1*, 170.

[47] Park, T.-H.; Hickman, A. J.; Koh, K.; Martin, S.; Wong-Foy, A.; Sanford, M. S.; Matzger, A. J. *Submitted* **2011**.

Chapter 2: An H/D Exchange Assay for Metal-Catalyzed C–H Activation

2.1 Introduction

The development of Pt-based catalysts for the oxidation of alkanes/arenes (R–H) to alcohols has been an important area of research for nearly 40 years. Pioneering studies by Shilov in the early 1970's demonstrated that a combination of simple Pt^{II} and Pt^{IV} salts promotes the oxidation of methane to methanol, and subsequent work in this field has aimed to improve this system through variation of the ancillary ligands at Pt^{II} (Scheme 2.1).[1,2] In one of the most important advances, Periana demonstrated that (bpym)$Pt^{II}Cl_2$ (bpym = κ-2,2′-bipyrimidine) catalyzes the conversion of methane to methylbisulfate in fuming sulfuric acid with a 72% first-pass yield and 81% selectivity.[3,4]

Scheme 2.1. Proposed mechanism of the Shilov oxidation

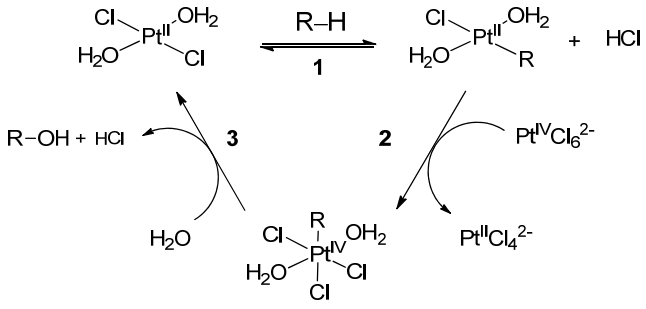

Carbon–hydrogen bond activation at Pt^{II} was identified as a key step in Pt-catalyzed alkane/arene oxidation in Shilov-type chemistry, and therefore, has been an important focus of recent studies (Scheme 2.1, step 1). The most common assay for C–H activation involves the stoichiometric reaction of an alkane or arene with a Pt^{II} alkyl complex (exemplified by **A** in Scheme 2.2).[5,6,7]

Many Pt^{II} complexes containing diverse bi- and tridentate nitrogen donor ligands participate in this model reaction, and studies of these systems have provided valuable insights into reactivity, mechanism, and selectivity.[8] However, their relevance to catalytic oxidation remains unclear, as C–H activation at Pt alkyl complexes like **A** is unlikely to be a key step within the catalytic cycle (see Scheme 2.1).[9]

Scheme 2.2. Common stoichiometric study of Pt-catalyzed C–H activation

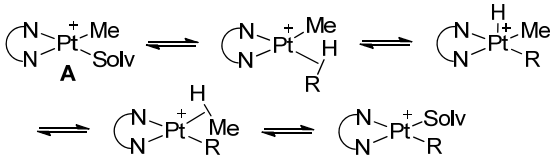

A second method for studying C–H activation involves Pt^{II}-catalyzed arene or alkane H/D exchange (Scheme 2.3). In contrast to the model systems in Scheme 2.2, H/D exchange does not rely on the ability to isolate stable organometallic complexes and is believed to proceed via intermediates directly relevant to those in catalytic R–H oxidation. The catalytic activity of simple Pt^{II} salts[10] as well as of nitrogen ligated Pt^{II} complexes[11,12,13,14] in H/D exchange reactions with both C_6H_6 and CH_4 has been examined. However, all of these studies used significantly different reaction conditions, with variable times, temperatures, concentrations, catalyst loadings, and deuterium sources. Therefore, there is currently insufficient data in the literature to systematically compare the reactivity of different Pt^{II} complexes. Herein, we present a standard assay of Pt-catalyzed H/D exchange between C_6H_6 and CF_3CO_2D, CD_3CO_2D, and CF_3CH_2COD (TFE-d_3) and utilize it to assess the reactivity (measured by turnover numbers) of a series of Pt^{II} complexes containing common nitrogen donor ligands. The work presented in sections 2.2 and 2.3 was conducted in collaboration with Dr. Janette Villalobos, who synthesized complex **2** and contributed to the development of the assay.

Scheme 2.3. Catalytic H/D exchange experiment for metal-catalyzed C–H activation

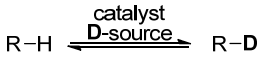

2.2 Results

Our investigations focused on comparing a series of Pt^{II} chloride complexes (**1-8,** Figure 2.1) as catalysts for H/D exchange between C_6H_6 and various deuterium sources. Complexes **1-8** were selected because Pt^{II} species containing these ligands have been reported to participate in stoichiometric R–H activation (complexes **5**,[6] **6**,[6] and **8**[15]) or its microscopic reverse (complex **1**[16]), and/or to catalyze H/D exchange reactions (complexes **2**,[3] **3**,[13] **4**,[11] and **7**[12]). However, despite many literature studies of these and related complexes, their reactivity has not been systematically compared by any metric. The chloride complexes were utilized because they can be conveniently synthesized in a single step from readily available Pt^{II} precursors.[17] Catalytic experiments were conducted with analytically pure samples of complexes **1**-**8**, which were stored at –35 ºC in vials sealed with Teflon-lined caps.[18]

Figure 2.1. Pt catalysts examined for H/D exchange reactions

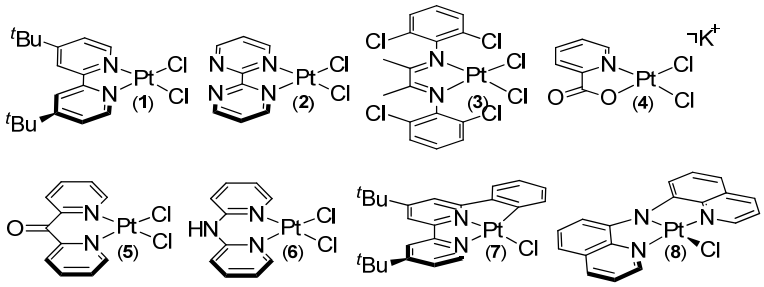

The H/D exchange between C_6H_6 and trifluoroacetic acid-d_1 (CF_3CO_2D) was selected as an initial test reaction. We felt that this would be an ideal benchmark because analogues of **2**, **4**, and **7** have been previously reported to catalyze this transformation under several different reaction conditions.[11,12] The H/D exchange reactions were conducted in 4 mL Teflon-sealed Schlenk tubes. These tubes

must be fully submerged in an oil bath in order to achieve maximum TONs and reproducible results. At the completion of the reactions, samples were subjected to a basic workup and then analyzed by GCMS. Isotope distributions were determined using a previously published worksheet that allows for deconvolution of mass spectral data for benzene isotopomers within ~5% error.[12] Herein the % deuterium incorporation is defined as the % of C–H bonds converted to C–D bonds. Turnover numbers (TONs) are calculated as moles D incorporated per mole of catalyst. The reported error is the standard deviation over at least three trials. It should be noted that the error in the deconvolution worksheet is equivalent to an error of ± 12 turnovers, which often exceeds the error in replicate trials.

We first examined the background reaction between benzene and CF_3CO_2D under standard conditions (0.50 M benzene in CF_3CO_2D). At 150 ºC, negligible (<2%) H/D exchange occurred after 2 h; however, after 24 h, 16 ± 3% D incorporation was observed. The background reaction was also investigated in the presence of silver salts (Table 2.1), which are common additives in metal-catalyzed C–H activation reactions.[11,19,20] The background reaction with silver chloride was also examined since it is the by-product of Cl abstraction from Pt^{II} chloride complexes. The addition of 4 mol % of AgOAc, AgTFA, or AgCl afforded comparable results to the reactions without Ag (with 13 ± 1%, 12 ± 1%, and 11 ± 1% D incorporation, respectively, after 24 h at 150 ºC).[21] Use of silver salts with less coordinating counterions such as tetrafluoroborate and triflate resulted in a large background reaction of 53 ± 1% and 80 ± 1%, respectively. As a result these silver salts were not used to study H/D exchange in CF_3CO_2D. At lower temperatures (between 75 and 125 ºC), < 5% D incorporation was observed in the presence of the AgOAc and AgCl salts (Table 2.2).

Table 2.1. Background H/D exchange between C_6H_6 and CF_3CO_2D as a function of time and silver additive

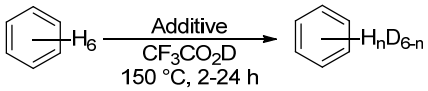

Additive	2 h	6 h	12 h	24 h
None	1 ± 1	4 ± 1	7 ± 1	16 ± 3
4 mol % AgOAc	1 ± 1	4 ± 1	5 ± 1	13 ± 1
4 mol % AgTFA	nd	nd	nd	12 ± 1
4 mol % $AgBF_4$	nd	nd	nd	53 ± 1
4 mol % AgOTf	nd	nd	nd	80 ± 1
4 mol % AgCl	1 ± 1	3 ± 1	5 ± 1	11 ± 1

Conditions: Benzene (23.2 µL, 0.26 mmol), AgX (4 mol %, 10 µmol) in CF_3CO_2D (0.5 mL, 6.5 mmol, 25 equiv relative to benzene) at 150 ºC. Data is reported as % D incorporation ± standard deviation. nd = not determined

Table 2.2. Background H/D exchange reaction between C_6H_6 and CF_3CO_2D as a function of temperature

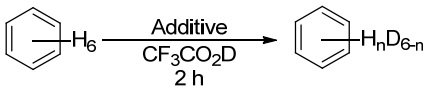

Salt	75 ºC	100 ºC	125 ºC	150 ºC
AgOAc	0.05 ± 0.01	0.20 ± 0.04	0.27 ± 0.05	1.2 ± 0.1
AgCl	0.03 ± 0.01	0.04 ± 0.01	0.2 ± 0.1	0.87 ± 0.03

Conditions: Benzene (23.2 µL, 0.26 mmol), AgOAc (1.7 mg, 10 µmol) or AgCl (1.4 mg, 10 µmol) in CF_3CO_2D (0.5 mL, 25 equiv relative to benzene) for 2 h. Reported as % D incorporation ± standard deviation.

We next measured the turnover number of Pt^{II} complexes **1** and **2** for H/D exchange between C_6H_6 and CF_3CO_2D at 150 ºC under standard conditions (2 mol % of [Pt], 0.5 M C_6H_6 in CF_3CO_2D). The parent chloride complexes exhibited modest H/D exchange activity (TON < 25) after 24 h. However, the addition of AgOAc[22] dramatically increased catalyst turnover, and optimal results (TON = 181 for **1** and 202 for **2** after 24 h) were obtained with 4 mol % of AgOAc (Figure

2.2).[21] These values are approaching the statistical maximum turnover, the TON required to achieve a statistical distribution of D between the solvent and the benzene after correcting for the AgCl background reaction [$TON_{max}(CF_3CO_2D)$ = 208 (24 h) and 239 (2 h)].

Figure 2.2. H/D exchange between C_6H_6 and CF_3CO_2D catalyzed by **1** and **2** as a function of equiv of AgOAc

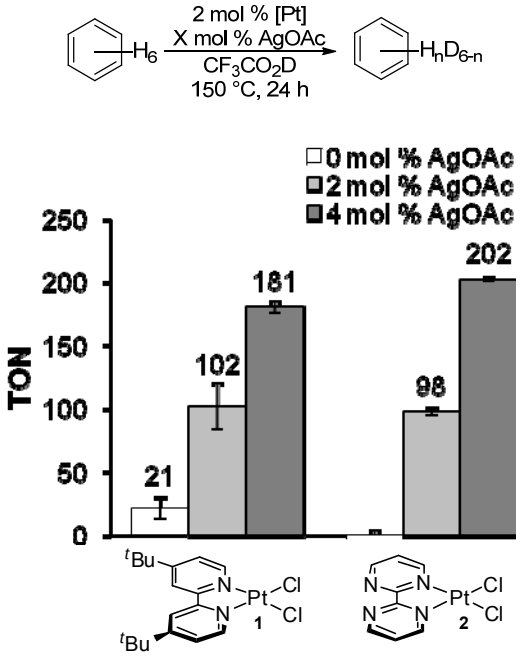

Conditions: Pt^{II} catalyst (2 mol %, 5 μmol), benzene (23.2 μL, 0.26 mmol), AgOAc (1 equiv, 0.85 mg, 5 μmol; 2 equiv, 1.7 mg, 10 μmol) in CF_3CO_2D (0.5 mL, 6.5 mmol, 25 equiv relative to benzene) at 150 ºC for 24 h. Reported as TON ± standard deviation.

To determine the identity of the Pt^{II} species generated under these conditions, **1** and **2** were treated with 2 equiv of AgOAc in trifluoroacetic acid, and the Pt-containing products were isolated (Scheme 2.4). After filtration to remove AgCl, the filtrate was concentrated, diluted with CH_2Cl_2 (for **1**) or MeCN (for **2**), and the product was precipitated by the addition of ether. This procedure provided the bis-trifluoroacetate complexes **1a** and **2a** in 80% and 75% isolated yield, respectively. Analytically pure samples of **1a** and **2a** were then used as catalysts

for H/D exchange between C_6H_6 and CF_3CO_2D, and, as summarized in Figure 3, essentially identical turnover numbers were observed to that with (N~N)$PtCl_2$/2 equiv of AgOAc. These results strongly suggest that the AgOAc serves to abstract the chloride ligands, but does not play an additional role in promoting H/D exchange. As such, the *in situ* generation of Pt^{II} H/D exchange catalysts by reaction of halide pre-catalysts with AgOAc appears to be a convenient and accurate means of assaying reactivity.

Scheme 2.4. Isolation of **1a** and **2a** from H/D exchange reaction conditions in CF_3CO_2H

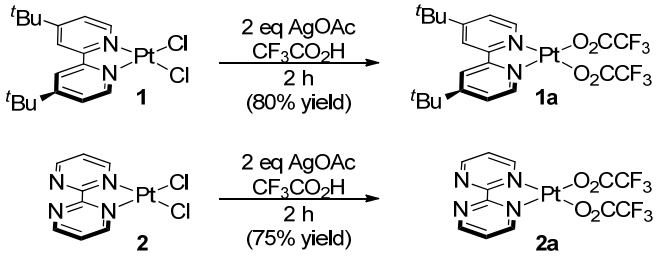

Figure 2.3. Comparison of reactivity of **1**/AgOAc to **1a** and of **2**/AgOAc to **2a**

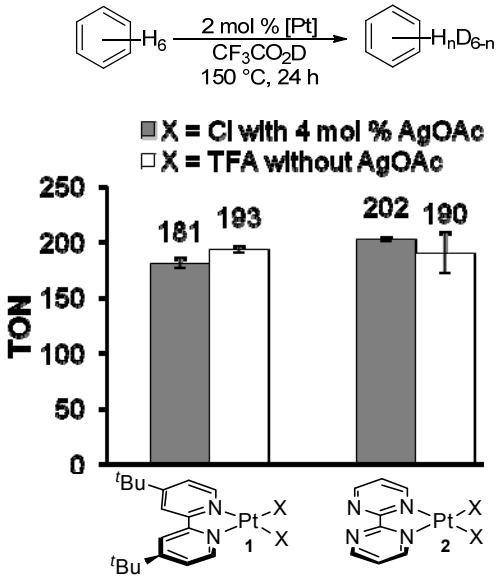

Conditions: Pt^{II} catalyst (2 mol %, 5 μmol), benzene (23.2 μL, 0.26 mmol), AgOAc (2 equiv, 1.7 mg, 10 μmol) in CF_3CO_2D (0.5 mL, 6.5 mmol, 25 equiv relative to benzene) at 150 ºC for 24 h. Reported as TON ± standard deviation.

Based on these findings, the reactivity of Pt^{II} complexes **1**-**8** for H/D exchange between C_6H_6 and CF_3CO_2D was evaluated in the presence of 4 mol % AgOAc under the standard reaction conditions. The simple Pt^{II} salts $PtCl_2$ and K_2PtCl_4 were also examined for comparison.[10] As summarized in Figure 2.4, (diimine)$PtCl_2$ (**3**) was the most active catalyst under these conditions reaching equilibrium (TON = 207 ± 4) after 2 h.[23]

Figure 2.4. Catalytic activity (measured by TON after 24 h) of **1**-**8** in H/D exchange between C_6H_6 and CF_3CO_2D

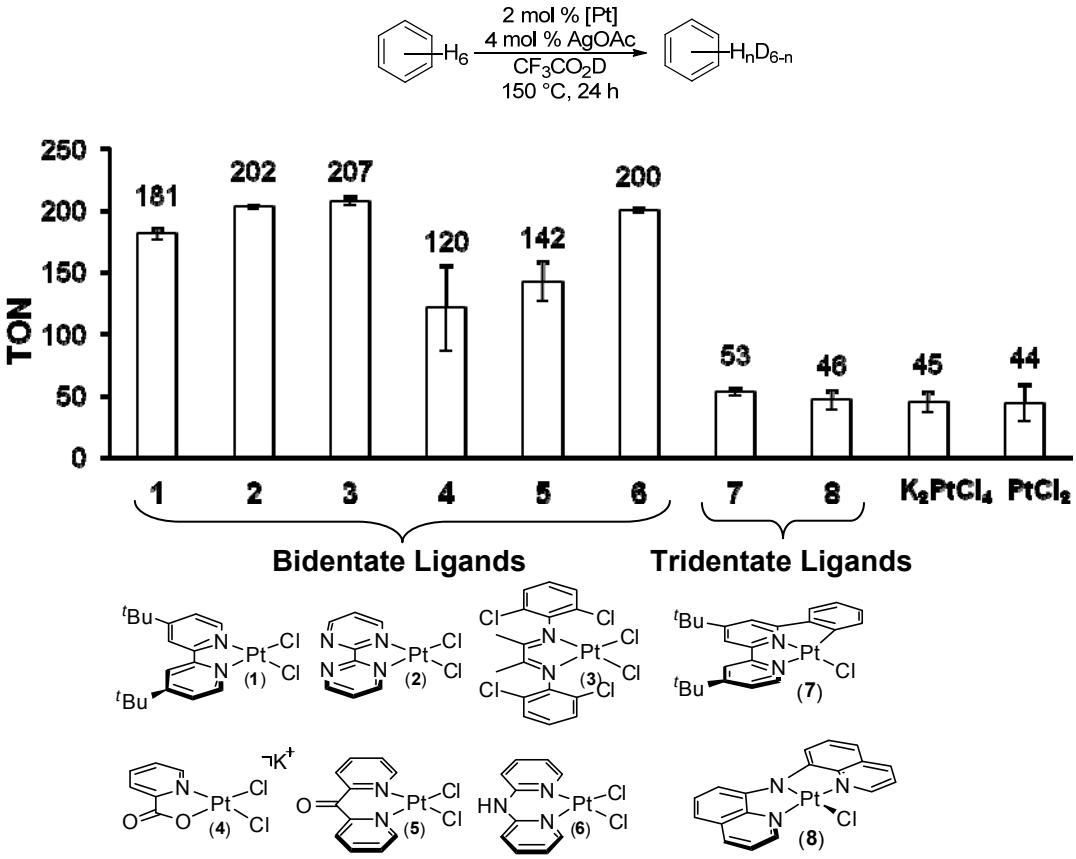

Conditions: Pt^{II} catalyst (2 mol %, 5 μmol), benzene (23.2 μL, 0.26 mmol), AgOAc (1.7 mg, 10 μmol) in CF_3CO_2D (0.5 mL, 6.5 mmol, 25 equiv relative to benzene) at 150 ºC for 2 h and 24 h. Reported as TON ± standard deviation.

While the data in Figure 2.4 offer a valuable initial metric for comparing these C–H activation catalysts, the results provide only a snapshot of catalyst performance under a single set of conditions and at a single time point. We next followed the progress of H/D exchange as a function of time for the best performing catalysts (**1**-**3**, and **6**) to gain further insights into catalyst activity. As illustrated in Figure 2.5, the H/D exchange between CF_3CO_2D and benzene proceeded fastest with diimine complex **3**. This catalyst displayed an initial turnover frequency (TOF) of 0.05 s^{-1} after 15 min at 150 °C. The bipyrimidine catalyst **2** was slower (TOF = 0.01 s^{-1}), and the bipyridine and dipyridylamine complexes **1** and **6** displayed comparable but significantly lower TOFs of 0.009 and 0.007 s^{-1}, respectively.

Figure 2.5. Turnover number versus time for H/D exchange between C_6H_6 and CF_3CO_2D catalyzed by **1**-**3** and **6.**

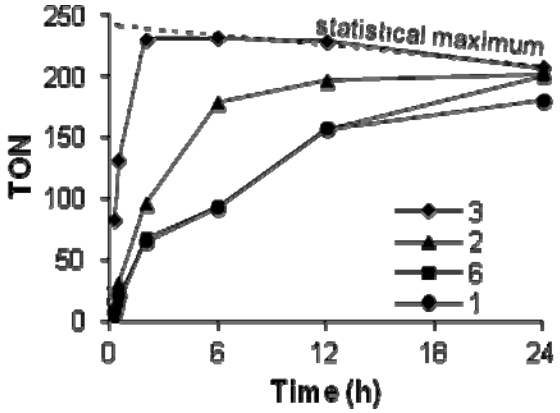

Conditions: Pt^{II} catalyst (2 mol %, 5 μmol), benzene (23.2 μL, 0.26 mmol), AgOAc (1.7 mg, 10 μmol) in CF_3CO_2D (0.5 mL, 6.5 mmol, 25 equiv relative to benzene) at 150 ºC. The statistical maximum TON at each time point is corrected for the background reaction; therefore, this value decreases with time.

In the case of catalyst **4**, the precipitation of Pt black was observed after 24 hours. These results suggest that catalyst decomposition is occurring under the reaction conditions, which is consistent with Periana's original studies of **4**.[11] In order to obtain a better benchmark for **4**, we also examined the performance of catalysts (**1**-**4** and **6**) at lower temperatures (25 ºC intervals from 75 to 150 ºC).

As summarized in Figure 2.6, catalyst **4** outperformed all others at 75 and 100 ºC; however, even at 75 ºC, decomposition of **4** by precipitation of platinum black began to occur within 2 h. This illustrates the careful balance between catalyst activity and stability required in catalyst design.[11] Notably, complex **3** performed significantly better at lower temperatures than **1**, **2**, or **6** and far surpassed all catalysts at 125 and 150 ºC.

Figure 2.6. Catalytic activity (as measured by TON after 2h) of **1**-**4** and **6** in H/D exchange between C_6H_6 and CF_3CO_2D as a function of temperature

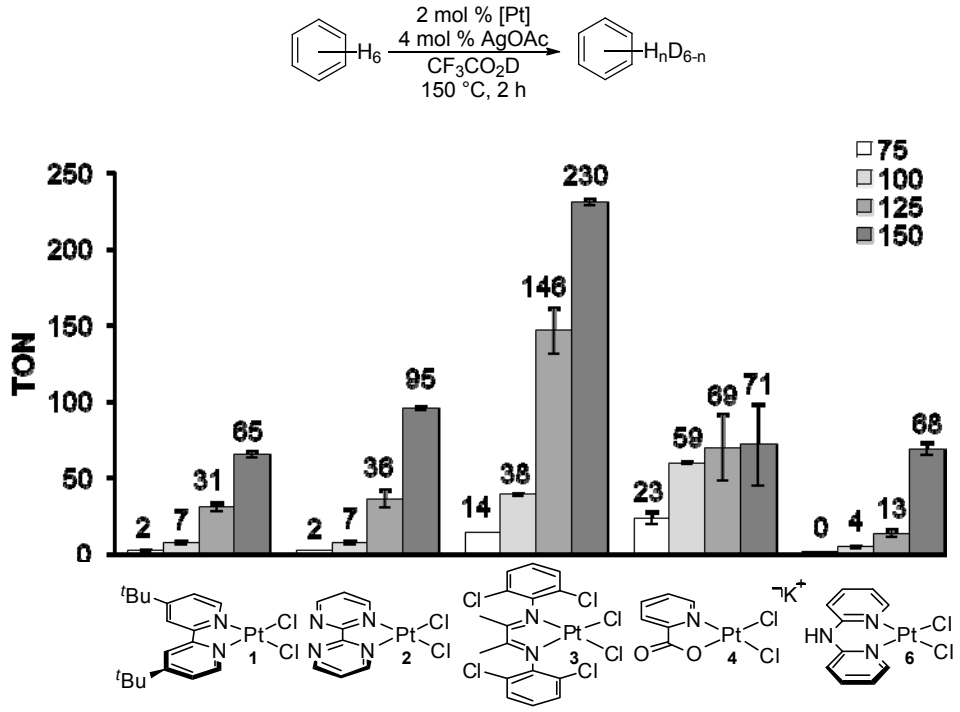

Conditions: Pt^{II} catalyst (2 mol %, 5 μmol), benzene (23.2 μL, 0.26 mmol), AgOAc (1.7 mg, 10 μmol) in CF_3CO_2D (0.5 mL, 6.5 mmol, 25 equiv relative to benzene) at 150 ºC for 2 h. Reported as TON ± standard deviation.

Finally, we examined H/D exchange between C_6H_6 and the less acidic deuterium sources CD_3CO_2D and trifluoroethanol-d_3 (TFE-d_3). C–H activation is expected to be more challenging under these conditions, because the solvents can compete with C–H bonds for coordination to the metal center. To date, there is only one example of Pt-catalyzed H/D exchange between C_6H_6 and CD_3CO_2D

(with a derivative of **3**).[13,24] Thus, we aimed to establish whether catalysts **1**-**8** displayed activity with these deuterium sources and to compare this reactivity to that with CF_3CO_2D.

The background reaction was negligible with both CD_3CO_2D and TFE-d_3; for example, <1% H/D exchange was observed after 24 h at 150 ºC in the presence or absence of 4 mol % of AgOAc, AgCl, or $AgBF_4$ (Table 2.3). Modest H/D exchange was observed in CD_3CO_2D upon the addition of 2 mol % of **1** or **2** along with 4 mol % of AgOAc (TON = 24 ± 8 and 26 ± 9, respectively). Furthermore, catalyst activity could be increased through the use of $AgBF_4$ in place of AgOAc under otherwise identical conditions (TON = 144 ± 12 and 94 ± 13, respectively, Figure 2.7).

Table 2.3. Background H/D exchange reaction with various deuterium sources

Deuterium Source	AgCl	AgOAc	$AgBF_4$
CD_3CO_2D	0.07 ± 0.03	0.10 ± 0.03	0.25 ± 0.02
TFE-d_3	0.02 ± 0.04	nd	0.10 ± 0.20

Conditions: benzene (23.2 µL, 0.26 mmol), AgOAc (1.7 mg, 10 µmol) or AgCl (1.4 mg, 10 µmol) or $AgBF_4$ (1.9 mg, 10 µmol) in CF_3CO_2D (0.5 mL, 6.5 mmol), CD_3CO_2D (0.37 mL, 6.5 mmol), or TFE-d_3 (0.47 mL, 6.5 mmol) at 150 ºC for 24 h; nd = not determined. Reported as % D incorporation ± standard deviation.

Figure 2.7. H/D exchange between C_6H_6 and CD_3CO_2D catalyzed by **1** and **2** as a function of Ag salt

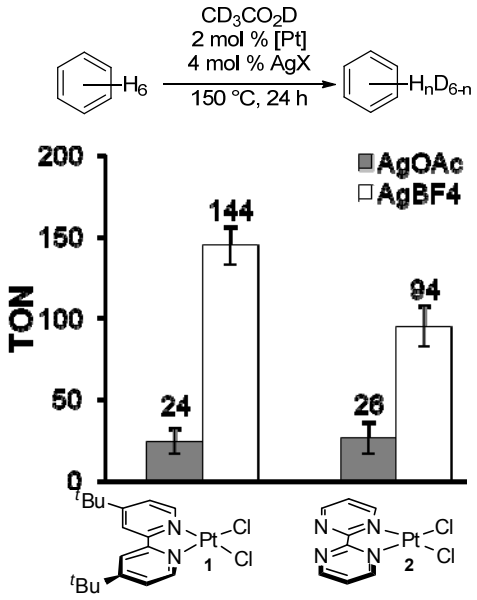

Conditions: Pt^{II} catalyst (2 mol %, 5 μmol), benzene (23.2 μL, 0.26 mmol), AgOAc (1.7 mg, 10 μmol) or $AgBF_4$ (1.9 mg, 10 μmol) in CD_3CO_2D (0.37 mL, 6.5 mmol, 25 equiv relative to benzene) at 150 ºC for 24 h. Reported as TON ± standard deviation.

With these conditions in hand, we investigated the reactivity of **1**-**6** as well as K_2PtCl_4 and $PtCl_2$ for H/D exchange between C_6H_6 and CD_3CO_2D in the presence of 4 mol % of $AgBF_4$ (Figure 2.8). A time study was conducted in acetic acid to further elucidate the reactivity profiles of the top three performing catalysts in this solvent (Figure 2.9). Additionally, H/D exchange was measured between C_6H_6 and TFE-d_3 in the presence of 4 mol % of $AgBF_4$ (Figure 2.10).[25] A time study was not undertaken in TFE-d_3 as it is prohibitively expensive.

With both deuterium sources, negligible reaction (<8 turnovers) was observed with the commercial Pt chloride salts. In contrast, all of the complexes **1-6** showed good to excellent levels of catalytic activity, with TON ranging from 65 to 230 using CD_3CO_2D and from 50 to 233 using TFE-d_3 after 24 h. Interestingly, the relative activity of the catalysts changed significantly as a function of

deuterium source; for example, **3** and **5** were the most active catalysts in CD_3CO_2D, while **1** and **3** were optimal in TFE-d_3.

Figure 2.8. H/D exchange between C_6H_6 and CD_3CO_2D catalyzed by **1**-**6**

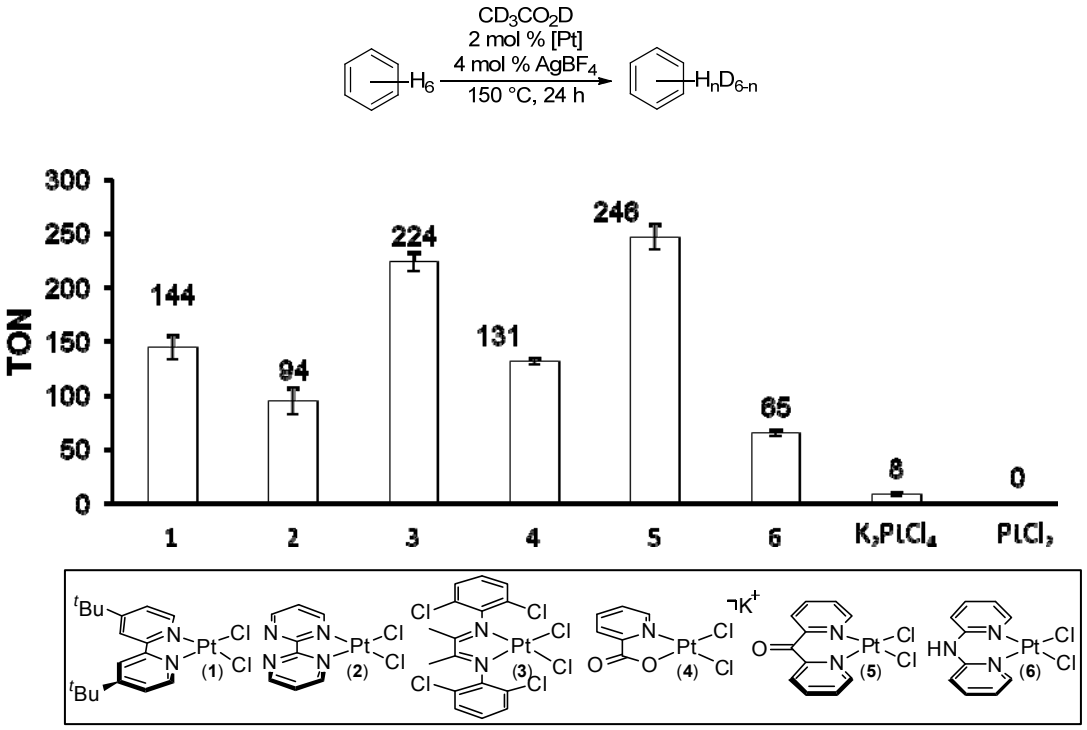

Conditions: Pt^{II} catalyst (2 mol %, 5 μmol), benzene (23.2 μL, 0.26 mmol), $AgBF_4$ (1.9 mg, 10 μmol) in CD_3CO_2D (0.37 mL, 6.5 mmol, 25 equiv relative to benzene) at 150 ºC for 24 h. Reported as TON ± standard deviation.

Figure 2.9. Turnover number versus time for H/D exchange between C_6H_6 and CD_3CO_2D catalyzed by **1**, **3**, and **5**

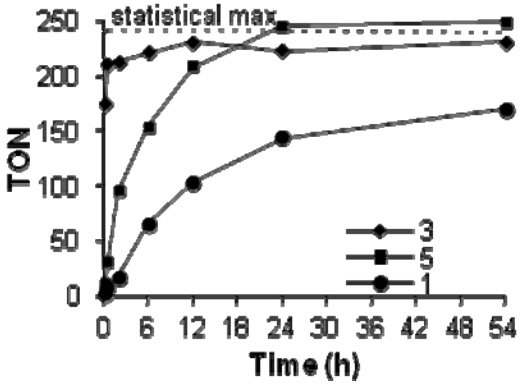

Conditions: Pt^{II} catalyst (2 mol %, 5 μmol), benzene (23.2 μL, 0.26 mmol), $AgBF_4$ (1.9 mg, 10 μmol) in CD_3CO_2D (0.37 mL, 6.5 mmol, 25 equiv relative to benzene) at 150 ºC.

Figure 2.10. H/D exchange between C_6H_6 and TFE-d_3 catalyzed by **1**-**3**, **5**, and **6**

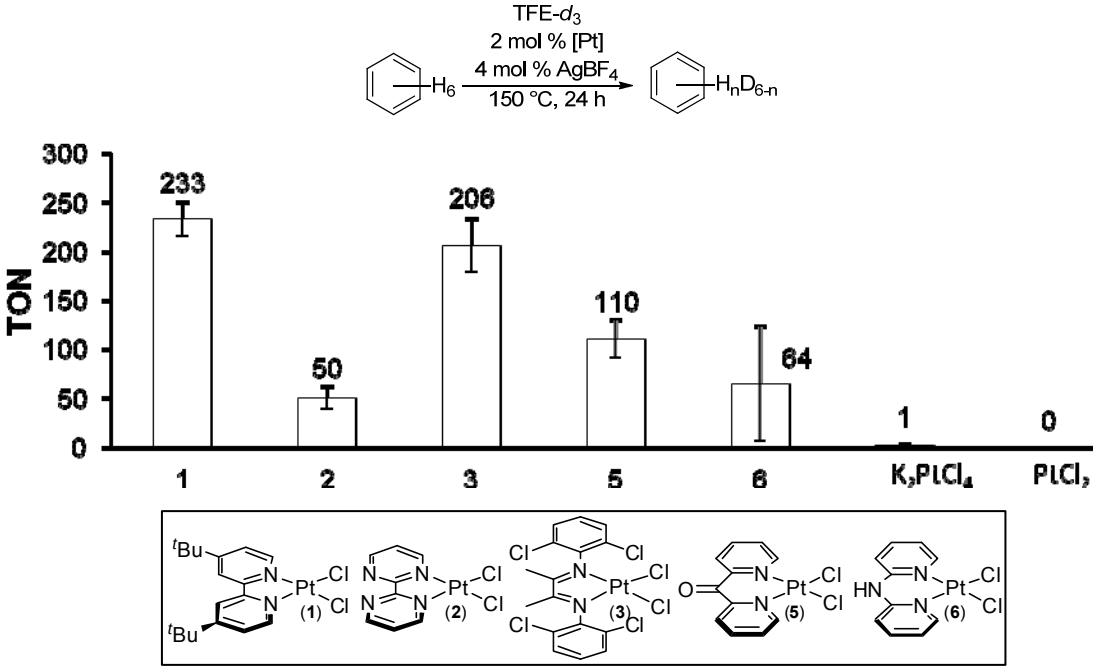

Conditions: Pt^{II} catalyst (2 mol %, 5 μmol), benzene (23.2 μL, 0.26 mmol), $AgBF_4$ (1.9 mg, 10 μmol) in TFE-d_3 (0.47 mL, 6.5 mmol, 25 equiv relative to benzene) at 150 ºC for 24 h. Reported as TON ± standard deviation.

Diimine complex **3** was consistently a top-performing catalyst with all three deuterium sources, and most H/D exchange reactions with **3** proceeded to equilibrium under our standard conditions. Thus, we sought to challenge catalyst **3** in order to establish the upper limits of its reactivity. Catalysts **3** and **5** (the two best catalysts in CD_3CO_2D) were therefore examined at 4-fold reduced Pt loading (0.5 mol % of Pt/1 mol % of $AgBF_4$) under otherwise identical conditions to the previous experiments. Catalyst **3** remained highly active under these conditions, and afforded 633 ± 43 turnovers for C_6H_6/CD_3CO_2D H/D exchange after 2 h. Complex **5** showed almost 3-fold lower activity with TON = 223 ± 3.

2.3 Discussion

Previous studies have examined the catalytic activity of simple Pt^{II} salts[10] and of nitrogen ligated Pt^{II} complexes[9-12] in benzene H/D exchange. However, these investigations were all conducted under different reaction conditions, with variable times, temperatures, concentrations, catalyst loadings, and deuterium sources. In this work, we have established a quick, first-pass standard protocol to assay the reactivity of Pt complexes for H/D exchange between C_6H_6 and various deuterium sources by measuring turnover numbers.

There are three discernible trends in the data reported herein. First, Pt^{II} complexes containing bidentate ligands (**1**-**6**) were significantly superior catalysts to simple Pt chloride salts under all of the H/D exchange conditions examined. In reactions with K_2PtCl_4 or $PtCl_2$, rapid formation of a black precipitate was observed, suggesting that decomposition to platinum black contributes to low TON's in these systems.[10]

Second, complexes containing bidentate ligands (**1**-**6**) generally exhibited higher H/D exchange activity than those with related tridentate ligands (**7** and **8**). This is clear from Figure 2.4 as well as from the fact that **7** and **8** showed negligible turnovers with either CD_3CO_2D or TFE-d_3 as a deuterium source. Computational studies in the literature have suggested that the low reactivity of **7** is due to a highly unfavorable ΔH associated with the C–H activation reaction.[11]

Third, complex **3** consistently showed high TON's for C_6H_6 H/D exchange at temperatures above 100 ºC. This was true over a range of different deuterium sources and reaction conditions. However, complex **3** does appear to suffer from some decomposition over the course of these transformations, as the catalytic solutions darkened considerably (changing color from orange to dark grey or black) after 24 h at 150 ºC in all of the solvents examined. These results suggest that the future development of related catalysts should focus on limiting catalyst decomposition pathways.

It is more difficult to make generalizations among the other complexes containing bidentate N-donor ligands, as both relative and absolute catalytic activity varied significantly upon changing the deuterium source. For example, the observed trends in catalytic activity were as follows: **3** > **2** > **6** > **1** > **5** > **4** (CF_3CO_2D), **5** ≈ **3** > **1** ≈ **4** > **2** > **6** (CD_3CO_2D), and **1** ≈ **3** > **5** > **6** ≈ **2** (TFE-d_3). This does not appear to track well with the reactivity of related complexes in stoichiometric C–H activation.[6] There is also no clear correlation with the electronic character of the ligands, although protonation of the basic nitrogens of **2** and **6** in CF_3CO_2D may be partially responsible for obscuring the expected trends. These differences may reflect a change in mechanism with the different deuterium sources, and/or competing electronic requirements of various steps of the H/D exchange process as a function of solvent. In general, a more systematic and detailed examination of ligand electronic and steric characteristics will be essential to definitively establish the parameters responsible for catalyst activity in these systems.

2.4 Application

With this assay in hand, we could now begin to study new complexes by quickly testing their reactivity in the H/D exchange assay and comparing it to the complexes benchmarked above. In collaboration with Dr. Janette Villalobos, we turned our attention to the study of bidentate N-donor ligands containing a quarternized nitrogen center. This ligand architecture has been implicated as the

active catalyst in the best Pt-based CH_4 oxidation process reported to date. It has been proposed that the conversion of methane to methylbisulfate in fuming H_2SO_4 is catalyzed by the cationic complex $[(N\text{-H-bpym})Pt(X)_2]^+$ (**9**, X = Cl or OSO_3H)[26] formed *in situ* by protonation of the precatalyst $(bpym)PtCl_2$ (**2**) (Scheme 2.5). Computational studies[26,27] suggest that this protonation is critical for limiting oxidative catalyst degradation and increasing the electrophilicity of the Pt center (and thereby its reactivity toward CH_4). However, these effects have proven difficult to study experimentally due to the challenges of working in fuming H_2SO_4 and the multiple accessible protonation states and X-type ligands in this medium. As such, the exact nature of the active catalyst remains the subject of some debate.[28] Additionally, limited experimental understanding of the effects of protonation on reactivity has hindered further catalyst development, which is required to render this methane oxidation process commercially viable.

In this work, Dr. Villalobos developed a synthesis for a Pt catalyst containing a quarternary nitrogen ligand. She then evaluated the reactivity of this complex for both benzene and methane H/D exchange with acidic deuterium sources using the standard assay developed above. Finally, I conducted NMR investigations to probe the stability and reactivity of this new catalyst under the H/D exchange reaction conditions.

Scheme 2.5. Oxidation of CH_4 to CH_3OSO_2H catalyzed by **2**

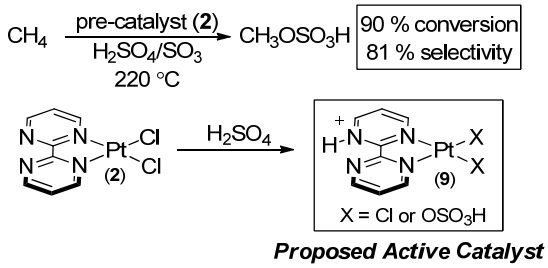

Proposed Active Catalyst

In an effort to address these challenges, we aimed to replace bpym with the cationic quaternized nitrogen-containing ligand *N*-CH_3-2,2'-bipyrimidininum (*N*-CH_3-$bpym^+$). Quaternary nitrogen substituents are highly electron withdrawing;

for example, the pK_a of *N*-methylisonicotinic acid (Figure 2.11) is 1.72, which corresponds to a Hammett σ_{para} value of +2.47 for the *N*-CH_3 group.[29, 30] We anticipated that the cationic Pt^{II} *N*-CH_3-bpym$^+$ complex **10** (Figure 2.12) would possess similar electronic properties to **9** but would be accessible in the absence of strong acids like fuming H_2SO_4[26] or HF/SbF_6.[31]

Figure 2.11. pK_a of *N*-methylisonicotinic acid

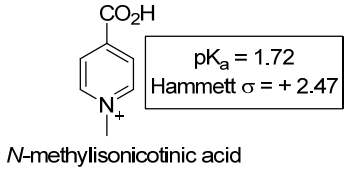

Figure 2.12. Pt^{II} complexes compared in this study

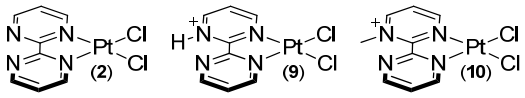

Our investigation focused on preparation of complex **10** via metalation of *N*-methyl bipyrimidinium [(*N*-CH_3-bpym)][BF_4]. However, treatment of $(DMSO)_2PtCl_2$[32] with [(*N*-CH_3-bpym)][BF_4] in methanol at 60 ºC did not afford the desired complex. Instead, metalation proceeded with concomitant addition of CH_3OH into the ligand to provide the neutral complex 2-(4-methoxy-3-methyl-4,5-dihydropyrimidin-2-yl)pyrimidine$PtCl_2$ (**11**) in 86% yield (Scheme 2.6, top). The ^1H and ^{13}C NMR spectra of **11** show signals consistent with loss of aromaticity in one ring of the bpym; for example, upfield ^1H NMR resonances at 5.49 and 5.69 ppm are observed for H_4 and H_5, respectively (Scheme 2.6, top). Crystals of **11** were obtained by diffusion of Et_2O into a solution of **11** in wet CH_3CN. This led to substitution of OH for OCH_3 to form complex **12** (Scheme 2.6, bottom), which was characterized by X-ray crystallography (Figure 2.13).

Scheme 2.6. Synthesis of complex **12**

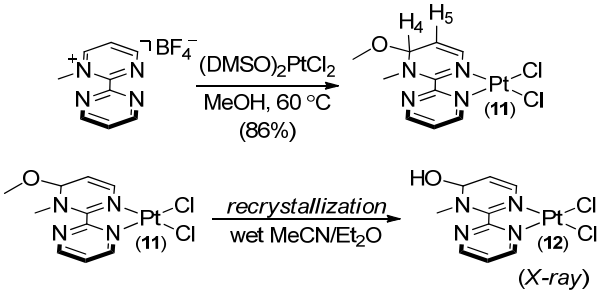

Figure 2.13. X-ray structure of complex **12**

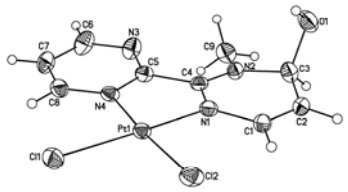

We hypothesized that **10** could be accessed from **11** via protonation of the CH_3O group followed by loss of CH_3OH. Gratifyingly, dissolving complex **11** in CF_3CO_2D led to instantaneous formation of a new inorganic species with concomitant release of 1 equiv of CH_3OD (which was converted *in situ* to $CF_3CO_2CH_3$) (Scheme 2.7). The ^1H and ^{13}C NMR resonances associated with the new complex (**10**) are shifted significantly downfield relative to those of **11**. For example, while the ligand proton resonances for **11** appear between 9.84 and 5.49 ppm, those in the product appear between 10.6 and 8.0 ppm. Similarly, in the ^{13}C NMR spectrum of **10**, 8 aromatic resonances are observed between 162.7 and 158.6 ppm, while the starting material **11** shows 8 peaks between 161.9 and 123.9 ppm. These data are all fully consistent with aromatization of the *N*-CH_3-bpym$^+$ ligand to form **10**.

Scheme 2.7. Synthesis of complex **10** containing a quaternized nitrogen ligand

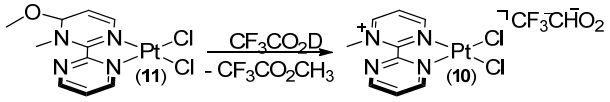

Having generated the desired complex in trifluoroacetic acid, we next examined the C–H activation reactivity of **2** and **10** (generated *in situ* from **11**) in CF_3CO_2D. In this solvent, the protonation of **2** to afford cationic complex **9** should be significantly less favorable than in more strongly acidic media typically employed in methane oxidation.[33,34,35]

Pre-catalysts **2** and **10** were evaluated under our standard H/D exchange conditions (2 mol % [Pt], 4 mol % AgOAc, 0.5 M C_6H_6 in CF_3CO_2D at 75 ºC and 150 ºC) after 2 h and 24 h. The extent of H/D exchange was assayed by GCMS, and the data are summarized in Figure 2.14. Interestingly, **2** and **10** provided very similar TON's under all conditions examined. In both cases, very little H/D exchange activity was observed at 75 ºC, even after 24 h (TON after 24 h = 19 and 15 respectively, for **2** and **10**). Both showed higher activity at 150 ºC, with similar TON (202 and 187 after 24 h) and turnover frequencies (TOF = 0.8 and 0.3 min^{-1} after 2 h) at this temperature.

Figure 2.14. Turnover numbers (TONs) for H/D exchange between C_6H_6 and CF_3CO_2D catalyzed by **2** and **10**.

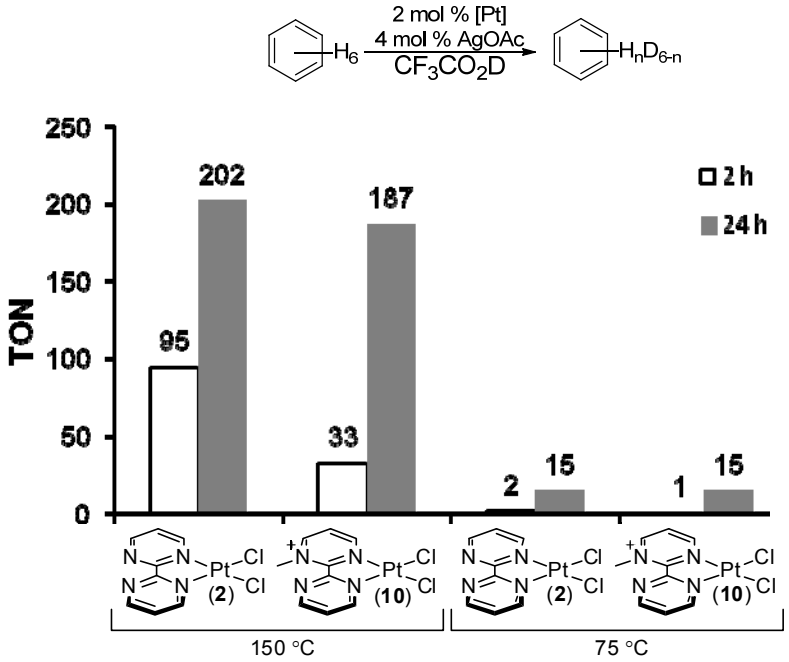

Conditions: Pt^{II} catalyst (2 mol %, 5 μmol), benzene (23.2 μL, 0.26 mmol), AgOAc (1 equiv, 0.85 mg, 5 μmol; 2 equiv, 1.7 mg, 10 μmol) in CF_3CO_2D (0.5 mL, 6.5 mmol, 25 equiv relative to benzene) at 75 or 150 ºC for 2 or 24 h. Reported TONs are the average of at least two trials.

To gain insights into the similar reactivity of **2** and **10** in C_6H_6/CF_3CO_2D H/D exchange, we probed the structure of the active Pt catalyst in both systems. As shown in Scheme 2.2, complex **2** reacts rapidly with AgOAc in CF_3CO_2D to form (bpym)Pt$(O_2CCF_3)_2$ (**2a**). Similarly, dissolving **10** in CF_3CO_2D at room temperature in the presence of 2 equiv of AgOAc led to the formation of a single detectable organometallic product, along with release of 1 equiv of $CF_3CO_2CH_3$ and 2 equiv of AcOD. On the basis of the stoichiometry of organic by-products as well as the observed ^1H and ^{13}C NMR resonances (which show an unsymmetrical species in which the *N*-methyl group is intact), this new complex is proposed to be [(*N*-CH_3-bpym)Pt$(O_2CCF_3)_2$](O_2CCF_3) (**10a**) (Figure 2.15).

Heating **10a** at 150 ºC for 15 min in CF_3CO_2D in a flame-sealed NMR tube resulted in complete disappearance of its diagnostic ^1H NMR resonances and concomitant formation of symmetrical (bpym)Pt$(O_2CCF_3)_2$ (**2a**) along with 1 equiv

of $CF_3CO_2CH_3$ (Figure 2.15). This result indicates that nucleophilic demethylation of the *N*-CH_3-bpym$^+$ ligand is very fast under the H/D exchange conditions. Although demethylation was slower at 75 ºC, significant (~30%) decomposition of **10a** to **2a** was observed after 24 h even at this temperature.[36] In sum, this data indicates that **10a** readily decomposes to **2a** at elevated temperatures in CF_3CO_2D. On this basis, we hypothesize that the similar H/D exchange reactivity of **2** and **10** is likely due to the generation of the same active catalyst, **2a**, under the reaction conditions.

Figure 2.15. Complex **10a** stability in CF_3CO_2D at 150 ºC. ^1H NMR spectra after 2 h at 25 ºC (top) and 15 min at 150 ºC (bottom)

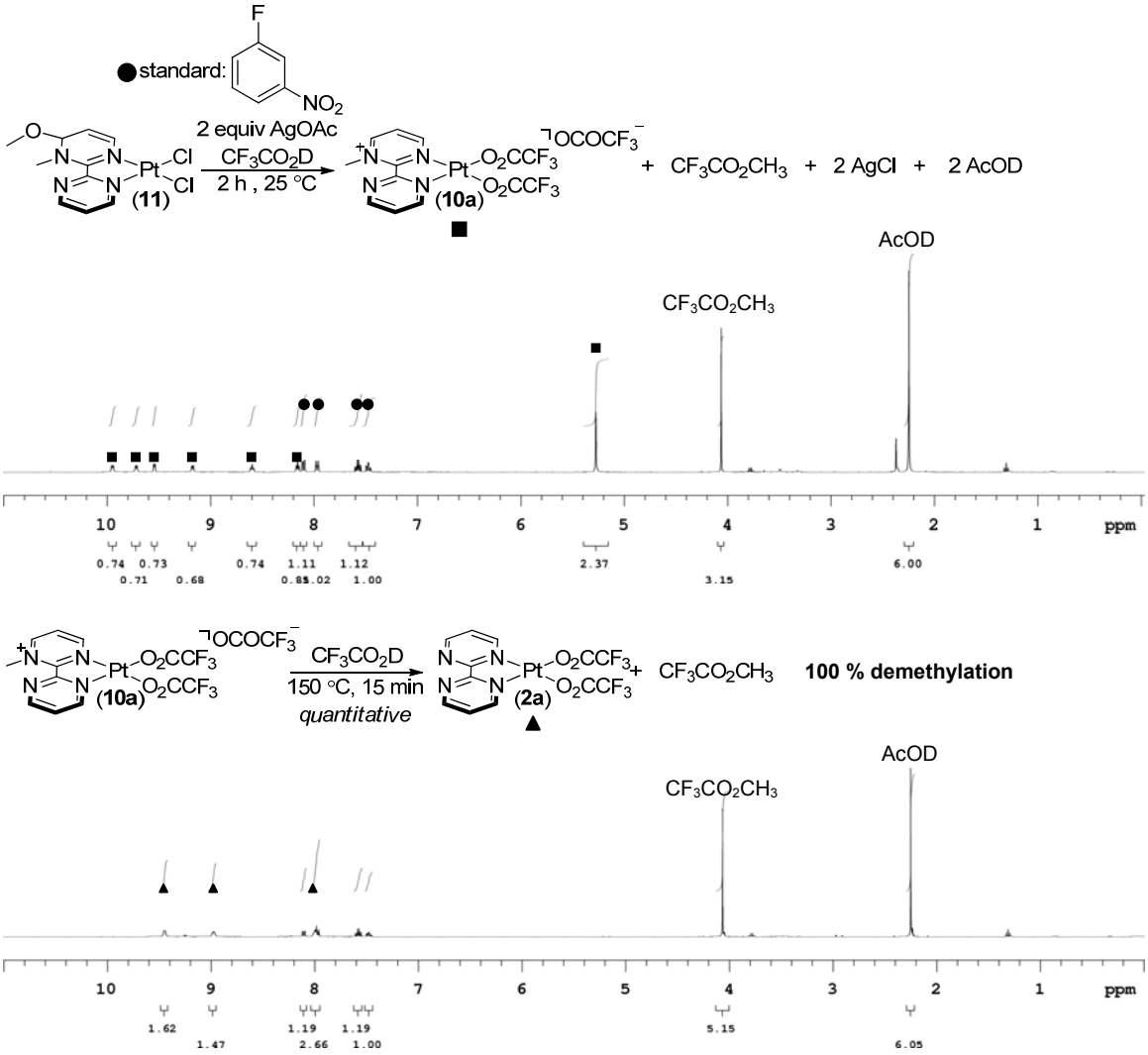

Conditions: To complex **11** (2.4 mg, 5 µmol, 1.0 equiv) in a NMR tube was added 0.25 mL of a 0.04 M stock solution of silver acetate in CF_3CO_2D (1.7 mg, 1.0 equiv). To this mixture was added an additional 0.25 mL of CF_3CO_2D and 1-fluoro-3-nitrobenzene as an internal standard. This sample was then flame sealed under vacuum and allowed to stand for 2 h at room temperature while shaking periodically (top). The sample was then heated at 150 ºC for 15 min and analyzed by ^1H NMR spectroscopy after cooling to room temperature.

We next examined the catalytic activity of **2** and **10** (generated *in situ* from **11**)[37] in the H/D exchange between CH_4 and D_2SO_4, which serves as a direct assay for methane C–H activation. The catalysts were compared under a

standard set of conditions (1 mol % of [Pt], 2 mmol CH_4, 1 mL D_2SO_4, 200 ºC, 24 h).[38] The headspace gases were analyzed by GCMS, and the distribution of CD_nH_{4-n} isotopologs was determined using a published worksheet.[39] As summarized in Figure 2.16, turnover numbers (TON's)[40] of 193 and 208 were obtained with **2** and **10**, respectively. The similarity between the TON's for **2** and **10** suggests that the *N*-methylated ligand does not offer a significant advantage over simple bpym under these conditions. Investigation of the active catalysts in D_2SO_4 by ^1H NMR spectroscopy is consistent with rapid demethylation of **10**. Therefore, it is likely that both **2** and **10** are converted to the *N*-protonated species **3** *in situ*; however, we were unable to definitively characterize the active species in sulfuric acid.[26,27]

Figure 2.16. Turnover numbers (TONs) for H/D exchange between CH_4 and D_2SO_4 catalyzed by **2** and **10**.

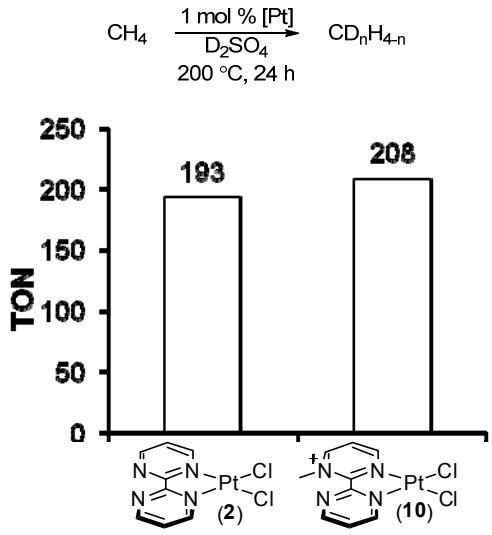

Conditions: Pt^{II} catalyst (1 mol %, 20 μmol), CH_4 (~13 bar, 2.0 mmol, 1 equiv), D_2SO_4 (1 mL, 20 mmol, 10 equiv) at 200 ºC for 24 h. Reported TON's are the average of two trials.

2.5 Conclusions

This chapter has described a protocol for the direct comparison of Pt-based catalysts for the H/D exchange between C_6H_6 and CF_3CO_2D, CD_3CO_2D, and

TFE-d_3. An initial survey of 10 different Pt catalysts under these conditions has established that diimine complex **3** is highly active for benzene H/D exchange with all three deuterium sources. However, intriguingly, the relative activity of the other catalysts was found to vary substantially depending on the nature of the deuterium source. The latter results reveal the importance of comparing new catalysts in *several different assays* in order to fully evaluate their reactivity.

The conditions developed here have served as a valuable method to rapidly screen and benchmark new transition metal catalysts for C–H activation. In particular, we have studied Pt catalysts with quaternary nitrogen ligands, which have previously been implicated in methane oxidation catalysis. Cationic complex **10** catalyzes H/D exchange between D_2SO_4 and CH_4 as well as between CF_3CO_2D and C_6H_6 with similar turnover numbers to (bpym)Pt$(Cl)_2$ (**2**). In both cases, the similar reactivities are proposed to result from rapid *in situ* demethylation of the *N*-CH_3-bpym$^+$ precatalyst. These results indicate that more stable ligands are needed to definitively establish the influence of quaternized nitrogen substituents on Pt C–H activation catalysts. The preparation of such ligands and their application in arene and alkane H/D exchange and oxidation reactions was recently reported by our group using the H/D exchange assay as a valuable tool for catalyst design and optimization.[41]

2.6 Experimental

General Procedures. ^{1}H and ^{13}C NMR spectra were recorded on Varian Inova 500 or 400 MHz NMR spectrometers with the residual solvent peak ($CDCl_3$: ^{1}H = 7.27 ppm, ^{13}C = 77.23 ppm) as the internal reference unless otherwise noted. Chemical shifts are reported in parts per million (ppm) (δ). Multiplicities are reported as follows: br (broad resonance), s (singlet), t (triplet), q (quartet), d (doublet), m (multiplet), app (apparent). Coupling constants (*J*) are reported in Hz. Infrared (IR) spectroscopy was performed on a Perkin Elmer FTIR. Peaks are reported in cm^{-1}. Elemental analyses were performed by Atlantic Microlab, Inc., Norcross, Georgia. Dichloromethane (CH_2Cl_2), dimethylsulfoxide (DMSO),

and methanol (CH_3OH) were purchased from Aldrich and used as received unless otherwise noted. Diethyl ether (Et_2O), ethyl acetate (EtOAc), and acetonitrile (MeCN) were obtained from EM Science and used as purchased. Ethanol (EtOH), 200 proof, was obtained from Deacon Labs, Inc., and used as received. Celite was purchased from EM Science. Silver acetate (AgOAc), Me_2SO_4, $NaPF_6$, bipyrimidine (bpym), and $[Me_3O]BF_4$ were purchased from Aldrich. $(DMSO)_2PtCl_2$ was prepared according to a literature procedure.[42] D_2SO_4 and CF_3CO_2D were purchased from Cambridge Isotopes Lab in 10 g ampules and were stored in Schlenk tubes under N_2. Ultra high purity methane gas was obtain from Airgas, Inc.

Stock solutions of AgOAc were prepared using volumetric glassware and all liquid reagents were dispensed by difference using gas-tight Hamilton syringes. All glassware and stir bars were treated with aqua regia, washed with copious water and acetone, and dried before each use. All reactions were conducted on the bench top (without rigorous exclusion of ambient air/moisture) unless otherwise noted. H/D exchange data was obtained on a Shimadzu GCMS-QP5000, and all raw data was deconvoluted using a benzene H/D exchange worksheet reported by Periana and coworkers.[43] One assumption in the worksheet is that the fragmentation pattern for each isotopomer is identical. To obtain the most accurate analysis, pure samples of each isotopomer were analyzed to determine the exact coefficients of the polynomial expansion for our GCMS instrument. Using this treatment, we confirmed the calculated percents of each isotopomer to be within the reported error of the worksheets. Every reported reaction was conducted at least twice. The average of all trials is reported herein; the reported error is the standard deviation of all trials (where more than two trials were done). The procedure for a typical H/D exchange reaction is as follows.

*C_6H_6/ CF_3CO_2D H/D exchange catalyzed by diiminePtCl$_2$ (**3**):*

To a 4 mL resealable schlenk tube was added a small stir bar and diiminePtCl$_2$ (**3**) (3.2 mg, 5 μmol, 2 mol % relative to benzene). 0.25 mL of CF_3CO_2D was then added to the schlenk tube, carefully rinsing the sides of the vessel. A stock solution of the silver acetate was prepared immediately prior to use (13.6 mg, 80 μmol, AgOAc was dissolved in 2 mL CF_3CO_2D). 0.25 mL of the stock solution (1.7 mg, 10 μmol, 4 mol % relative to benzene of silver acetate) was then added to the vessel such that a total of 25 equiv of CF_3CO_2D was delivered relative to benzene, and the solution was stirred for 1 min. Benzene (23.2 μL, 0.26 mmol), stored over 4 Å molecular sieves, was then added. The reaction vessel was sealed and completely submerged in a preheated oil bath, and the mixture was heated with vigorous stirring for the appropriate time. At the end of the reaction, the vessel was cooled to room temperature, and the reaction mixture was filtered through a plug of Celite and washed with ethyl acetate (2 mL) into a 20 mL scintillation vial. A saturated aqueous solution of potassium carbonate (2 x 1 mL) was added carefully to the vial to quench the residual acid. The organic layer was separated and diluted to afford a 12.8 mM solution of benzene in EtOAc (~1 mg/mL), which was analyzed by GCMS.

CH_4/ CF_3CO_2D H/D exchange:

All glassware and stir bars were treated with aqua regia, washed with copious amounts of water and acetone, and dried before each use. A 7 mL glass Schlenk tube with 1.6 mm walls capable of sustaining pressures up to 200 psi equipped with a resealable Teflon stopcock and sidearm 14/20 female adaptor was attached to a 50 mL bulb equipped with a screw cap septum, a 14/20 male adaptor, and a gas/vacuum inlet. The Schlenk tube was charged with catalyst (0.02 mmol, 0.01 equiv, 1 mol %) in D_2SO_4 (1 mL, 20 mmol, 10 equiv). The entire system was then degassed by three freeze-pump-thaw cycles. The 50 mL bulb was backfilled with ultra pure methane (2.0 mmol, 1.0 equiv) three times to 1 atm at room temperature. The Schlenk tube was submerged in liquid N_2 and then

opened to the methane filled bulb. The methane condensed into the reaction vessel for over 10 min. After the Schlenk tube was resealed and warmed to room temperature, it was submerged up to the stopcock channel in a 200 ºC oil bath for 18 h. At the end of the reaction, the reaction vessel was cooled to room temperature. The gas was re-expanded in the same 50 mL bulb and analyzed by GC-MS using a GS-CarbonPLOT column obtained from Agilent Technologies. The % deuterium incorporation was defined as the percent of C–H bonds converted to C–D bonds. Turnover numbers (TON's) are calculated as mol D incorporated per mol of catalyst. Reported values have been corrected for the background reaction in the presence of AgCl, which is formed *in situ*. The reported TON is the average of at least two trials. The error associated with deconvolution is 5%.

2.7 Characterization

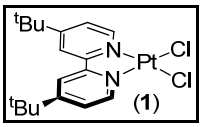

(**1**)

Complex **1** was prepared from 4,4'-di-*tert*-butylbipyridine (Aldrich) and *cis*-$(Me_2SO)_2Pt(Cl)_2$[44] using the procedure of Vicente and coworkers.[45] The ^{1}H NMR spectrum of **1** matched that reported in the literature. In addition, the purity of samples of **1** used for catalysis was confirmed by elemental analysis. Anal. calcd. for $C_{18}H_{24}Cl_2N_2Pt$: C, 40.46; H, 4.53; N, 5.24; Found: C, 40.34; H, 4.51; N, 5.17.

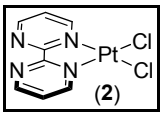

(**2**)

Complex **2** was prepared from bipyrimidine (Aldrich) and *cis*-$(Me_2SO)_2Pt(Cl)_2$[44] following the procedure of Neumann and coworkers.[46] The ^{1}H NMR spectrum of **2** matched that reported in the literature. In addition, the purity of samples of **2** used for catalysis was confirmed by elemental analysis. Anal. calcd. for $C_8H_6Cl_2N_4Pt$: C, 22.65; H, 1.43; N, 13.21; Found: C, 22.83; H, 1.32; N; 13.16.

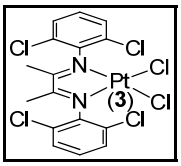

The diimine ligand[47] (115 mg, 0.31 mmol) and *cis*-$(Me_2SO)_2Pt(Cl)_2$[44] (100 mg, 0.24 mmol) were dissolved in acetone (10 mL) in a 20 mL scintillation vial. The vial was sealed with a Teflon-lined cap, and the reaction mixture was heated to 70 ºC for 4 h. During heating, the mixture changed color from yellow to red, and a reddish-brown precipitate was observed. The reaction was filtered while still hot, and the reddish-brown precipitate was collected and dried under vacuum to afford **3** (32.9 mg, 22% yield). ^{1}H NMR (400 MHz, DMF-d_7): δ 7.73 (d, J = 8 Hz, 4H), 7.55 (t, J = 8 Hz, 2H), 2.02 (s, 6H). ^{13}C NMR (100 MHz, DMF-d_7): δ 182.83, 140.42, 130.63, 128.84, 128.76, 20.08. The purity of samples of **3** used for catalysis was confirmed by elemental analysis. Anal. calcd. for $C_{16}H_{12}Cl_6N_2Pt$: C, 30.02; H, 1.89; N, 4.38; Found: C, 30.00; H, 1.83; N, 4.33.

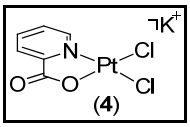

Complex **4** was prepared from picolinic acid (Fluka) and K_2PtCl_4 (Pressure Chemical) using a modification of the procedure reported by Annibale and coworkers.[48] After 4 h at 70 ºC the reaction had not gone to completion; therefore, it was stirred at 70 ºC for a total of 14 h. A workup analogous to that reported in the literature[48] afforded **4** in 21% yield. ^{1}H NMR (400 MHz, DMF-d_7): δ 9.25 (d w/Pt satellites, J_{Pt-H} = 15.6 Hz, J = 5 Hz, 1H), 8.28 (m, 1H), 7.77-7.69 (multiple peaks, 2H). ^{13}C NMR (100 MHz, DMF-d_7): δ 175.63, 150.59, 146.38, 139.19, 128.76, 127.12. ^{195}Pt NMR (100 MHz, DMF-d_7): δ –1598.45. HRMS-electrospray (m/z): $[M - K]^-$ calcd for $C_6H_4Cl_2NO_2Pt$, 387.9268; Found, 387.9258. Anal. calcd. for $C_6H_4Cl_2NO_2PtK$: C, 16.87; H, 0.94; N, 3.28; Found: C, 18.30; H, 1.24; N, 3.92; Cl, 16.75. The elemental analysis for this complex was consistently elevated in carbon and nitrogen, even after multiple recrystallizations. This

appears to result from residual DMF (from recrystallization). Numerous attempts to prepare analytically pure samples of **4** were unsuccessful.

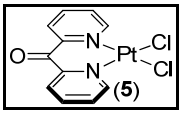

cis-$(Me_2SO)_2Pt(Cl)_2$[44] (36 mg, 0.11 mmol, 1.0 equiv) was dissolved in CH_3OH (13 mL) under an inert atmosphere. This solution was heated to 60 ºC, and then 2,2'-dipyridyl ketone (Aldrich) (20 mg, 0.11 mmol, 1.0 equiv) was added. The reaction was refluxed overnight and then cooled to room temperature. The volume was reduced to 2 mL, resulting in the precipitation of a light yellow solid. The precipitate was collected, washed with Et_2O (3 x 5 mL), and dried under vacuum to afford **5** as a yellow solid (25 mg, 51% yield). ^{1}H NMR (500 MHz, DMSO-d_6): δ 9.13 (m, 1H), 8.38 (m, 1H), 8.16 (m, 1H), 7.88 (m, 1H). ^{13}C NMR (100 MHz, DMSO-d_6): δ 185.92, 153.90, 149.85, 141.63, 130.02, 127.30. IR (KBr pellet, cm^{-1}): 1681 (s). The purity of samples of **5** used for catalysis was confirmed by elemental analysis. Anal. calcd. for $C_{11}H_8Cl_2N_2OPt$: C, 29.35; H, 1.79; N, 6.22; Found: C, 29.15; H, 1.92; N, 6.22.

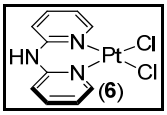

Complex **6** was prepared from 2,2'-dipyridyl amine (Aldrich) and *cis*-$(Me_2SO)_2Pt(Cl)_2$[44] following the procedure of Tu and coworkers.[49] ^{1}H NMR (400 MHz, DMSO-d_6): δ 11.07 (s, 1H), 8.78 (m, 2H), 7.97 (m, 2H), 7.27 (m, 1H), 7.11 (m, 1H). ^{13}C NMR (100 MHz, DMSO-d_6) δ 150.59, 150.14, 141.04, 119.58, 114.29. The purity of samples of **6** used for catalysis was confirmed by elemental analysis. Anal. calcd. for $C_{10}H_9Cl_2N_3Pt$: C, 27.67; H, 2.07; N, 9.61; Found: C, 27.72; H, 2.10; N, 9.79.

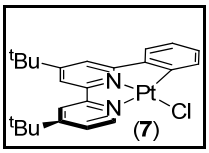

(**7**)

Complex **7** was prepared from 6-phenyl-4,4'-di-*tert*-butylbipyridine[50] and K_2PtCl_4 (Pressure) in glacial acetic acid following the procedure of Periana.[43] The ^1H NMR spectrum of **7** matched that reported in the literature. In addition, the purity of samples of **7** used for catalysis was confirmed by elemental analysis. Anal. calcd for $C_{25}H_{30}ClN_2Pt$: C, 50.22; H, 4.74; N, 4.88; Found: C, 49.96; H, 4.87; N, 4.86.

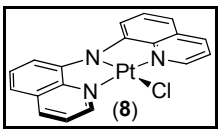

(**8**)

Complex **8** was prepared from bis-quinoline amine (BQAH)[51] and $(COD)PtCl_2$ (Strem) following the procedure of Peters.[51] The ^1H NMR spectrum of **8** matched that reported in the literature. In addition, the purity of samples of **8** used for catalysis was confirmed by elemental analysis. Anal. calcd for $C_{18}H_{12}Cl_2N_3Pt$: C, 43.17; H, 2.42; N, 8.39; Found: C, 42.76; H, 2.24; N, 8.11

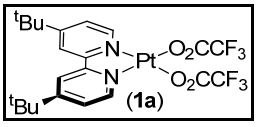

(**1a**)

Complex **1** (100 mg, 0.185 mmol) and AgOAc (Aldrich) (61.8 mg, 0.370 mmol) were dissolved in trifluoroacetic acid (10 mL), and the resulting solution was stirred at room temperature for 1 h. The reaction mixture was filtered through a plug of Celite to remove AgCl, and the filtrate was then concentrated by rotary evaporation. The resulting yellow oil was taken up in CH_2Cl_2, and Et_2O was added to precipitate an off-white powder. This solid was collected by filtration and dried under vacuum to afford **1a** (93.2 mg, 80% yield). ^1H NMR (400 MHz, acetone-d_6): δ 8.64 (d, J = 2 Hz, 2H), 8.41 (d, J = 6 Hz, 2H), 7.90 (dd, J = 6 Hz, 2 Hz, 2H), 1.47 (s, 18H). ^{13}C NMR (100 MHz, acetone-d_6): δ 165.89, 161.28 (q, $J_{C\text{-}F}$ = 36 Hz), 156.84, 148.37, 124.63, 121.63, 115.09 (q, $J_{C\text{-}F}$ = 290 Hz), 35.96,

29.29. ^{19}F NMR (400 MHz, acetone-d_6): δ –75.08. IR (KBr pellet, cm^{-1}) 1722 (s). The purity of samples of **1a** used for catalysis was confirmed by elemental analysis. Anal. calcd. for $C_{18}H_{24}Cl_2N_2Pt$: C, 38.32; H, 3.51; N, 4.06; Found: C, 38.22; H, 3.39; N, 4.05.

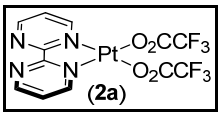

(**2a**)

Complex **2** (30 mg, 0.071 mmol) and AgOAc (Aldrich) (23.6 mg, 0.141 mmol) were dissolved in trifluoroacetic acid (5 mL), and the resulting solution was stirred at room temperature for 1 h. The reaction mixture was filtered through a plug of Celite to remove AgCl, and the filtrate was then concentrated by rotary evaporation. The resulting yellow oil was taken up in MeCN, and Et_2O was added to precipitate a yellow powder. This solid was collected by filtration and dried under vacuum to afford **2a** (29.2 mg, 75% yield). The ^1H NMR spectrum of **2a** matched that reported in the literature.[43] In addition, the purity of samples of **2a** used for catalysis was confirmed by elemental analysis. Anal. calcd. for $C_{18}H_{24}Cl_2N_2Pt$: C, 24.88; H, 1.04; N, 9.67; Found: C, 24.59; H, 1.06; N, 9.51.

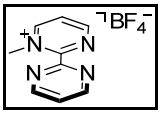

Under N_2, bipyrimidine (bpym) (100 mg, 0.63 mmol, 1.0 equiv) was dissolved in CH_2Cl_2 (13 mL, dried over 4 Å molecular sieves). The mixture was cooled to –5 ^oC in an ice bath. $[Me_3O]BF_4$ (103 mg, 0.69 mmol, 1.1 equiv) was then added as a solid, and the resulting mixture was stirred for 2 h at –5 ºC. A white precipitate slowly formed that was subsequently filtered. The crude product was washed with CH_2Cl_2 (2 x 5 mL) and Et_2O (3 x 5 mL) to remove unreacted bipyrimidine. The resulting mixture of mono- and dimethylated bipyrimidine was purified by recrystallization from MeOH/Et_2O at –35 ºC to give the product as a white powder (78 mg, 48% yield). This product was unstable; therefore, it was stored at –15 ºC

and used for subsequent reactions within 12 h. ^{1}H NMR (500 MHz, CD_3CN): δ 9.54 (d, *J* = 4.9 Hz, 1H), 9.13 (d, *J* = 4.9 Hz, 2H), 9.09 (d, *J* = 6.6 Hz, 1H), 8.26 (app t, *J* = 5.6 Hz, 1H), 7.78 (app t, *J* = 4.9 Hz, 1H), 4.39 (s, 3H). HRMS (EI) Calcd for $C_9H_9N_4$: 173.0827. Found: 173.0819.

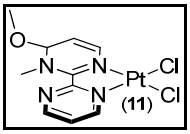

(**11**)

Under an inert atmosphere, $(DMSO)_2PtCl_2$ (74.2 mg, 0.22 mmol, 1.0 equiv) was dissolved in CH_3OH (27 mL). This mixture was heated to 60 ºC, and then [*N*-Me(bpym)]BF_4 (58 mg, 0.22 mmol, 1.0 equiv) was added. The reaction was refluxed overnight and then cooled to room temperature, resulting in the precipitation of a pale yellow solid. The precipitate was collected, washed with Et_2O (3 x 5 mL), and dried under vacuum to afford the product as a yellow solid (77 mg, 75% yield). ^{1}H NMR (500 MHz, CD_3CN): δ 9.84 (dd, *J* = 5.7, 1.9 Hz, 1H), 9.09 (dd, *J* = 4.5, 1.9 Hz, 1H), 7.79 (d, *J* = 7.6 Hz, 1H), 7.68 (app t, *J* = 4.5 Hz, 1H), 5.69 (dd, *J* = 7.3, 5.0 Hz, 1H), 5.49 (d, *J* = 5.0 Hz, 1H), 3.89 (s, 3H), 3.22 (s, 3H). ^{13}C NMR (100 MHz, CD_3CN): δ 161.9, 157.2, 155.3, 155.2, 133.4, 123.9, 106.7, 85.8, 51.6, 42.0. IR (KBr pellet, cm^{-1}): 1562 (s). Anal. Calcd. for $C_{10}H_{12}Cl_2N_4OPt$: C, 25.54; H, 2.57; N, 11.92; Found: C, 25.69; H, 2.51; N, 11.82.

2.8 Reference

[1] Goldshleger, N. F.; Eskova, V. V.; Shilov, A. E.; Shteinmann, A. A. *Zh. Fiz. Khim.* **1972**, *46*, 1353.

[2] Stahl, S. S.; Labinger, J. A.; Bercaw, J. E. *Angew. Chem., Int. Ed.* **1998**, *37*, 2180.

[3] Periana, R. A.; Taube, D. J.; Gamble, S.; Taube, H.; Satoh, T.; Fujii, H. *Science* **1998**, *280*, 560.

[4] Conley, B. L.; Tenn, W. J., III; Young, K. J. H.; Ganesh, S. K.; Meier, S. K.; Ziatdinov, V. R.; Mironov, O.; Oxgaard, J.; Gonzales, J.; Goddard, W. A., III; Periana, R. A. *J. Mol. Catal., A.*, **2006**, *251*, 8.

[5] (a) Holtcamp, M. W.; Labinger, J. A.; Bercaw, J. E. *J. Am. Chem. Soc.* **1997**, *119*, 848. (b) Wick, D. D.; Goldberg, K. I. *J. Am. Chem. Soc.* **1997**, *119*, 10235. (c) Holtcamp, M. W.; Henling, L. M.; Day, M. W.; Labinger, J. A.; Bercaw, J.E. *Inorg. Chim. Acta* **1998**, *270*, 467. (d) Johansson, L.; Ryan, O. B.; Tilset, M. *J. Am. Chem. Soc.* **1999**, *121*, 1974. (e) Johansson, L. Tilset, M.; Labinger, J. A.; Bercaw, J. E. *J. Am. Chem. Soc.* **2000**, *122*, 10846. (f) Heiberg, H.; Johansson, L.; Gropen, O.; Ryan, O. B.; Swang, O.; Tilset, M. *J. Am. Chem. Soc.* **2000**, *122*, 10831. (g) Zhong, H. A.; Labinger, J. A.; Bercaw, J. E. *J. Am. Chem. Soc.* **2001**, *124*, 1378. (h) Thomas, J. C.; Peters, J. C. *J. Am. Chem. Soc.* **2001**, *123*, 5100. (i) Johansson, L.; Ryan, O. B.; Rømming, C.; Tilset, M. *J. Am. Chem. Soc.* **2001**, *123*, 6579. (j) Iverson, C. N.; Carter, C. A.; Baker, R. T.; Scollard, J. D.; Labinger, J. A.; Bercaw, J. E. *J. Am. Chem. Soc.* **2003**, *125*, 12674. (k) Gerdes, G.; Chen, P. *Organometallics* **2003**, *22*, 2217. (l) Driver, T. G.; Day, M. W.; Labinger, J. A.; Bercaw, J. E. *Organometallics* **2005**, *24*, 3644. (m) Thomas, C. M.; Peters, J. C. *Organometallics*, **2005**, *24*, 5858. (n) Karshtedt, D.; McBee, J. L.; Bell, A. T.; Tilley, T. D. *Organometallics*, **2006**, *25*, 1801. (o) Owen, J. S.; Labinger, J. A.; Bercaw, J. E. *J. Am. Chem. Soc.* **2006**, *128*, 2005. (p) Driver, T. G.; Williams, T. J.; Labinger, J. A.; Bercaw, J. E. *Organometallics*, **2007**, *26*, 294. (q) Williams, T. J.; Caffyn, A. J. M.; Hazari, N.; Oblad, P. F.; Labinger, J. A.; Bercaw, J. E. *J. Am. Chem. Soc.* **2008**, *130*, 2418.

[6] Zhang, F.; Kirby, C. W.; Hairsine, D. W.; Jennings, M. C.; Puddephatt, R. J. *J. Am. Chem. Soc.* **2005**, *127*, 14196.

[7] Ong, C. M.; Jennings, M. C.; Puddephatt, R. J. *Organometallics* **2004**, *23*, 1396.

[8] For a review of C–H activation at Pt(II), see: Lersch, M.; Tilset, M. *Chem. Rev.* **2005**, *105*, 2471 and references therein.

[9] Stahl, S. S.; Labinger, J. A.; Bercaw, J. E.; *J. Am. Chem. Soc.* **1996**, *118*, 5961.

[10] (a) Hodges, R. J; Webster, D. E.; Wells, P. B *J. Chem. Soc., Chem. Comm.* **1971**, 462. (b) Hodges, R. J; Webster, D. E.; Wells, P. B. *J. Chem. Soc. A* **1971**, 3230. (c) Hodges, R. J; Webster, D. E.; Wells, P. B. *J. Chem. Soc., Dalton Trans.* **1972**, 2571.

[11] Ziatdinov, V. R.; Oxgaard, J.; Mironov, O. A.; Young, K. J. H.; Goddard, W. A., III; Periana, R. A. *J. Am. Chem. Soc.* **2006**, *128*, 7404.

[12] Young, K. J. H.; Meier, S. K.; Gonzales, J. M.; Oxgaard, J.; Goddard, W. A., III; Periana, R. A. *Organometallics* **2006**, *25*, 4734.

[13] Gerdes, G.; Chen, P. *Organometallics* **2004**, *23*, 3031.

[14] Kloek, S. M.; Goldberg, K. I. *J. Am. Chem. Soc.* **2007**, *129*, 3460.

[15] Harkins, S. B.; Peters, J. C.; *Organometallics*, **2002**, *21*, 1753.

[16] Ong, C. M.; Jennings, M. C.; Puddephatt, R. J. *Can. J. Chem.* **2003**, *81*, 1196.

[17] Complex **1**: Vicente, J.; Cazlez-Herrero, P.; Prez-Cadenas, M.; Jones, P. G.; Bautista, D. *Inorg. Chem.* **2007**, *46*, 4718. Complex **2**: Neumann, R.; Bar-Nahum, I.; Khenkin, A. M. *J. Am. Chem. Soc.* **2004**, *126*, 10236. Complex **3**: See supporting information. Complex **4**: Annibale, G.; Cattalini, L.; Chessa, G.; Marangoni, G.; Pitteri, B.; Tobe, M. L. *Gazz. Chim. Ital.* **1985**, *115*, 279. Complex **5**: Rauterkus, M. J.; Krebs, B. *Angew. Chem., Int. Ed.* **2004**, *43*, 1300. Complex **6**: Tu, C.; Wu, X.; Liu, Q.; Wang, X.; Xu, Q.; Guo, Z. *Inorg. Chim. Acta.* **2004**, *357*, 95. Complex **7**: ref. [12]. Complex **8**: Peters, J. C.; Harkins, S. B.; Brown, S. D.; Day, M. W. *Inorg. Chem.* **2001**, *40*, 5083.

[18] Complex **4** was isolated with 0.05 mol % residual K_2PtCl_4 as well as some residual DMF from recrystallization. The identity of the complex was confirmed by HRMS.

[19] Wong-Foy, A. G.; Henling, L. M.; Day, M.; Labinger, J. A.; Bercaw, J. E.; *J. Mol. Cat. A.* **2002**, *189*, 3.

[20] Corbern, R.; Sana, M.; Peris, E. *J. Am. Chem. Soc.* **2006**, *128*, 3974.

[21] The raw H/D exchange data for all catalytic transformations with TFA-d_1 was corrected by subtraction of the % deuterium incorporation observed in the background reaction between TFA-d_1 and C_6H_6 in the presence of AgCl.

[22] Use of AgTFA yielded identical results; however, AgOAc was used as it was on hand and moderately less expensive.

[23] The apparently lower TONs observed at extended times are an artifact of subtraction of the AgCl background reaction at the respective time points.

[24] K_2PtCl_4 and $PtCl_2$ also catalyze this reaction, but the addition of a mineral acid is required. See ref. 10 for details.

[25] Complexes **7** and **8** showed negligible activity for H/D exchange with CD_3CO_2D or TFE-d_3 under our standard conditions.

[26] (a) Kua, J.; Xu, X.; Periana, R. A. Goddard, W. A. *Organometallics* **2002**, *21*, 511. (b) Xu, X.; Kua, J.; Periana, R. A.; Goddard, W. A. *Organometallics* **2003**, *22*, 2057. (c) Ahlquist, M.; Periana, R. A.; Goddard, W. A. *Chem. Commun.* **2009**, 2373.

[27] Paul, A.; Musgrave, C. B. *Organometallics* **2007**, *26*, 793.

[28] (a) Gilbert, T. M.; Hristov, I.; Ziegler, T. *Organometallics* **2001**, *20*, 1183. (b) Hristov, I. H.; Ziegler, T. *Organometallics* **2003**, *22*, 1668.

[29] Black, M. L. *J. Phys. Chem.* **1955**, *59*, 670.

[30] For examples of other metal complexes containing ligands with quaternized nitrogen substituents, see: (a) Johnson, C. R.; Shepherd, R. E. *Inorg. Chem.* **1983**, *22*, 2439. (b) Wishart, J. F.; Bino, A.; Taube, H. *Inorg. Chem.* **1986**, *25*, 3318. (c) Kaim, W.; Matheis, W. *Chem. Ber.* **1990**, *123*, 1323. (d) Matheis, W.; Kaim, W. *J. Chem. Soc., Faraday Trans.* **1990**, *86*, 3337. (e) Matheis, W.; Poppe, J.; Kaim, W.; Zaliz, S. *J. Chem. Soc., Perkin Trans. 2* **1994**, 1923. (f) Waldhör, E.; Kaim, W.; Olabe, J. A.; Slep, L. D.; Fiedler, J. *Inorg. Chem.* **1997**, *36*, 2969. (g) Coe, B. J.; Chamberlain, M. C.; Essex-Lopresti, J. P.; Gaines, S.; Jeffery, J. C.; Houbrechts, S.; Persoons, A. *Inorg. Chem.* **1997**, *36*, 3284. (h) Fujihara, T.; Wada, T.; Tanaka, K. *Inorg. Chim. Acta* **2004**, *357*, 1205.

[31] Seidel, S.; Seppelt, K. *Inorg. Chem.* **2003**, *42*, 3846.

[32] Price, J. H; Williamson, A. N; Schramm, R. F.; Wayland, B. B. *Inorg. Chem.* **1972**, *11*, 1280.

[33] K_{eq} for protonation of coordinated bpym in TFA should be greater than two orders of magnitude lower than in H_2SO_4. The pK_a of H_2SO_4 is –3, while the pK_a of trifluoroacetic acid is –0.3 in H_2O.

[34] Ernst, S.; Kaim, W. *J. Am. Chem. Soc.* **1986**, *108*, 3578.

[35] Negligible H/D exchange was observed between CH_4 and CF_3CO_2D with pre-catalyst **2** or **10**.

[36] Complex **2a** was also the sole inorganic product observed when **2** was heated to 150 ºC for 15 min in TFA-d_1 in the presence of 2 equiv of AgOAc.

[37] Complex **10** is expected to be generated *in situ* by protonation of the OCH_3 group by D_2SO_4 followed by an S_N1 reaction to aromatize the *N*-CH_3-bpym$^+$ ligand.

[38] Young, K. J. H.; Meier, S. K.; Gonzales, J. M.; Oxgaard, J.; Goddard, W. A.; Periana, R. A. *Organometallics* **2006**, *25*, 4734.

[39] Notably, under these conditions, all three of the catalytic reaction solutions remained homogeneous, and no Pt black or other precipitate was observed after 24 h.

[40] Turnover numbers were calculated as: mol of D incorporated per mol of catalyst minus the background D incorporation in the absence of catalyst

[41] Emmert, M. H.; Villalobos, J. M.; Gary, J. B.; Sanford, M. S. *Angew. Chem. Int. Ed.* **2010**, *49*, 5884-5886.

[42] Price, J. H; Williamson, A. N; Schramm, R. F.; Wayland, B. B. *Inorg. Chem.* **1972**, *11*, 1280.

[43] Young, K. J. H.; Meier, S. K.; Gonzales, J. M.; Oxgaard, J.; Goddard, W. A., III; Periana, R. A. *Organometallics* **2006**, *25*, 4734.

[44] Hill, G. S.; Irwin, M. J.; Levy, C. J.; Rendina, L. M.; Puddephatt, R. J. *Inorg. Synth.* **1998**, *32,* 149.

[45] Vicente, J.; Cazlez-Herrero, P.; Prez-Cadenas, M.; Jones, P. G.; Bautista, D. *Inorg. Chem.* **2007**, *46*, 4718.

[46] Neumann, R.; Bar-Nahum, I.; Khenkin, A. M. *J. Am. Chem. Soc.* **2004**, *126*, 10236.

[47] Gerdes, G.; Chen, P. *Organometallics*, **2003**, *22*, 2217.

[48] Annibale, G.; Cattalini, L.; Chessa, G.; Marangoni, G.; Pitteri, B.; Tobe, M. L. *Gazz. Chim. Ital.* **1985**, *115*, 279.

[49] Tu, C.; Wu, X.; Liu, Q.; Wang, X.; Xu, Q.; Guo, Z. *Inorg. Chim. Acta.*, **2004**, *357*, 95.

[50] Lu, W.; Mi, B-X.; Chan, M. C. W.; Hui, Z.; Che, C. M.; Zhu, N.; Lee, S. T. *J. Am. Chem. Soc.* **2004**, *126*, 4958.

[51] Peters, J. C.; Harkins, S. B.; Brown, S. D.; Day, M. W. *Inorg. Chem.* **2001**, *40*, 5083.

Chapter 3: Structure Activity Relationship of Pt-Catalyzed C–H Activation

3.1 Introduction

The development of Pt-based catalysts for the oxidation of alkanes/arenes (R–H) to alcohols has been an important area of research for nearly 40 years. Pioneering studies by Shilov in the early 1970's demonstrated that a combination of Pt^{II} and Pt^{IV} salts promotes the oxidation of methane to methanol.[1] Subsequent work has sought to improve this system through variation of the ancillary ligands at Pt^{II}.[2] Carbon–hydrogen bond activation at Pt^{II} is believed to be a key step in Pt-catalyzed R–H oxidation, and has therefore been an important focus of recent studies.

One method for studying C–H activation involves Pt^{II}-catalyzed H/D exchange. H/D exchange is believed to proceed via intermediates directly relevant to those in catalytic R–H oxidation. As discussed in Chapter 2, we previously examined the catalytic activity of simple Pt^{II} salts and nitrogen ligated Pt^{II} complexes in an H/D exchange assay with C_6H_6 and several RCO_2D sources.[3] In each case the diimine Pt^{II} dichloride catalyst **1** exhibited high reactivity, with turnover frequencies an order of magnitude greater than the other top performing catalysts examined (Figure 3.1).

Figure 3.1. Diimine catalyst **1** exhibits enhanced C–H activation reactivity in standard H/D exchange assay.

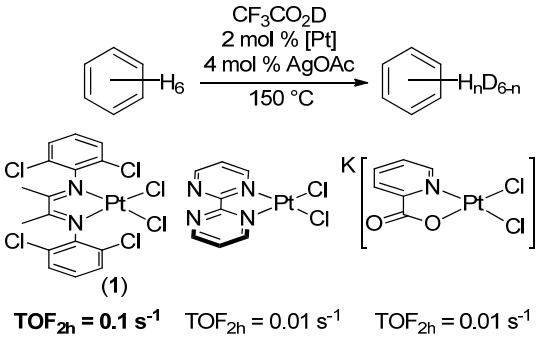

Diimines are particularly attractive ligands for catalyst design because they are highly modular. As such diimines have been used widely as model systems for stoichiometric studies of the mechanism of C–H activation in "Shilov" chemistry. In particular, work by Bercaw, Labinger, and Tilset has shown correlations between diimine structure and kinetic isotope effects, rate determining steps,[4] and formation and stability of intermediates in C–H activation at [(N~N)Pt(CH_3)(Solv)]X, where (N~N) is a diimine ligand (Scheme 3.1).[5,6,7] Although these studies have elegantly probed the fundamental reactivity of Pt-mediated C–H activation, the built in driving force of methane liberation deviates considerably from the proposed catalytic cycle for C–H oxidation reactions.[3]

Scheme 3.1. Stoichiometric studies of ligand effects on Pt-mediated C–H activation

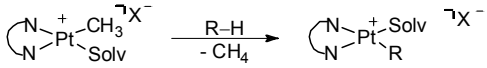

In the current work, we have examined the structure activity relationship of several different diimine Pt^{II} dichloride complexes using our previously published catalytic H/D exchange assay of C_6H_6 and RCO_2D. The chloride complexes were utilized because they are all conveniently available in a single step from readily available Pt^{II} precursors.[8] Importantly, this assay is conducted under acidic conditions very similar to those employed for many C–H functionalization

reactions.[2d,9] As a result, the observed trends have the potential to be directly relevant to catalytic C–H oxidation reactions. The effect of substitution at the *N*-aryl group, electron density at the metal, and presence of halogen substitution on the ligand have been examined in detail and are reported herein. This work was conducted in collaboration with an undergraduate summer research student Megan Cismesia. She developed optimized synthetic protocols for both diimine ligands and their platinum dichloride catalysts and conducted initial evaluations of turnover number at 2 and 24 h.

3.2 Results

We first investigated the impact of steric hindrance near the active site by studying a series of 2,6- and 3,5-disubstituted *N*-aryl diimines (**1**-**7**) (Figure 3.2). The initial rate of the H/D exchange reaction was measured for each catalyst in both CF_3CO_2D and CD_3CO_2D (Figure 3.3). Notably, in a few cases, the observed initial rates were fast relative to heat transfer from the oil bath resulting in a low estimate of the rate (Figure 3.3 (a) and (c), for example). The 2,6-dichlorodiimine Pt dichloride complex **1** exhibits dramatically higher reactivity than all other catalysts studied in CF_3CO_2D (Table 3.1, entry 1 vs entries 2-5). Both 2,6-disubstituted diimine Pt dichloride complexes **1** and **2** significantly outperform the 3,5-disubstituted diimine Pt dichloride analogs **3** and **4** in CD_3CO_2D (Table 3.1, entries 1 and 2 vs entries 3 and 4). These results indicate a large steric impact on catalyst reactivity in both solvents. In all cases the dichlorosubstituted complexes (**1** and **3**) exhibit faster rates than their analogous dimethyl complexes (**2** and **4**, respectively).

Figure 3.2. Diimine catalysts for H/D exchange of C_6H_6 and RCO_2D

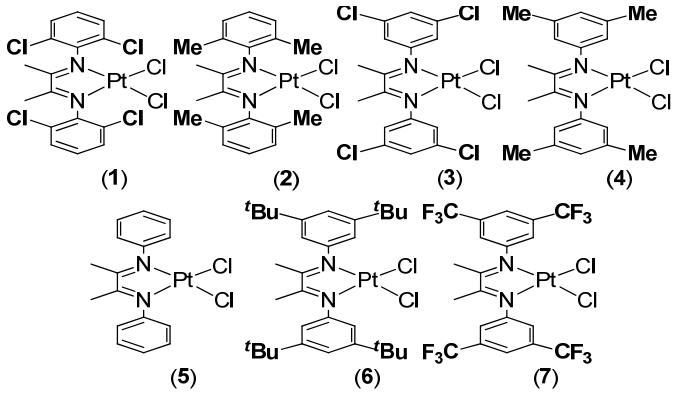

Figure 3.3. Representative plots of initial rates. (a) (**1**)-catalyzed H/D exchange in CF_3CO_2D (b) (**2**)-catalyzed H/D exchange in CF_3CO_2D (c) (**3**)-catalyzed H/D exchange in CD_3CO_2D (d) (**5**)-catalyzed H/D exchange in CD_3CO_2D

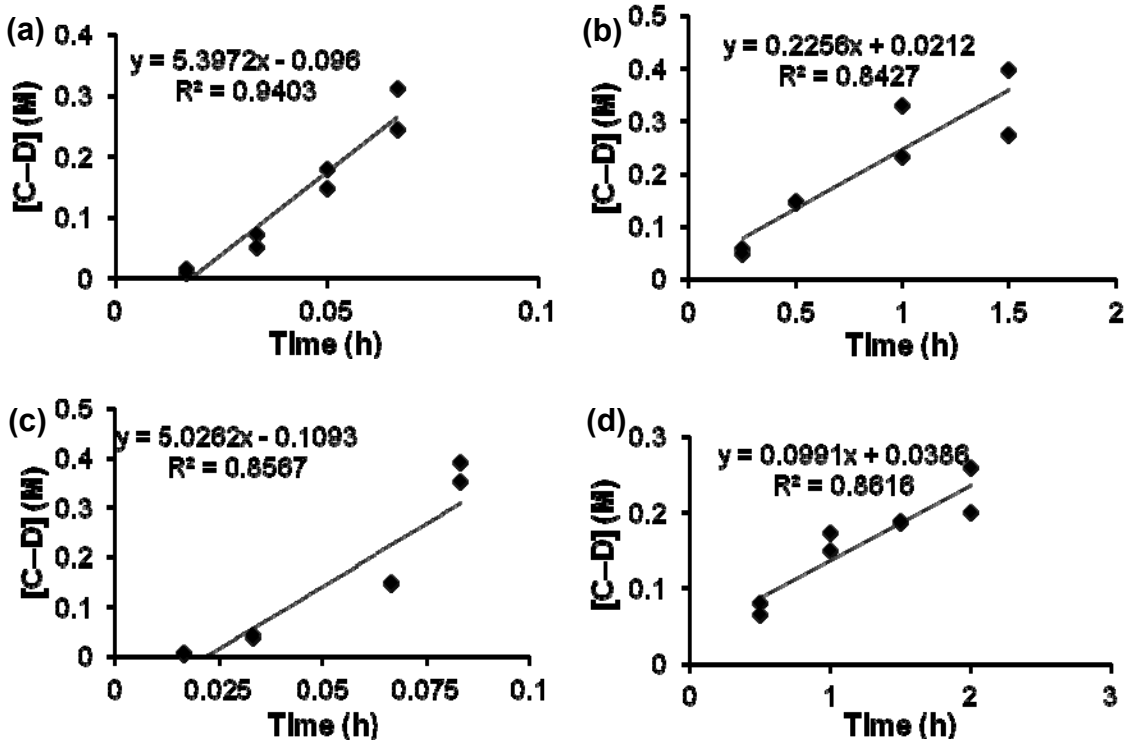

Conditions: (a) and (b): Pt^{II} catalyst (2 mol %, 5 μmol), benzene (23.2 μL, 0.26 mmol), AgOAc (1.7 mg, 10 μmol) in CF_3CO_2D (0.5 mL, 6.5 mmol, 25 equiv relative to benzene) at 150 ºC. (c) and (d): Pt^{II} catalyst (2 mol %, 5 μmol), benzene (23.2 μL, 0.26 mmol), $AgBF_4$ (1.9 mg, 10 μmol) in CD_3CO_2D (0.37 mL, 6.5 mmol, 25 equiv relative to benzene) at 150 ºC.

Table 3.1. Initial rate of H/D exchange between C_6H_6 and RCO_2D catalyzed by complexes **1**-**7.**

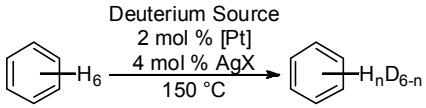

Entry	Catalyst	Initial rates (M/h)	
		CF_3CO_2D, AgOAc	CD_3CO_2D, $AgBF_4$
1	**1**	5.39	5.66
2	**2**	0.68	5.03
3	**3**	0.23	0.92
4	**4**	0.17	0.26
5	**5**	0.09	0.10

Based on these results, we hypothesized that the observed differences in activity might be due to differences in electron density at the metal center. We measured the electron density of the platinum center using two different methods. First, an experimental measurement of electron density was obtained from the CO stretching frequency of analogous Pt diimine complexes **8**-**14** (Figure 3.4). More electron-rich ligands donate more electron density into the carbonyl anti-bonding orbitals resulting in a lower observed stretching frequency. This metric has been used extensively in organometallic chemistry, including investigation of platinum diimine complexes.[4,10]

Figure 3.4. Diimine Pt methyl carbonyl complexes and their carbonyl stretching frequency in CH_2Cl_2.[4,10]

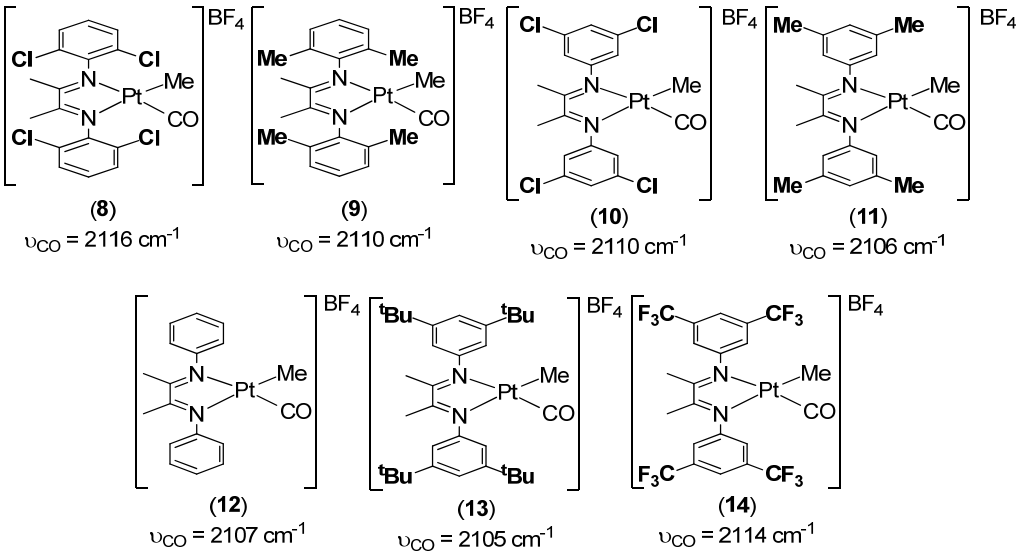

Second, density functional theory (DFT) and natural bond order (NBO) analysis were employed to computationally determine the natural charge of the Pt atom in complexes **1**-**7**. The geometry of complexes **1**-**7** were optimized using Gaussian 03 suite of programs.[11] All DFT calculations were performed with the B3LYP functional[12,13,14,15] along with the LanL2DZ basis set.[16,17,18] NBO analysis was then used to predict the natural charge at the platinum atom (Table 3.2).

Table 3.2. The natural charge at Pt for complexes **1**-**7**.

Catalyst	Natural Charge
1	0.773
2	0.742
3	0.730
4	0.744
5	0.745
6	0.736
7	0.744

With this data in hand, we then plotted the initial rates of Pt-catalyzed H/D exchange in CF_3CO_2D and CD_3CO_2D as a function of both CO stretching frequency of analogous complexes **8**-**14** (Figure 3.5) and the calculated natural charge of the Pt atom in complexes **1**-**7** (Figure 3.6). Under catalytic H/D exchange conditions, there is no correlation between the observed initial rate in CF_3CO_2D or CD_3CO_2D and either the carbonyl stretching frequency or Pt-atom natural charge.

Figure 3.5. Initial rates of H/D exchange between C_6H_6 and RCO_2D catalyzed by complexes **1**-**7** versus ν_{CO} of analogous complexes **8**-**14.**

(○ = 2,6-disubstituted, ■ = 3,5-disubstituted ▲ = unsubstituted)

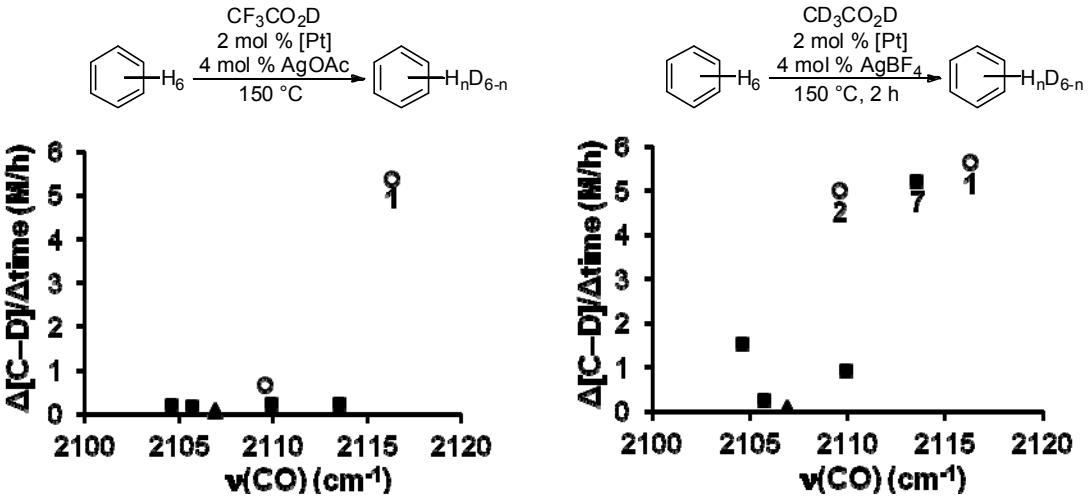

Figure 3.6. Initial rates of H/D exchange between C_6H_6 and RCO_2D catalyzed by complexes **1**-**7** versus the calculated natural charge of Pt**.**

(♦ = 2,6-disubstituted, ■ = 3,5-disubstituted ▲ = unsubstituted)

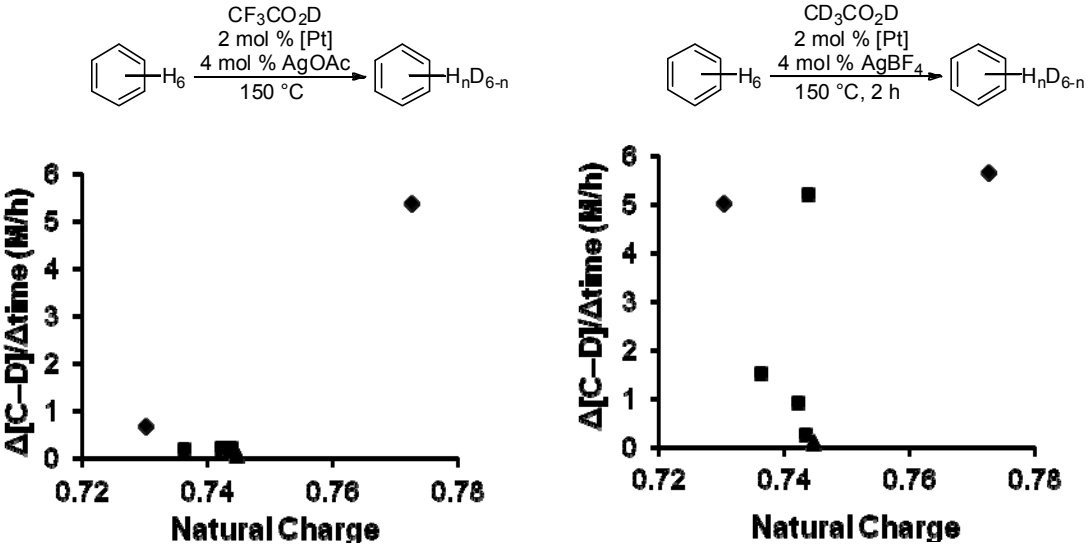

Notably, enhanced initial rates were observed in acetic acid for both 2,6-disubstituted diimine Pt dichloride catalysts **1** and **2** and the 3,5-bis(trifluoromethyl)substituted diimine Pt dichloride catalyst **7**. The suprising

reactivity of **7** led us to hypothesize that there may be a unique impact on reactivity in the presence of halogen substitution. In order to probe this effect, a new series of halogen substituted diimine Pt dichloride catalysts were prepared and their reactivity was evaluated for Pt-catalyzed H/D exchange between benzene and RCO_2D (**15**-**18**, Figure 3.7).

Figure 3.7. Diimine catalysts for H/D exchange between C_6H_6 and RCO_2D

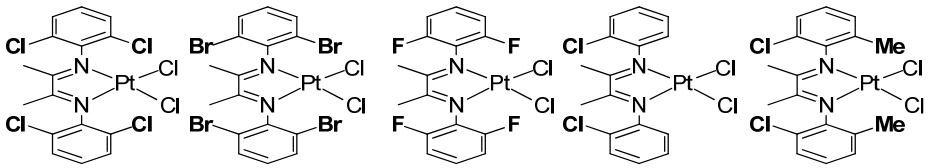

First, 2,6-dichloro, 2,6-dibromo-, and 2,6-difluorodiimine Pt^{II} dichloride complexes (**1**, **15**, and **16**, respectively) were evaluated as catalysts for H/D exchange between C_6H_6 and both CF_3CO_2D (Figure 3.8) and CD_3CO_2D (Figure 3.9) over 24 h. This study was carried out at 100 °C where the rate of H/D exchange is slow enough to easily distinguish trends in reactivity, and the results were compared to the 2,6-dimethyldiimine Pt^{II} dichloride complex **2**. With both deuterium sources, the reaction rate increased moving from methyl to halogen substitution. A large increase in rate was observed for chloro- and bromo-substituted diimines, whereas fluoro-subsitution only demonstrated a moderate increase in rate (Figures 3.8 and 3.9).

Figure 3.8. Turnover number for H/D exchange between C_6H_6 and CF_3CO_2D catalyzed by complexes **1**, **2**, **15**, and **16** as a function of time

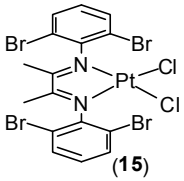

(**15**)

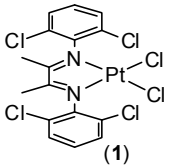

(**1**)

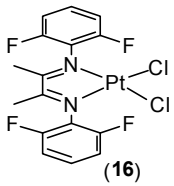

(**16**)

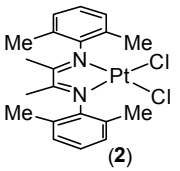

(**2**)

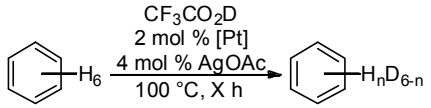

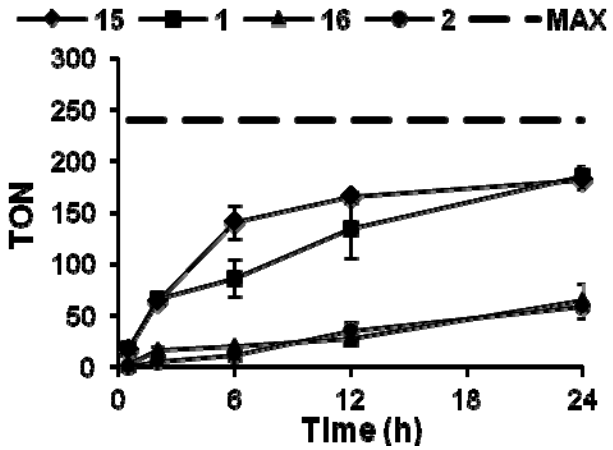

Conditions: Pt^{II} catalyst (2 mol %, 5 μmol), benzene (23.2 μL, 0.26 mmol), AgOAc (1.7 mg, 10 μmol) in CF_3CO_2D (0.5 mL, 6.5 mmol, 25 equiv relative to benzene) at 100 ºC.

Figure 3.9. Turnover number for H/D exchange between C_6H_6 and CD_3CO_2D catalyzed by complexes **1**, **2**, **15**, and **16** as a function of time

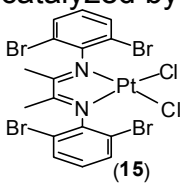

(**15**)

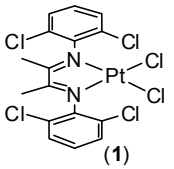

(**1**)

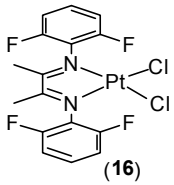

(**16**)

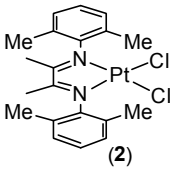

(**2**)

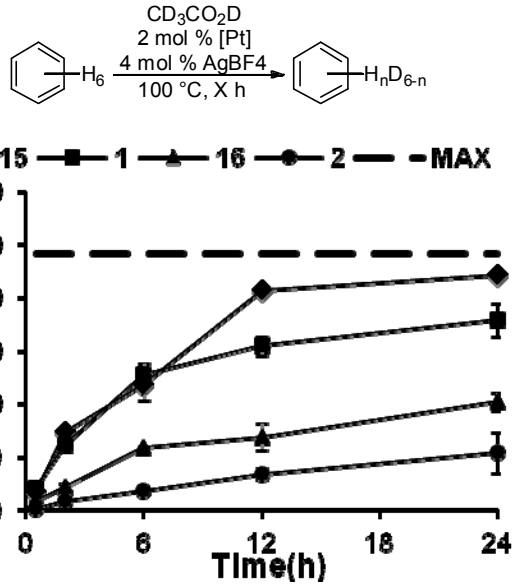

Conditions: Pt^{II} catalyst (2 mol %, 5 μmol), benzene (23.2 μL, 0.26 mmol), $AgBF_4$ (1.9 mg, 10 μmol) in CD_3CO_2D (0.37 mL, 6.5 mmol, 25 equiv relative to benzene) at 100 ºC.

To further probe the effect of halogen substitution, we sought to deconvolute the steric impact of substitution at the 2 and 6 positions of the *N*-aryl group and the enhanced reactivity of halogen substitution. We therefore synthesized two additional complexes and examined their reactivity using the H/D exchange assay in both CF_3CO_2D and CD_3CO_2D. The first complex contains mono-substituted aryl rings with only chloro-substitution at the 2 position (**17**, Figure 3.7). The second complex features a methyl group in the 2 position and a chloride in the 6 position of the *N*-aryl group (**18**, Figure 3.7). As seen in Figures 3.10 and 3.11, the observed order of reactivity is **1** > **18** > **17** with both deuterium sources.

Figure 3.10. Turnover number for H/D exchange between C_6H_6 and CF_3CO_2D catalyzed by complexes **1**, **17**, and **18** as a function of time

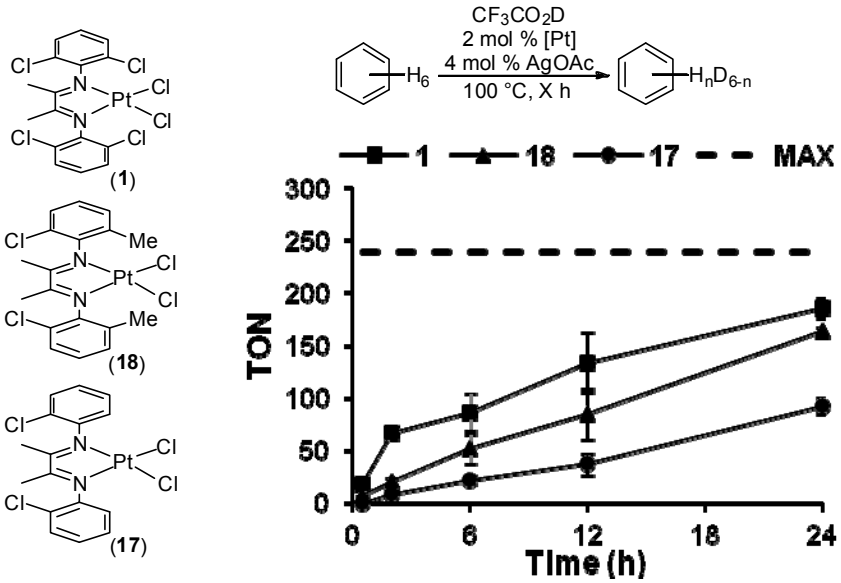

Conditions: Pt^{II} catalyst (2 mol %, 5 μmol), benzene (23.2 μL, 0.26 mmol), AgOAc (1.7 mg, 10 μmol) in CF_3CO_2D (0.5 mL, 6.5 mmol, 25 equiv relative to benzene) at 100 ºC.

Figure 3.11. Turnover number for H/D exchange between C_6H_6 and CD_3CO_2D catalyzed by complexes **1**, **17**, and **18** as a function of time

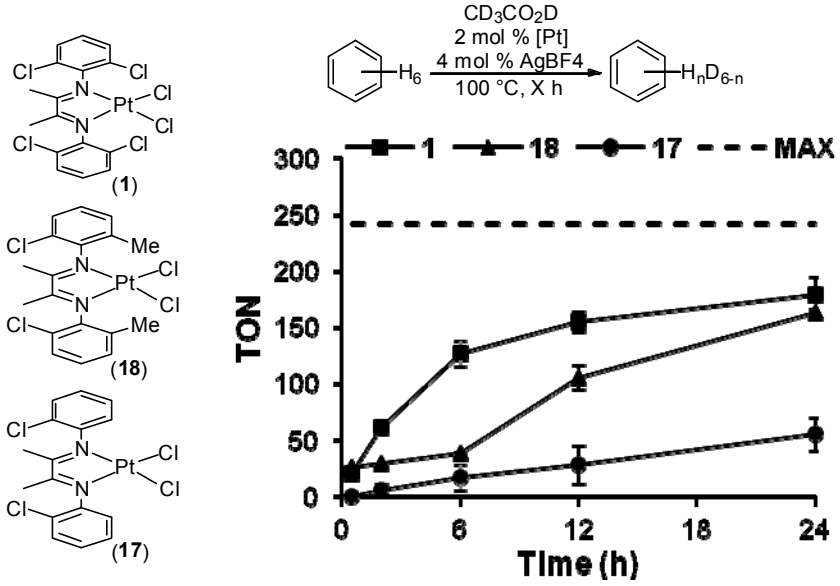

Conditions: Pt^{II} catalyst (2 mol %, 5 μmol), benzene (23.2 μL, 0.26 mmol), $AgBF_4$ (1.9 mg, 10 μmol) in CD_3CO_2D (0.37 mL, 6.5 mmol, 25 equiv relative to benzene) at 100 ºC.

3.3 Discussion

Our investigations revealed a significant correlation between structure and activity of diimine Pt^{II} dichloride catalysts for H/D exchange between C_6H_6 and RCO_2D. Pt catalysts bearing 2,6 disubstituted diimine ligands exhibited enhanced rates compared to both 3,5-disubstituted and unsubstituted ligands (Table 3.1). There is no clear correlation between reactivity and the electron density of the metal center, as measured by both the carbonyl stretching frequencies of analogous complexes **8**-**14** (Figure 3.5) and the natural charge of Pt in complexes **1**-**7** calculated with NBO analysis (Figure 3.6). However, a special enhancement in reactivity was observed when halogens were present on the *N*-aryl group.

Intriguingly, different reactivity patterns were observed in stoichiometric C–H activation reactions at Pt diimine organometallic complexes. Zhong and Bercaw

reported an extensive investigation of diimine ligand effects in the stoichiometric C–H activation of benzene by diimine Pt^{II} monomethyl complexes (**19**-**23,** Figure 3.12).[4] In particular they examined the electronic effect of the ligand by plotting the log of the rate of C–H activation versus the carbonyl stretching frequency of analogous complexes **24**-**28** (Figure 3.12). Diimines with 3,5-disubstitution (**19**-**22**) exhibited a linear correlation between the log of the rate constant of C–H activation and the carbonyl stretching frequency of complexes **24**-**27** (Figure 3.13). More electron rich complexes showed an increased rate of C–H activation, which was attributed to a ground state effect (accelerated dissociation of a coordinated solvent molecule). The authors also compared the reactivity of 2,6- and 3,5-disubstituted diimines. The 2,6-disubstituted complexes investigated react an order of magnitude more *slowly* than 3,5-disubstituted complexes (**23**, Figure 3.13).

Figure 3.12. A subset of Pt diimine complexes studied by Zhong and Bercaw[4] for the stoichiometric C–H activation of C_6D_6

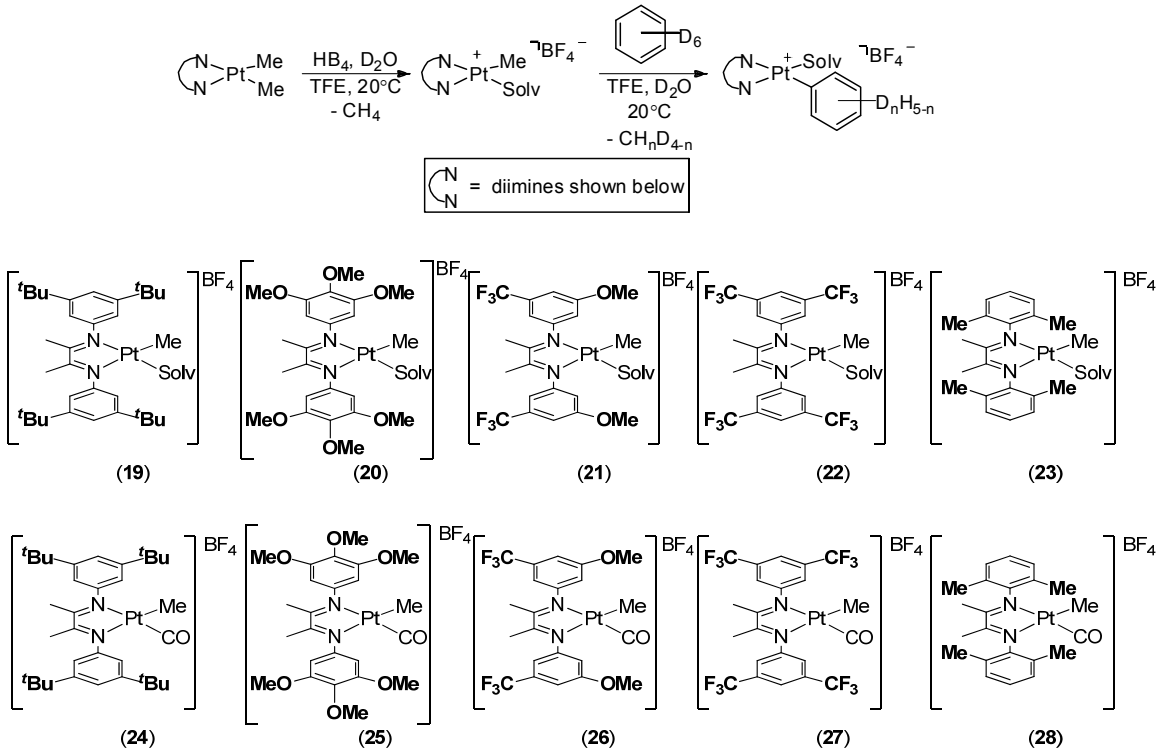

Figure 3.13. The log of the rate constant of C_6D_6 activation by complexes **19**-**23** versus ν_{CO} of analogous complexes **24**-**28** reported by Zhong and Bercaw[4]

(♦ = 3,5-disubstituted ■ = 2,6-disubstituted)

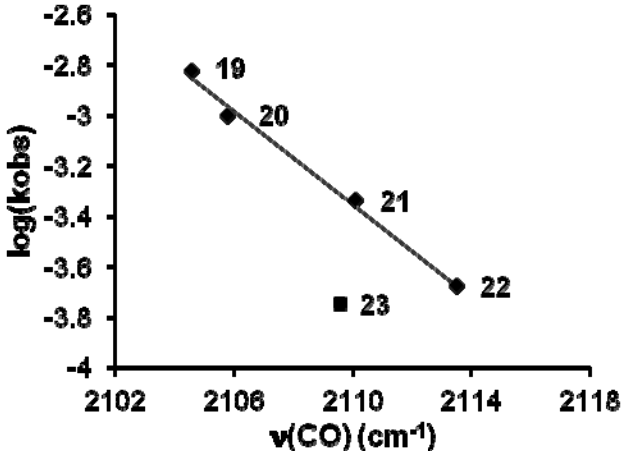

Zhong and Bercaw's stoichiometric study of diimine ligand effects also revealed significant mechanistic differences between 3,5- and 2,6-disubstituted ligands. For example, 3,5-disubstituted complexes exhibit a kinetic isotope effect of ~2, whereas platinum complexes with 2,6-disubstituted ligands show an isotope effect of ~1. Additionally, large differences in the amount of deuterium scrambling between C_6D_6 and the liberated methane were observed. Isotope scrambling can occur when the rate of oxidative addition of CH_3D ($k_{scramble}$, Scheme 3.2) is faster than the rate of CH_3D ligand exchange ($k_{exchange}$, Scheme 3.2). Interestingly, little isotope scrambling was observed for complexes with 3,5-disubstituted ligands, whereas near statistical isotope scrambling between C_6D_6 and the methyl of the Pt starting material was observed for 2,6-disubstituted complexes. The authors conclude that the two ligand classes give rise to a change in rate determining step – benzene coordination for 2,6-disubstitution and C–H bond cleavage for 3,5-disubstitution. Based on semiempirical calculations, they suggest that the increased steric demands of the 2,6-disubstitution result in a perpendicular orientation of the aryl ring relative to the square plane, which in turn retards associative ligand substitution.

Scheme 3.2. Proposed mechanism of isotope scrambling

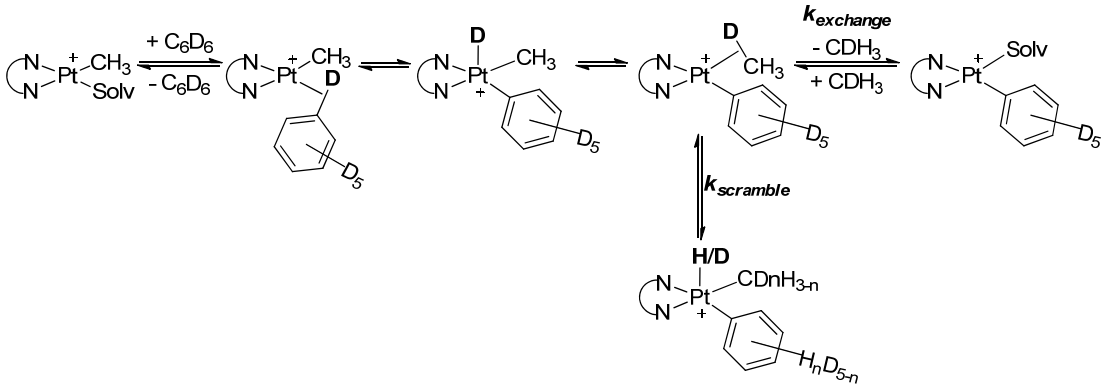

In marked contrast to Bercaw's results, our H/D exchange data showed no trend in initial rates of reaction and carbonyl stretching frequency when plotted as k_{obs} versus ν(CO) (Figure 3.5). For an exact comparison to the Bercaw data, the

logarithm of k_{obs} was instead plotted versus ν(CO) in Figure 3.14. Plotted in this fashion, there is still no clear correlation between rate and carbonyl stretching frequency.

Figure 3.14. Log of the initial rates of H/D exchange between C_6H_6 and RCO_2D catalyzed by complexes **1**-**7** versus ν_{CO} of analogous complexes **8**-**14.**

(○ = 2,6-disubstituted, ■ = 3,5-disubstituted ▲ = unsubstituted)

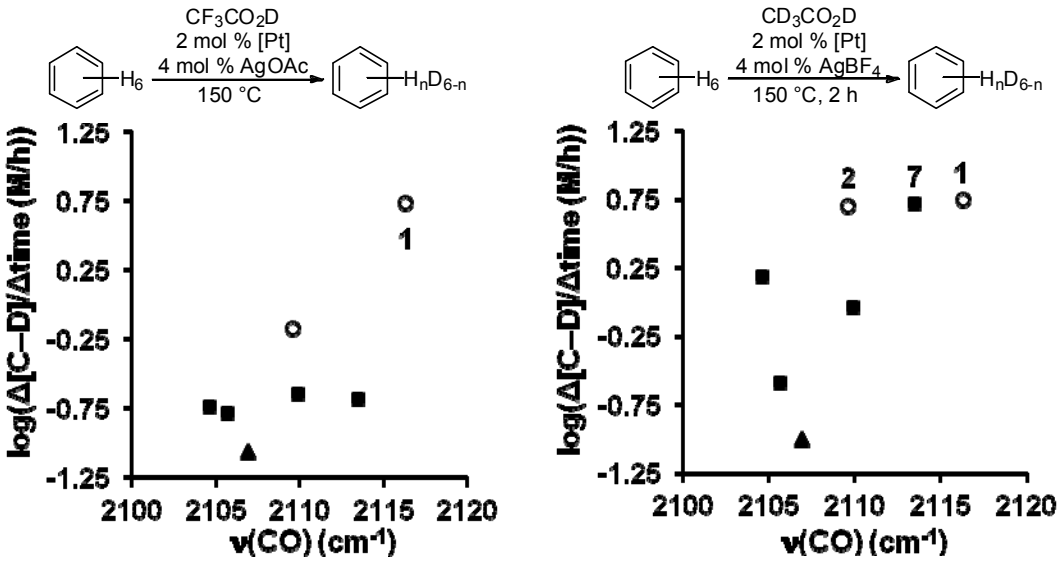

Our catalytic assay does corroborate the large impact of diimine ligand structure on Pt-catalyzed C–H activation. However, based on Bercaw's stoichiometric investigations, one might hypothesize that an electron rich 3,5-disubstituted diimine ligand would give the highest rates for catalytic C–H activation. On the contrary, our assay reveals that Pt catalysts with 2,6-disubstituted diimine ligands result in up to a 30-fold increase in initial rate of reactivity over those with 3,5-disubstituted ligands. Furthermore, our assay demonstrates no electronic trend in reactivity. Some of the enhanced reactivity of the platinum complexes with 2,6-disubstituted ligands may be the result of an increased propensity to undergo multiple reversible C–H activations and

deuterations without dissociation of the substrate as predicted by the increased isotope scrambling observed by Bercaw in the stoichiometric study.

Our studies have also revealed the special reactivity of halogen substitution for diimine Pt dichloride C–H activation. The most active catalysts we studied were 2,6-dichloro- and 2,6-dibromodiimine Pt dichloride in both deuterium sources (**1** and **15**, respectively). These catalysts exhibit dramatically higher turnover frequencies than the alkyl substituted analogs. Reactivity was attenuated by replacing one of the halogens with a methyl (**18**) or hydrogen (**17**) (Figure 10) as well as by replacement of chloride with fluoride (**16**). The reduced activity of complexes **16** and **17** may be attributed to reduced steric hinderance at the active site. However, the observed increase in reactivity from dimethyl-substitution (**2**) to mono-methyl mono-chloro (**18**) to dichloro-substitution (**1**) is indicative of a unique effect of halogen substitution.

Halogen substitution in the *ortho* positions of *N*-aryl diimine ligands have been shown to result in uniquely high reactivity for other metal-catalyzed reactions as well. For example use of 2,3-dichloro-substituted diimine ligands for Pd-catalyzed Heck and Suzuki reactions led to a significant increase in yield over analogous methyl substituted ligands (Figure 3.15).[19] In this case the authors note a “conspicuous” increase in yield with chloro-substitution but suggest the effect may be due to decreased electron density at the metal center.

Figure 3.15. Halogen substitution of Pd-diimine catalysts gives increased yields for Suzuki coupling versus methyl substitution[19]

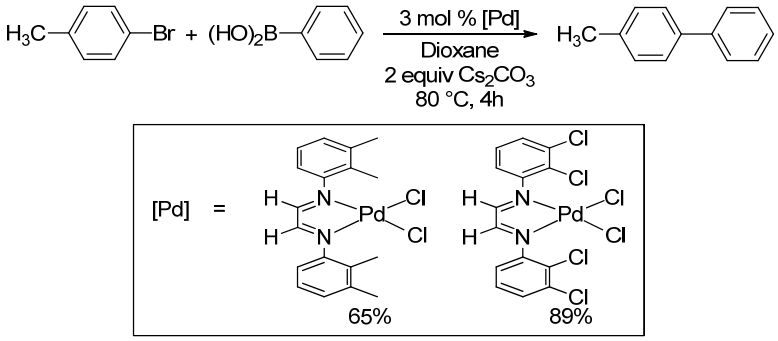

Additionally, diimine Ni dibromide catalysts have been studied extensively for the metal-catalyzed polymerization of ethylene. As shown in Figure 3.16, catalysts with *ortho* substiutents on the *N*-aryl ring have higher activities for olefin polymerization than those with the same substituent in the meta or para position.[20] Furthermore, chloro-substitution at the *ortho* position leads to an increase in activity compared to methyl substitution. Based on crystal structures and a proposed "chain-running" mechanism, the authors propose that these trends are the result of axial coordination of the *ortho*-substituent to the metal center. In the case of halogen, this interaction is presumed to further stabilize the metal center. A similar interaction has also been proposed for Ru-catalyzed olefin metathesis with halogenated *N*-heterocyclic carbene ligands.[21]

Figure 3.16. Halogen substitution of Ni-diimine catalysts gives increased activity for ethylene oligomerization[20]

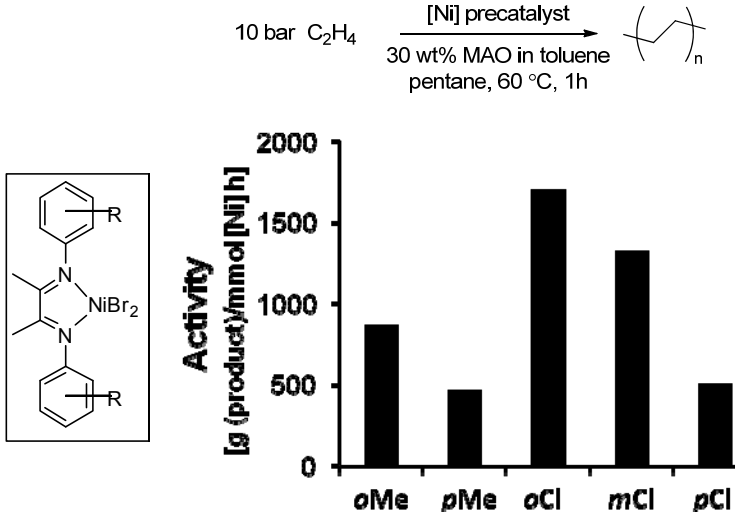

Our study of Pt-catalyzed C–H activation adds another example to the list of organometallic transformations where diimine ligated catalyst reactivity is enhanced with *N*-aryl halogen substitution. Contrary to the proposal for increased yields in Suzuki and Heck couplings, we have demonstrated that this effect is not due to a change in electron density at the metal center. Semi-empirical

calculations by Bercaw and by us[22] suggest that the *N*-aryl rings of the diimine ligand exhibit hindered rotation. In the case of 2,6-disubstitution, crystal structures of related complexes[23] and DFT geometry optimizations suggest that the aryl rings are positioned nearly perpendicular to the Pt square plane. This structural difference is the most likely explanation for the observed increased rates of C–H activation for 2,6-disubstitution. Whereas axial coordination of the *ortho*-substituent was proposed for the Ni-catalyzed polymerization reaction, the distance between the metal center and the 2,6-substituents in the diimine Pt dichloride complexes is nearly 4 Å based on DFT geometry optimizations, which exceeds typical values for metal-halogen coordination.[24]

3.4 Conclusion

In summary this work has demonstrated a remarkable relationship between diimine ligand substitution at the *N*-aryl group and catalyst activity for H/D exchange between C_6H_6 and RCO_2D. This assay directly studies Pt catalysts that are viable for development in C–H functionalization reactions[10] under conditions similar to previously reported methodology.[9] Intriguingly, marked differences in trends of structure of the diimine ligand and the activity of the Pt-catalyst were observed between previously published stoichiometric assays and our catalytic investigations. Our study identified substitution in the 2 and 6 positions of the *N*-aryl group of the diimine ligand, especially incorporation of halogens in these positions, leads to dramatic increases in catalyst reactivity. Further optimization of catalyst activity could be explored using this straightforward assay.

3.5 Experimental

General: ^{1}H, ^{19}F, and ^{13}C NMR spectra were recorded on Varian Inova 500 or 400 MHz NMR spectrometers with the residual solvent peak as the internal reference. Chemical shifts are reported in parts per million (ppm) (δ). Multiplicities are reported as follows: br (broad resonance), s (singlet), t (triplet), q (quartet), d

(doublet), dd (doublet of doublets), m (multiplet). Coupling constants (*J*) are reported in Hz. Infrared (IR) spectroscopy was performed on a Perkin Elmer FTIR. Peaks are reported in cm^{-1}. Elemental analyses were performed by Atlantic Microlab, Inc., Norcross, Georgia. CF_3CO_2D was purchased from Cambridge Isotopes Lab and stored in a Schlenk tube under N_2. Stock solutions of silver salts were prepared using volumetric glassware, and all liquid reagents were dispensed by difference. Benzene was obtained from Fisher Scientific and stored over 4 Angstrom molecular sieves. $(DMSO)_2PtCl_2$[25]and Zeise's salt[26] were prepared according to literature procedures. All reactions were prepared on the benchtop and run under air. H/D exchange data was measured on a Shimadzu GCMS-QP5000, and all raw data was deconvoluted using a benzene H/D exchange worksheet prepared by Periana and coworkers.[27] Every reported reaction was conducted at least twice. The average of all trials is reported herein.

Computational Methods: Using Gaussian 03 suite of programs,[11] all density functional theory (DFT) calculations were performed with the B3LYP functional[12,13,14,15] along with the LanL2DZ basis set.[16,17,18] All geometries were optimized using LanL2DZ/B3LYP without symmetry constraints using the restricted Kohn-Sham formalism for all complexes. All minima were confirmed by the absence of imaginary frequencies. Thermochemical data was calculated using unscaled vibrational frequencies and default parameters at 298.15 K and 1 atm. NBO analysis[28] was used to determine relevant charge distribution in ground states.

Example H/D Exchange: All glassware and stir bars were treated with aqua regia, washed with copious amounts of water and acetone, and dried before each use. To a 4 mL resealable schlenk tube was added a small stir bar and 2 mol % catalyst. A 0.04 M in CF_3CO_2D stock solution of silver acetate was prepared immediately prior to use. The silver solution (if specified) and catalyst were combined in a total of 0.5 mL of CF_3CO_2D and stirred for one minute. Benzene (23.2 µL, 0.26 mmol), stored over 4 Angstrom molecular sieves, was

added to the reaction vessel, which was subsequently sealed. The vessel was submerged up to the stopcock channel in a preheated oil bath. At the end of the reaction, the vessel was cooled to room temperature. The reaction mixture was then filtered over celite to remove any particulates and rinsed with ethyl acetate into a 20 mL scintillation vial. A saturated aqueous solution of potassium carbonate (500 g in 400 mL deionized H_2O) was added to the vial to quench and separate the acid (2 x 1 mL). The organic layer was carefully separated and diluted with additional ethyl acetate to a 1 mg/mL sample for analysis by GC-MS.

Example Initial Rates: All glassware and stir bars were treated with aqua regia, washed with copious amounts of water, and dried before each use. The Pt^{II} catalyst (5 μmol) was dissolved in CF_3CO_2D (0.25 mL) in a 4 mL Schlenk flask fitted with a resealable Teflon stopcock. A 0.04 M stock solution of AgOAc in CF_3CO_2D was prepared immediately before use. This AgOAc solution (0.25 mL of a 0.04 M stock solution in CF_3CO_2D, 0.01 mmol, 4 mol %) was added to the flask, this mixture was stirred for 1 min, and then benzene (23 μL, 0.26 mmol) was added. The reaction vessel was sealed and then completely submerged in an oil bath that was pre-heated to 150 ºC. After the desired time, the vessel was removed from the oil bath and immediately submerged in an ice bath. The reaction was then worked up as described in the manuscript. Three to four time points were acquired for each catalyst to assess the reactivity up to approximately 10% conversion (10% of the statistical maximum turnover number, TON = 21 and TON = 24 for CF_3CO_2D and CD_3CO_2D, respectively). To obtain the observed rate, the concentration of C–D bonds was plotted vs. reaction time. For reactions that proceed very fast, the rates are at best a low approximation of the rate as a result of slow heat transfer relative to the reaction kinetics.

Example Time Study: All glassware and stir bars were treated with aqua regia, washed with copious amounts of water, and dried before each use. The Pt^{II} catalyst (5 μmol) was dissolved in CF_3CO_2D (0.25 mL) in a 4 mL Schlenk flask fitted with a resealable Teflon stopcock. A 0.04 M stock solution of AgOAc in

CF_3CO_2D was prepared immediately before use. This AgOAc solution (0.25 mL of a 0.04 M stock solution in CF_3CO_2D, 0.01 mmol, 4 mol %) was added to the flask, this mixture was stirred for 1 min, and then benzene (23 μL, 0.26 mmol) was added. The reaction vessel was sealed and then completely submerged in an oil bath that was pre-heated to 100 ºC. After the allotted time, the mixture was cooled to room temperature and worked up as described above.

3.6 Characterization

*General procedure for synthesis of compounds **S1-S11**:*

The diimine ligands were prepared according to literature procedures.[10,29,30,31] Diimine ligand **S1** was prepared according to a procedure reported by Chen[31] and Sanford.[10] Diimine ligands **S2**-**S7** were prepared according to procedures reported by Bercaw[82] and Tilset,[30] and their characterization is reported in Chapter 4.[10] The appropriate aniline and 2,3-butanedione were dissolved in methanol. Formic acid (1-6 drops) was added, and the reaction was allowed to stand unstirred until crystals began to form (typically overnight). The reaction mixture was then stirred overnight. The precipitate was collected on a fritted filter, washed with methanol, and dried under vacuum.

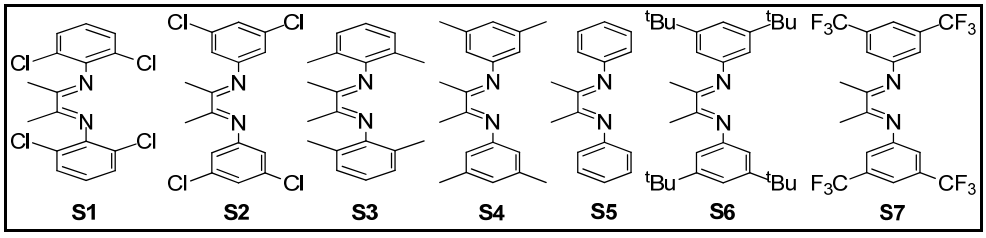

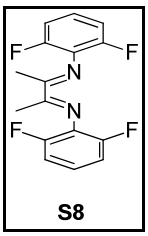

Diimine ligand **S8** was synthesized by an adaptation of a published preparation.[32] 2,6-difluoroaniline (1.08 mL, 10 mmol, SynQuest) was dissolved in anhydrous

methanol (7.5 mL) in a 25 mL round bottom flask. 2,3-Butanedione (0.64 mL, 7 mmol, TCI), *p*-toulenesulfonic acid (0.021 g, Aldrich), and trimethyl *ortho*-formate (2 mL) were added to the solution and the reaction was stirred overnight. The next day, the precipitate was collected by filtration and dried under vacuum to yield a yellow solid (322 mg, 21%). ^{1}H NMR (400 MHz, Acetone-d_6): δ 7.25 (m, 2H), 7.14 (m, 4H), 2.22 (s, 6H). ^{19}F NMR (376 MHz, Acetone- d_6): δ 124.72 (m) ^{13}C NMR (100 MHz, Acetone-d_6): δ173.32 (s), 153.03 (dd, J^1 = 245.4, J^3 = 5.83),' 127.79 (t, J^2 = 16.7), 126.22 (t, J^3 = 9.3), 112.66 (m), 16.80 (s).

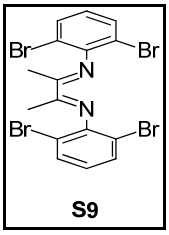

S9

Diimine ligand **S9** was synthesized by an adaptation of a published preparation by Chen et al.[4] 2,6-Dibromoaniline (2.361 g, 9.4 mmol, Alfa Aesar) and 2,3-butanedione (0.41 mL, 4.7 mmol, TCI) were dissolved in dry toluene (4.5 mL) in a 10 mL round bottom flask equipped with a Dean Stark trap and reflux condenser. Trifluoroacetic acid (0.11 mL, Aldrich) was added to the solution and the reaction was stirred at reflux overnight. The reaction was then cooled to room temperature and the solvent was concentrated to a brown oil. Cold acetone was added to the oil to precipitate a solid that was collected by filtration, washed with cold acetone, and dried under vacuum to yield a yellow solid (404 mg, 16%). ^{1}H NMR (400 MHz, $CDCl_3$): δ 7.56 (d, *J*= 8.0 Hz, 2H), 6.85 (t, *J*= 8.0 Hz, 4H), 2.14 (s, 6H). ^{13}C NMR (100 MHz, $CDCl_3$): δ 171.21, 147.52, 131.93, 125.60, 112.71, 17.02.

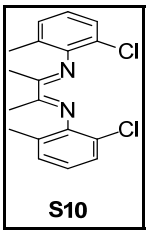

S10

Diimine ligand **S10** was synthesized by an adaptation of a published preparation by Chen et al.[4] 2-chloro, 6-methylaniline (4.4 mL, 35.7 mmol, Pfaltz and Bauer) and 2,3-butanedione (1.7 mL, 19.8 mmol, TCI) were dissolved in dry toluene (15 mL) in a 25 mL round bottom flask equipped with a Dean Stark trap and reflux condenser. Trifluoroacetic acid (0.38 mL, Aldrich) was added to the solution and the reaction was stirred at reflux overnight. The reaction was then cooled to room temperature and the solvent was concentrated to a brown oil. Ether was added to the oil to precipitate a solid that was collected by filtration, washed with ether, and dried under vacuum to yield a yellow-brown solid (1.94 g, 33%). Proton NMR analysis at room temperature is consistent with hindered rotation. Coalescence of the aliphatic peaks was above 75 °C. ^{1}H NMR (500 MHz, DMSO-d_6, 75°C): δ 7.35 (d, *J*= 8 Hz, 2H), 7.25 (d, *J*= 8 Hz, 2H), 7.05 (m, 2H), 2.07 (s, 6H), 2.04 (s, 6H) . ^{13}C NMR (100 MHz, DMSO-d_6, 100°C): δ 168.73, 145.35, 128.28, 126.97, 126.30, 123.70, 120.38, 16.62, 15.43 (br).

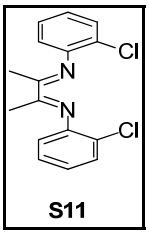

S11

Diimine ligand **S11** was synthesized by following a published preparation.[20] 2-Chloroaniline (1.6 mL, 15.5 mmol, Acros) and 2,3 butanedione (0.5 mL, 5.7 mmol, TCI) were dissolved in dry methylene chloride (5 mL) in a 20 mL scintillation vial. Tosic acid monohydrate (108 mg, 5 mol %, Aldrich) was added to the solution and the reaction was stirred at reflux for 24 h. The reaction was then cooled to room temperature and filtered over a plug of silica in a pipet. The filtrate was concentrated in vacuo to a viscous oil. Cold methanol (10 mL) was added, and then the reaction was stored in the freezer to facilitate precipitation of a pale yellow microcystalline solid that was collected by filtration (255.9 mg, 15%). ^{1}H NMR (400 MHz, $CDCl_3$): δ 7.42 (d, *J*= 8 Hz, 2H), 7.26 (t, *J*= 8 Hz, 2H),

7.05 (t, *J*= 8 Hz,2H), 6.79 (d, *J*= 8 Hz, 2H), 2.14 (s, 6H). ^{13}C NMR (100 MHz, $CDCl_3$): δ 169.66, 147.68, 129.86, 127.31, 124.85, 123.13, 119.67, 16.10.

*General Procedure for synthesis of complexes **1**-**7**:*

The diimine Pt dichloride complexes were prepared according to published literature methods A, B, or C. **Method A**: The diimine ligand and *cis*-$(Me_2SO)_2Pt(Cl)_2$ were heated in acetone at 70 ºC for 4 h, then the precipitate was collected by hot filtration, and dried under vacuum.[3] **Method B:** Zeise's dimer was suspended in tetrahydrofuran and the diimine added slowly with vigorous stirring. The solution was stirred overnight, and then the precipitate was collected by filtration and dried under vacuum.[8] **Method C:** Zeise's salt[26] was suspended in methanol at 0 °C and the diimine added slowly with vigorous stirring. The solution was stirred for three hours and slowly warmed to room temperature. The precipitate was collected by filtration, washed with methanol and ether, and dried under vacuum.[Error! Bookmark not defined.] ^{13}C NMR spectral data is not reported for any of the dichloride complexes due to their poor solubility.

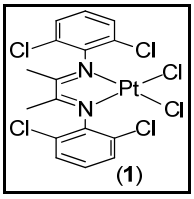

(**1**)

Method A: The diimine ligand **S1** (115 mg, 0.31 mmol) and *cis*-$(Me_2SO)_2Pt(Cl)_2$ (100 mg, 0.24 mmol) were dissolved in acetone (10 mL) in a 20 mL scintillation vial. During heating, the mixture changed color from yellow to red, and a reddish-brown precipitate was observed (32.9 mg, 22% yield). ^{1}H NMR (400 MHz, DMF-d_7): δ 7.73 (d, *J* = 8 Hz, 4H), 7.55 (t, *J* = 8 Hz, 2H), 2.02 (s, 6H). The purity of samples of complex **1** used for catalysis was confirmed by elemental analysis. Anal. calcd. for $C_{16}H_{12}Cl_6N_2Pt$: C, 30.02; H, 1.89; N, 4.38; Found: C, 30.00; H, 1.83; N, 4.33.

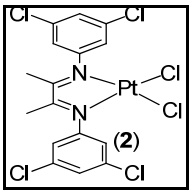

Method B: $[Pt_2Cl_4(C_2H_4)_2]$ (80 mg, 0.136 mmol, Strem) was suspended in tetrahydrofuran (5.4 mL) in a 20 mL scintillation vial. Slowly, the diimine ligand **S2** (110.7 mg, 0.295 mmol) was added to the reaction with constant stirring. The clear yellow liquid turned murky brown with the addition of the diimine and the reaction was allowed to stir overnight yielding a brown solid which was collected by filtration and washed with ether (2 x 3 mL) (145.4 mg, 83%). ^{1}H NMR (400 MHz, DMSO-d_6): δ 7.72 (m, 2H), 7.23 (d, J = 2 Hz, 4H), 1.90 (s, 6H). The purity of samples of complex **2** used for catalysis was confirmed by elemental analysis. Anal. Calcd. for $C_{16}H_{12}Cl_6N_2Pt$: C, 30.02; H, 1.89; N, 4.38; Found: C, 30.30; H, 2.06; N, 4.19.

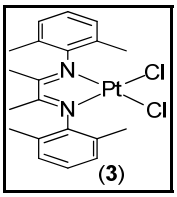

Method B: $[Pt_2Cl_4(C_2H_4)_2]$ (105 mg, 0.18 mmol, Strem) was suspended in tetrahydrofuran (7 mL) in a 20 mL scintillation vial. Slowly, the diimine ligand **S3** (114.0 mg, 0.39 mmol) was added to the reaction with constant stirring. The clear yellow liquid turned murky brown with the addition of the diimine and the reaction was allowed to stir overnight yielding a brown solid (154.3 mg, 77%). ^{1}H NMR (400 MHz, DMSO-d_6): δ 7.18 (s, 6H), 2.12 (s, 12H), 1.75 (s, 6H). The purity of samples of complex **3** used for catalysis was confirmed by elemental analysis. Anal. Calcd. for $C_{20}H_{24}Cl_2N_2Pt$: C, 43.02; H, 4.33; N, 5.02; Found: C, 42.97; H, 4.37; N, 4.86.

Method C: $K[PtCl_3(C_2H_4)]\bullet H_2O$[26] (140 mg, 0.36 mmol) was suspended in methanol (7 mL) in a 20 mL scintillation vial at 0˚C. Slowly, the diimine ligand **S3**

(115 mg, 0.39 mmol) was added to the chilled reaction with constant stirring. The clear yellow liquid turned murky brown with the addition of the diimine and the reaction was allowed to stir and warm up to room temperature yielding a brown solid (165 mg, 83%). The purity of samples of complex **3** used for catalysis was confirmed by elemental analysis. Anal. Calcd. for $C_{20}H_{24}Cl_2N_2Pt$: C, 43.02; H, 4.33; N, 5.02; Found: C, 42.93; H, 4.31; N, 5.15.

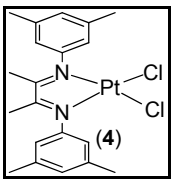

(**4**)

Method C: $K[PtCl_3(C_2H_4)]•H_2O$ (138 mg, 0.36 mmol) was suspended in methanol (7 mL) in a 20 mL scintillation vial at 0˚C. Slowly, the diimine ligand **S4** (115 mg, 0.39 mmol) was added to the chilled reaction with constant stirring. The clear yellow liquid turned murky brown with the addition of the diimine and the reaction was allowed to stir and warm up to room temperature yielding a brown solid (173 mg, 86%). ^{1}H NMR (400 MHz, CD_3CN): δ 7.22 (s, 6H), 2.27 (s, 12H), 1.69 (s, 6H). The purity of samples of complex **4** used for catalysis was confirmed by elemental analysis. Anal. Calcd. for $C_{20}H_{24}Cl_2N_2Pt$: C, 43.02; H, 4.33; N, 5.02; Found: C, 43.04; H, 4.25; N, 5.11.

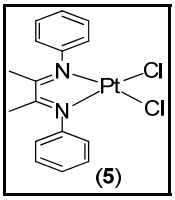

(**5**)

Method B: $[Pt_2Cl_4(C_2H_4)_2]$ (105 mg, 0.18 mmol, Strem) was suspended in tetrahydrofuran (7 mL) in a 20 mL scintillation vial. Slowly, the diimine ligand **S5** (92.1 mg, 0.39 mmol) was added to the reaction with constant stirring. The clear yellow liquid turned murky brown with the addition of the diimine and the reaction was allowed to stir overnight yielding a brown solid (165.1 mg, 91%). ^{1}H NMR (400 MHz, Acetone-d_6): δ 7.50 (t, *J*= 7.2 Hz, 4H), 7.38 (t, *J*= 7.2 Hz, 2H), 7.17 (d,

J= 7.2 Hz, 4H), 1.95 (s, 6H). The purity of samples of complex **5** used for catalysis was confirmed by elemental analysis. Anal. Calcd. for $C_{16}H_{16}Cl_2N_2Pt$: C, 38.26; H, 3.21; N, 5.58; Found: C, 38.36; H, 3.14; N, 5.52.

Method C: $K[PtCl_3(C_2H_4)]•H_2O$ (138 mg, 0.36 mmol) was suspended in methanol (7 mL) in a 20 mL scintillation vial at 0˚C. Slowly, the diimine ligand **S5** (56 mg, 0.39 mmol) was added to the chilled reaction with constant stirring. The clear yellow liquid turned murky brown with the addition of the diimine and the reaction was allowed to stir and warm up to room temperature yielding a brown solid (76 mg, 42%). The purity of samples of complex **5** used for catalysis was confirmed by elemental analysis. Anal. Calcd. for $C_{16}H_{16}Cl_2N_2Pt$: C, 38.26; H, 3.21; N, 5.58; Found: C, 38.24; H, 3.10; N, 5.61.

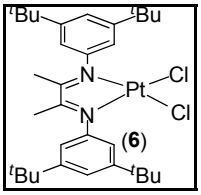

Method C: $K[PtCl_3(C_2H_4)]•H_2O$ (140 mg, 0.36 mmol) was dissolved in methanol (10 mL) in a 20 mL scintillation vial at 0˚C. Slowly, the diimine ligand **S6** (183 mg, 0.40 mmol) was added to the chilled reaction with constant stirring. The clear yellow liquid turned murky brown with the addition of the diimine and the reaction was allowed to stir and warm up to room temperature yielding a brown solid (233 mg, 89%). ^{1}H NMR (400 MHz, Acetone-d_6): δ 7.47 (s, 2H), 7.06 (s, 4H), 1.96 (s, 6H), 1.36 (s, 36H). The purity of samples of complex **6** used for catalysis was confirmed by elemental analysis. Anal. Calcd. for $C_{32}H_{48}Cl_2N_2Pt$: C, 52.89; H, 6.66; N, 3.85; Found: C, 52.69; H, 6.59; N, 3.89.

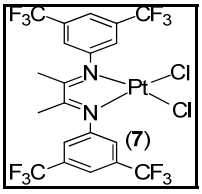

Method B: $[Pt_2Cl_4(C_2H_4)_2]$ (105 mg, 0.18 mmol, Strem) was suspended in tetrahydrofuran (7 mL) in a 20 mL scintillation vial. Slowly, the diimine ligand **S7** (105.0 mg, 0.39 mmol) was added to the reaction with constant stirring. The clear yellow liquid turned murky brown with the addition of the diimine and the reaction was allowed to stir overnight yielding a brown solid (212.2 mg, 76%). ^{1}H NMR (400 MHz, DMSO-d_6): δ 8.26 (s, 2H), 7.85 (s, 4H), 1.94 (s, 6H). ^{19}F NMR (376 MHz, DMSO-d_6) δ 61.36. The purity of samples of complex **7** used for catalysis was confirmed by elemental analysis. Anal. Calcd. for $C_{20}H_{12}Cl_2F_{12}N_2Pt$: C, 31.02; H, 1.56; N, 3.62; Found: C, 30.92; H, 1.46; N, 3.48.

Method C: $K[PtCl_3(C_2H_4)]•H_2O$ (144 mg, 0.37 mmol) was suspended in methanol (12 mL) in a 20 mL scintillation vial at 0˚C. Slowly, the diimine ligand **S7** (208 mg, 0.41 mmol) was added to the chilled reaction with constant stirring. The clear yellow liquid turned murky brown with the addition of the diimine and the reaction was allowed to stir and warm up to room temperature yielding a brown solid (90 mg, 31%). The purity of samples of complex **7** used for catalysis was confirmed by elemental analysis. Anal. Calcd. for $C_{20}H_{12}Cl_2F_{12}N_2Pt$: C, 31.02; H, 1.56; N, 3.62; Found: C, 30.90; H, 1.41; N, 3.75.

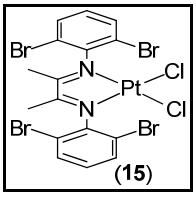

(**15**)

Method A: The diimine ligand **S9** (171 mg, 0.31 mmol) and *cis*-$(Me_2SO)_2Pt(Cl)_2$ (100 mg, 0.24 mmol) were dissolved in acetone (10 mL) in a 20 mL scintillation vial. During heating, the mixture changed color from yellow to red, and a reddish-brown precipitate was observed (58.9 mg, 30%). ^{1}H NMR (500 MHz, Acetone-d_6): δ 7.83 (d, *J*= 8 Hz, 4H), 7.32 (t, *J*= 8 Hz, 2H), 2.08 (s, 6H). The purity of samples of complex **15** used for catalysis was confirmed by elemental analysis. Anal. Calcd. For $C_{16}H_{12}Br_4Cl_2N_2Pt$: C, 23.50; H, 1.48; N, 3.43; Found: C, 23.49; H, 1.24; N, 3.27.

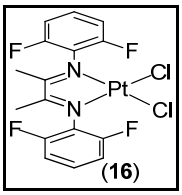

(**16**)

Method B: $[Pt_2Cl_4(C_2H_4)_2]$ (105mg, 0.18 mmol, Strem) was suspended in tetrahydrofuran (7 mL) in a 20 mL scintillation vial. Slowly, the diimine ligand **S8** (120 mg, 0.39 mmol) was added to the reaction with constant stirring. The clear yellow liquid turned murky brown with the addition of the diimine and the reaction was allowed to stir overnight. The next day, the solution was filtered and dried under vacuum to yield a brown solid (115 mg, 56%). ^{1}H NMR (400 MHz, Acetone-d_6): δ 7.54 (m, 2H), 7.24 (m, 4H), 2.09 (s, 6H). ^{19}F NMR (376 MHz, Acetone-d_6) δ 119.62 (m). The purity of samples of complex **16** used for catalysis was confirmed by elemental analysis. Anal. Calcd. for $C_{16}H_{12}Cl_2F_4N_2Pt$: C, 33.46; H, 2.11; N, 4.88; Found: C, 33.35; H, 1.96; N, 4.84.

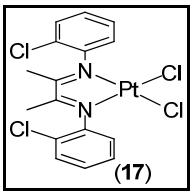

(**17**)

Method B: $[Pt_2Cl_4(C_2H_4)_2]$ (80 mg, 0.136 mmol, Strem) was suspended in tetrahydrofuran (5.4 mL) in a 20 mL scintillation vial. Slowly, the diimine ligand **S11** (90.0 mg, 0.295 mmol) was added to the reaction with constant stirring. The clear yellow liquid turned murky brown with the addition of the diimine and the reaction was allowed to stir overnight. The next day, the solution was filtered and dried under vacuum to yield a brown solid (131.3 mg, 85%). ^{1}H NMR (400 MHz, CD_3CN): δ 7.61 (m, 2H), 7.50 (m, 2H), 7.43 (m, 2H), 7.26 (m, 2H), 1.76 (s, 6H). The purity of samples of complex **17** used for catalysis was confirmed by elemental analysis. Anal. Calcd. for $C_{16}H_{14}Cl_4N_2Pt$: C, 33.64; H, 2.47; N, 4.90; Found: C, 33.35; H, 2.33; N, 4.69.

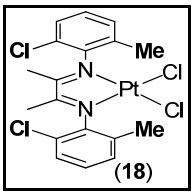

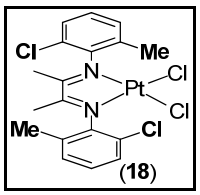

Method B: $[Pt_2Cl_4(C_2H_4)_2]$ (80 mg, 0.136 mmol, Strem) was suspended in tetrahydrofuran (5.4 mL) in a 20 mL scintillation vial. Slowly, the diimine ligand **S10** (120 mg, 0.295 mmol) was added to the reaction with constant stirring. The clear yellow liquid turned murky brown with the addition of the diimine and the reaction was allowed to stir overnight. The next day, the solution was filtered and dried under vacuum to yield a brown solid (132.2 mg, 81%). Proton NMR analysis is consistent with the formation of two isomers. Coalescence of the aliphatic peaks was not observed up to 100 °C. ^{1}H NMR (500 MHz, DMSO-d_6): δ 7.50 (d, J= 8 Hz, 2H, both isomers), 7.38 (m, 2H, both isomers), 7.33 (m, 2H, both isomers), 2.33 (s, 4.7H, major isomer), 2.29 (s, 1.8H, minor isomer), 1.83 (s, 1.6 H, minor isomer), 1.82 (s, 5.0H, major isomer). The purity of samples of complex **18** used for catalysis was confirmed by elemental analysis. Anal. Calcd. for $C_{18}H_{18}Cl_4N_2Pt$: C, 36.08; H, 3.03; N, 4.67; Found: C, 35.98; H, 3.12; N, 4.52.

3.7 References

[1] Gol'dshleger, N. F.; Eskova, V. V.; Shilov, A. E.; Shteinman, A. A. *Zh. Fiz. Khim.* **1972**, *46*, 1353.

[2] For select pertinent reviews, see: (a) Stahl, S. S.; Labinger, J. A.; Bercaw, J. E. *Angew. Chem., Int. Ed.* **1998**, *37*, 2180-2192. (b) Lersch, M.; Tilset, M. *Chem. Rev.* **2005**, *105*, 2471-2526. (c) Fekl, U.; Goldberg, K. I. *Adv. Inorg. Chem.* **2003**, *54*, 259-320. (d) Conley, B. L.; Tenn, W. J.; Young, K. J. H.; Ganesh, S. K.; Meier, S. K.; Ziatdinov, V. R.; Mironov, O.; Oxgaard, J.; Gonzales, J.; Goddard, W. A.; Periana, R. A. *J. Mol. Cat. A.*, **2006**, *251*, 8-23.

[3] Hickman, A. J.; Villalobos, J. M.; Sanford, M. S. *Organometallics* **2009**, *28*, 5316-5322.

[4] Zhong, H. A.; Labinger, J. A.; Bercaw, J. E. *J. Am. Chem. Soc.* **2002**, *124*, 1378-1399.

[5] Wik, B. J.; Lersch, M.; Krivokapic, A.; Tilset, M. *J. Am. Chem. Soc.* **2006**, *128*, 2682-2696**.**

[6] Driver, T. G.; Williams, T. J.; Labinger, J. A.; Bercaw, J. E. *Organometallics* **2007**, *26*, 294-301.

[7] Parmene, J.; Krivokapic, A.; Tilset, M. *Eur. J. Inorg. Chem.* **2010**, 1381-1394.

[8] Wong-Foy, A. G.; Henling, L. M.; Day, M.; Labinger, J. A.; Bercaw, J. E. *J. Mol. Catal. A Chem.* **2002**, *189,* 3-16.

[9] (a) Lyons, T. W.; Sanford, M. S. *Chem. Rev.* **2010**, *110*, 1147-1169. (b) Ahrens, S.; Strassner, T. *Inorganica Chimica Acta* **2006**, *359*, 4789-4796. (c) Strassner, T.; Muehlhofer, M.; Zeller, A.; Herdtweck, E.; Herrmann, W. A. *J. Organometallic Chem.* **2004**, *689*, 1418-1424. (d) Muehlhofer, M.; Strassner, T.; Herrmann, W. A. *Angew. Chem., Int. Ed.* **2002**, *41*, 1745-1747. (e) Periana, R. A.; Taube, D. J.; Gamble, S.; Taube, H.; Satoh, T.; Fujii, H. *Science* **1998**, *280*, 560-564.

[10] Hickman, A. J.; Sanford, M. S. *ACS Catalysis*, **2011**, *1*, 170-174.

[11]Gaussian 03, Revision C.02, M. J. Frisch, G. W. Trucks, H. B. Schlegel, G. E. Scuseria, M. A. Robb, J. R. Cheeseman, J. A. Montgomery, Jr., T. Vreven, K. N. Kudin, J. C. Burant, J. M. Millam, S. S. Iyengar, J. Tomasi, V. Barone, B. Mennucci, M. Cossi, G. Scalmani, N. Rega, G. A. Petersson, H. Nakatsuji, M. Hada, M. Ehara, K. Toyota, R. Fukuda, J. Hasegawa, M. Ishida, T. Nakajima, Y. Honda, O. Kitao, H. Nakai, M. Klene, X. Li, J. E. Knox, H. P. Hratchian, J. B. Cross, C. Adamo, J. Jaramillo, R. Gomperts, R. E. Stratmann, O. Yazyev, A. J. Austin, R. Cammi, C. Pomelli, J. W. Ochterski, P. Y. Ayala, K. Morokuma, G. A. Voth, P. Salvador, J. J. Dannenberg, V. G. Zakrzewski, S. Dapprich, A. D. Daniels, M. C. Strain, O. Farkas, D. K. Malick, A. D. Rabuck, K. Raghavachari, J. B. Foresman, J. V. Ortiz, Q. Cui, A. G. Baboul, S. Clifford, J. Cioslowski, B. B. Stefanov, G. Liu, A. Liashenko, P. Piskorz, I. Komaromi, R. L. Martin, D. J. Fox, T. Keith, M. A. Al-Laham, C. Y. Peng, A. Nanayakkara, M. Challacombe, P. M. W. Gill, B. Johnson, W. Chen, M. W. Wong, C. Gonzalez, and J. A. Pople, Gaussian, Inc., Wallingford CT, 2004.

[12] Becke, A. D. *J. Chem. Phys.***1993**, *98*, 5648-5652.

[13] Lee, C.; Yang, W.; Parr, R. G. *Phys. Rev. B* **1988**, *37*, 785-789.

[14] Vosko, S. H.; Wilk, L.; Nusair, M. *Can. J. Phys.* **1980**, *58*, 1200-1211.

[15] Stephens, P. J.; Devlin, F. J.; Chabalowski, C. F.; Frisch, M. J. *J. Phys. Chem.* **1994**, *98*, 11623-11627.

[16] Hay, P. J.; Wadt, W. R. *J. Chem. Phys.* **1985**, *82*, 270-283.

[17] Wadt, W. R.; Hay, P. J. *J. Chem. Phys.* **1985**, *82*, 284-298.

[18] Hay, P. J.; Wadt, W. R. *J. Chem. Phys.* **1985**, *82*, 299-310.

[19] Hanhan, M. E. *App. Organometal. Chem.* **2008**, *22*, 270-275.

[20] Helldörfer, M.; Miliu, W.; Alt, H. G. *J. Mol. Catal. A: Chem.* **2003**, *197*, 1-13.

[21] Ritter, T.; Day, M. W.; Grubbs, R. H. *J. Am. Chem. Soc.* **2006**, *128*, 11768-11769.

[22] Preliminary semi-empirical calculations predict a rotational barrier >25 kcal/mol.

[23] (a) van Asselt, R.; Elsevier, C. J.; Smeets, W. J. J.; Spek, A. L. Benedix, R. *Recl. Trav. Chim. Pays-Bas* **1994**, *113*, 88-98. (b) Yang, K.; Lachicotte, R. J.; Eisenberg, R. *Organometallics* **1997**, *16*, 52344-5243. (c) Johansson, L.; Ryan, O. B.; Rømming, C.; Tilset, M. *Organometallics* **1998**, *17*¸ 3957-3966. (d) Yang, K.; Lachicotte, R. J.; Eisenberg, R. *Organometallics* **1998**, *17*, 5102-5113. (e) Gates, D. P.; Svejda, S. A.; Oñate, Killian, C. M.; Johnson, L. K.; White, P. S.; Brookhart, M. *Macromolecules* **2000**, *33*, 2320-2334. (f) Paulovicova, A.; El-Ayaan, U.; Shibayama, K.; Morita, T.; Fukuda, Y. *Eur. J. Inorg. Chem.* **2001**, 2641-2646. (g) Johansson, L.; Ryan. O. B.; Rømming, C.; Tilset, M. *J. Am. Chem. Soc.* **2001**, *123*, 6579-6590. (h) Gerdes, G.; Chen, P. *Organometallics* **2003**, *22*, 2217-2225. (i) Heyduk, A. F.; Driver, T. G.; Labinger, J. A.; Bercaw, J. E. *J. Am. Chem. Soc.* **2004**, *126*, 15034-15035. (j) Coventry, D. N.; Batsanov, A. S.; Goeta, A. E.; Howard, J. A. K.; Marder, T. B. *Polyhedron* **2004**, *23*, 2789-2795. (k) Wik, B. J.; Lersch, M.; Krivokapic, A.; Tilset, M. *J. Am. Chem. Soc.* **2006**, *128*, 2682-2696. (l) Shiotsuki, M.; White, P.S.; Brookhart, M.; Templeton, J. L. *J. Am. Chem. Soc.* **2007**, *129*, 4058-4067. (m) Parmene, J.; Krivokapic, A.; Tilset, M. *Eur. J. Inorg. Chem.* **2010**, 1381-1394.

[24] Kulawiec, R. J.; Crabtree, R. H. *Coord. Chem. Rev.* **1990**, *99*, 89-115.

[25] Price, J. H; Williamson, A. N; Schramm, R. F.; Wayland, B. B. *Inorg. Chem.* **1972**, *11*, 1280-1284.

[26] Cramer, R. D.; Jenner, E. L.; Lindsey, R. V.; Stolberg, U. G. *J. Am. Chem. Soc.* **1963**, *85*, 1691-1692.

[27] Young, K. J. H.; Meier, S. K.; Gonzales, J. M.; Oxgaard, J.; Goddard, W. A., III; Periana, R. A. *Organometallics* **2006**, *25*, 4734-4737.

[28] NBO Version 3.1, E. D. Glendening, A. E. Reed, J. E. Carpenter, and F. Weinhold.

[29] Zhong, H. A.; Labinger, J. A.; Bercaw, J. E. *J. Am. Chem. Soc*. **2002**, *124*, 1378-1399.

[30] Johansson, L.; Ryan, O. B.; Tilset, M. *J. Am. Chem. Soc.* **1999**, *121*, 1974-1975.

[31]Gerdes, G.; Chen, P. *Organometallics* **2003**, *22*, 2217-2225.

[32] Khusniyarov, M. M.; Harms, K.; Burghaus, O.; Sundermeyer, J. *Eur. J. Inorg. Chem.* **2006**, 2985-2996.

Chapter 4: Catalyst-Controlled Site-Selective Pd-Catalyzed C–H Arylation

4.1 Introduction

Aryl-aryl bonds are ubiquitous in organic molecules including pharmaceuticals, agrochemicals, and natural products.[1] While these linkages are most commonly formed via the cross-coupling of two prefunctionalized arenes,[1] there has been tremendous recent progress in the development of metal-catalyzed C–H arylation reactions.[2,3,4,5] In these systems, the aryl-aryl bond is formed by directly merging an arene or heteroarene with an aryl halide, aryl organometallic (*e.g.,* $ArB(OH)_2$, $ArSnBu_3$, $ArSiX_3$), or aryl iodonium salt (Scheme 4.1).

Scheme 4.1. Direct C–H arylation

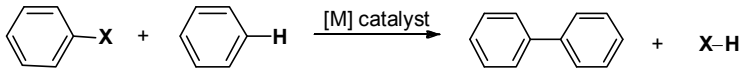

A major challenge in the field of direct arylation is achieving site selective C–H functionalization. The three most common strategies are to use: (1) arene substrates that contain directing groups,[6,7,8,9] (2) arene substrates bearing intramolecular coupling partners,[10,11] or (3) heteroarene substrates with highly activated C–H bonds (*e.g.*, indoles, pyrroles) (Figure 4.1).[12,13,14,15,16] All three approaches have provided powerful methods for the selective assembly of complex molecules. However, the requirement for substrate-based control over selectivity inherently restricts the scope of these transformations.

Figure 4.1. Substrate-control of site-selective C–H activation

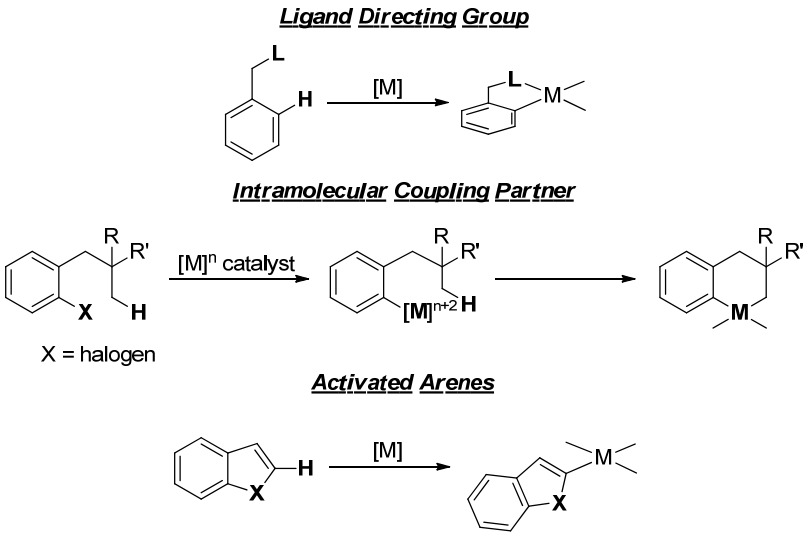

In contrast, the site selective direct arylation of unactivated aromatics remains extremely rare.[17,18,19,20] Naphthalene has proven to be a particularly challenging substrate for this type of reaction, and previously reported methods have provided either low yields[21] or only modest (< 3.5 : 1) preference for formation of the α isomer (Table 4.1).[22,23,24] Catalyst-based control (*i.e.* using steric and electronic modification of ancillary ligands at the metal to dictate the preferred site of C–H arylation) would be a powerful approach for modulating the selectivity of such transformations. While catalyst control of selectivity and reactivity is common in other areas of Pd catalysis,[25,26,27,28,29,30] C–H functionalization reactions often work best with simple Pd salts like $Pd(OAc)_2$ and $PdCl_2$ (for example, Table 4.1, entries 1, 2, and 4), which do not contain readily tunable ligands.

Table 4.1. Metal-catalyzed direct arylation of naphthalene

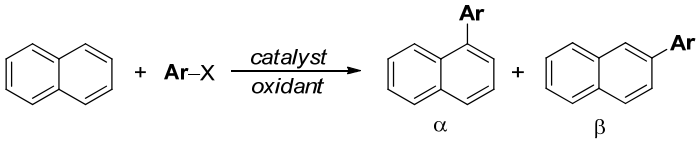

Entry	Ar–X	Catalyst/Oxidant	Yield	α : β
1[23]	*p*-$NO_2C_6H_4I$	$Pd(OAc)_2$/none	88%	3.3 : 1
2[24]	$PhSnCl_3$	$PdCl_2/CuCl_2$	40%	3.4 : 1
3[22]	PhBr	Cp_2Ni-KO^{t}Bu-BEt_3	70%	2.3 : 1
4[21]	PhH	$Pd(OAc)_2$/TFA/$K_2S_2O_8$	32%	>20:1

This chapter describes the first systematic examination of catalyst-controlled selectivity in the Pd-catalyzed arylation of an unactivated arene.[31,32,33,34,35] We demonstrate that modular diimine-ligated Pd-catalysts can be tuned to enhance both the reaction yield and site selectivity of naphthalene arylation with $[Ar_2I]BF_4$. Preliminary investigations implicate a mechanism in which naphthalene π-coordination and subsequent metalation occur at a high oxidation state Pd center.[36]

4.2 Results

Our initial investigations focused on the Pd-catalyzed C–H phenylation of naphthalene with Ph_2IBF_4. $Pd(OAc)_2$ was the first catalyst examined, since it has been used for other C–H functionalization reactions with $[Ar_2I]^+$ reagents.[24,37,38,39,40,41,42] We were pleased to find that phenylated products **A** and **B** were formed in a variety of different solvents. Under the optimal conditions (NO_2Ph at 130 ºC for 16 h), $Pd(OAc)_2$ provided 24% yield and 5 : 1 selectivity for isomer **A** (Table 4.2, entry 1). This selectivity is comparable to that observed in many other naphthalene arylation reactions (Table 4.1, entries 1-3).[22-24] A survey of Pd salts (Table 4.2, entries 2-4) revealed that the X-type ligand has a significant influence on selectivity, with $PdCl_2$ providing the best results (**A** : **B** = 13 : 1, entry 2).

Table 4.2. Catalyst effects in the phenylation of naphthalene with $[Ph_2I]BF_4$

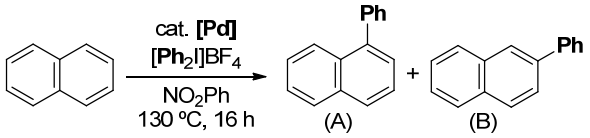

Entry	Catalyst	Yield	A : B
1	$Pd(OAc)_2$	24%	5 : 1
2	$PdCl_2$	22%	13 : 1
3	$PdBr_2$	21%	8 : 1
4	PdI_2	12%	8 : 1

Conditions: Pd catalyst (3.68 μmol, 5 mol %), naphthalene (47.1 mg, 0.368 mmol, 5 equiv), Ph_2IBF_4 (27.1 mg, 0.0735 mmol, 1 equiv) in NO_2Ph (0.75 mL) at 130 ºC for 16 h. Yield and selectivity determined by GCMS.

We next examined naphthalene phenylation with $PdCl_2$ complexes of 1,4-bisphenyl-2,3-dimethyl-1,4-diaza-1,3-butadiene ($^{Ph}DAB^{Me}$), di-*tert*-butyl bipyridine (dtbpy), and 1,10-phenanthroline (phen) (**1-3**). These ligands were selected because they are all known to support Pd^{II} and/or Pt^{II} complexes that promote arene C–H activation.[43,44,45] Gratifyingly, distinct changes in both reactivity and selectivity were observed as a function of catalyst structure. For example, complex **1** afforded double the yield of $PdCl_2$ (Table 4.3, entry 1), while **2** provided dramatically enhanced selectivity for isomer **A** (**A** : **B** = 78 : 1, entry 2). *These results clearly demonstrate the potential for catalyst control in Pd-catalyzed C–H arylation.*

Complex **1** is an attractive starting point for systematically evaluating ligand effects because electronically and sterically diverse diimine analogues are readily available.[46] A series of bis(aryl)diimine$PdCl_2$ complexes containing various R and R^1 substituents (**4a-d, 5a, b**) were prepared, and substitution at both R and R^1 had a significant influence on selectivity and yield (Table 4.3). The 2,6-Cl diimine complex **5b** was particularly effective for this transformation (entry 9), providing

the highest yield (70%) and **A** : **B** selectivity (71 : 1) of the series.[47,48,49] Notably, the **5b**-catalyzed reaction was also very clean and afforded <5% yield of diarylated naphthalene, biphenyl, or binaphthyl side products.

Table 4.3. Substituted diimine Pd^{II} catalysts for the phenylation of naphthalene with $[Ph_2I]BF_4$

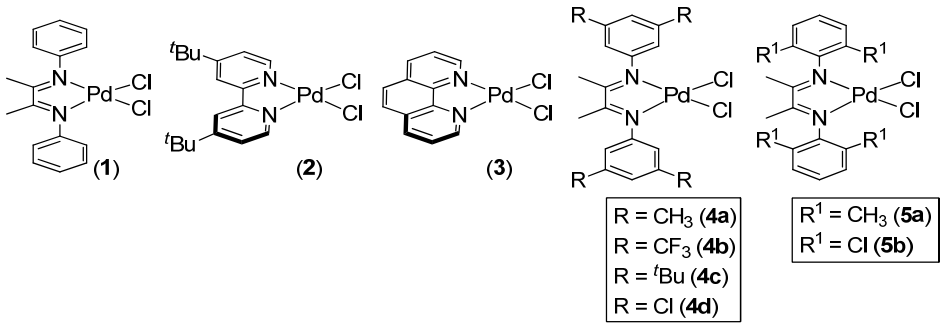

Entry	Catalyst	Yield	A : B
1	**1**	54%	9 : 1
2	**2**	22%	78 : 1
3	**3**	12%	10 : 1
4	**4a**	47%	9 : 1
5	**4b**	50%	10 : 1
6	**4c**	32%	18 : 1
7	**4d**	42%	22 : 1
8	**5a**	43%	27 : 1
9	**5b**	70%	71 : 1

Conditions: Pd catalyst (3.68 μmol, 5 mol %), naphthalene (47.1 mg, 0.368 mmol, 5 equiv), Ph_2IBF_4 (27.1 mg, 0.0735 mmol, 1 equiv) in NO_2Ph (0.75 mL) at 130 ºC for 16 h. Yield and selectivity determined by GCMS.

The **5b**-catalyzed reaction was optimized to maximize yield and selectivity. The reaction was evaluated in a variety of solvents known to facilitate C–H activation and functionalization reactions (Table 4.4). Although dichloroethane gave slightly higher yields and better selectivity, a large uncatalyzed reaction was observed in

this solvent (Table 4.4, entry 3). From this study nitrobenzene was determined to be the optimal solvent for further development (Table 4.4, entry 4). Additionally, substrate to oxidant ratio and temperature were also investigated (Table 4.5). Remarkably, excellent yield and selectivity could be obtained with as a few as 3 equiv of naphthalene relative to oxidant at 130 °C (Table 4.5, entry 5).

Table 4.4. Solvent study of **5b**-catalyzed naphthalene phenylation with $[Ph_2I]BF_4$[a]

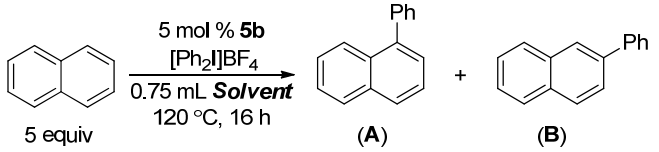

Entry	Solvent	Total Yield	Selectivity A : B
1	AcOH	23%	11 : 1
2	TFE	37%	56 : 1
3	DCE[b]	60%	171 : 1
4	NO_2Ph	51%	89 : 1
5	NO_2CH_3	5%	29 : 1

[a] Conditions: Catalyst **5b** (4.1 mg, 7.35 μmol, 10 mol %), naphthalene (47.1 mg, 0.368 mmol, 5 equiv), $[Ph_2I]BF_4$ (27.1 mg, 0.0735 mmol, 1 equiv) in solvent (0.75 mL) for 16 h. Yields and selectivities were determined by GC analysis. [b] A large background (uncatalyzed) reaction (45% yield) was observed in DCE with ~4:1 selectivity.

Table 4.5. Reaction optimization with **5b** and $[Ph_2I]BF_4$[a]

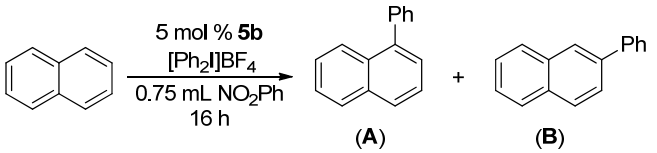

Entry	Substrate : Oxidant	Temp	Yield	Selectivity (A : B)
1	5 : 1	100 ºC	14%	5 : 1
2	5 : 1	120 ºC	51%	89 : 1
3	5 : 1	130 ºC	74%	78 : 1
4[b]	5 : 1	150 ºC	67%	50 : 1
5	3 : 1	130 ºC	73%	110 : 1
6	1 : 1	130 ºC	49%	113 : 1

[a] Conditions: Catalyst **5b** (2.0 mg, 3.68 μmol, 5 mol %), naphthalene (47.1 mg, 0.368 mmol, 5 equiv; 28.3 mg, 0.221 mmol, 3 equiv; 9.4 mg, 0.0735 mmol, 1 equiv), $[Ph_2I]BF_4$ (27.1 mg, 0.0735 mmol, 1 equiv) in nitrobenzene (0.75 mL) for 16 h. Yield and selectivity were determined by GC analysis. [b] 24 h

To obtain more quantitative information about the influence of ligand structure on selectivity, we examined the yield and **A** : **B** ratio as a function of the electronic character of the diimine [as measured by ν_{CO} for (diimine)Pt$(CH_3)(CO)^+$], as discussed in Chapter 3.[50] As shown in Figure 4.2, there is no clear relationship between ν_{CO} and yield or the **A** : **B** ratio, even when potential steric contributions were eliminated (3,5-substituted derivatives, Figure 4.2, circles). This data suggests that the observed ligand effects are not predominantly electronic in nature. Additionally, the poor correlation between ligand electronic properties and selectivity/yield suggests against a Lewis-acid catalyzed mechanism, since the Lewis acidity of the Pd center is expected to track closely with the electron withdrawing ability of the ligand.[51]

Figure 4.2. A : **B** ratio versus diimine electronics (as measured by ν_{CO} for (diimine)Pt(CH_3)$(CO)^+$).

(■ = 2,6-disubstituted, ● = 3,5-disubstituted)

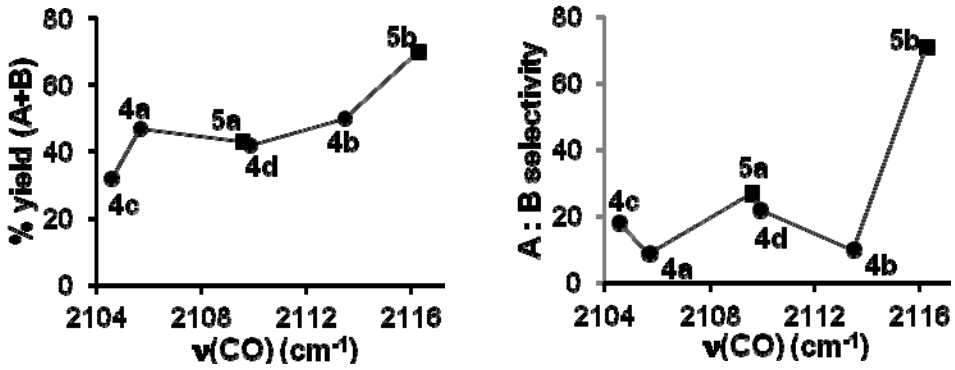

We also probed the chemoselectivity of **5b**-catalyzed C–H arylation. A 1 : 1 mixture of naphthalene and other electron rich and electron deficient arenes was subjected to the standard conditions in the presence of 0.2 equiv of $[Ph_2I]BF_4$. In all cases, the reaction was remarkably selective for naphthalene, with (**A**+**B**):**C** ratios ranging from >600 : 1 (trifluorotoluene, benzene) to 12 : 1 (veratrole) (Table 4.6).[52] Chemoselectivity did not track well with nucleophilicity (N),[53,54] as substrates that are much more nucleophilic than naphthalene (1,3-dimethoxybenzene, anisole) were significantly less reactive in this competition experiment. These results indicate that the chemoselectivity-determining step does not proceed via a classical electrophilic aromatic substitution pathway.[55]

Table 4.6. Chemoselectivity of C–H phenylation catalyzed by **5b**

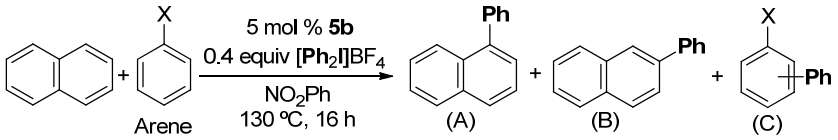

Entry	Arene	N[53]	Total Yield	(A+B):C
1	1,3-dimethoxybenzene	2.4	39%	43 : 1
2	veratrole	na	52%	12 : 1
3	anisole	–1.6	63%	210 : 1
4	*o*-xylene	–3.7	60%	597 : 1
5	naphthalene	–3.8	70%	----
6	*p*-xylene	–4.2	60%	>600 : 1
7	benzene[a]	–6.3	27%	>600 : 1
8	trifluorotoluene	–10.3	55%	>600 : 1

Conditions: Catalyst **5b** (2.0 mg, 3.68 μmol, 5 mol %), naphthalene (23.6 mg, 0.184 mmol, 2.5 equiv), arene (0.184 mmol, 2.5 equiv), Ph_2IBF_4 (27.1 mg, 0.0735 mmol, 1 equiv) in NO_2Ph (0.75 mL) for 16 h at 130 ºC. Yield and selectivity determined by GCMS. [a] Using *p*-tol_2IBF_4.

Next the kinetic isotope effect (KIE) was determined by comparing the initial rate of naphthalene phenylation (Figure 4.3) to that of naphthalene-d_8 (Figure 4.4). Both reactions were conducted using the standard kinetics procedure in the experimental section 4.5, using arene substrate (0.368 mmol, 5 equiv), $[Ph_2I]BF_4$ (0.0735 mmol, 1 equiv), and **5b** (3.68 μmol, 5 mol %, added as a pre-initiated solution). These experiments provided a KIE of 1.0 ± 0.1, indicating that C–H bond-cleavage is not involved in the rate-determining step of the catalytic cycle.

Figure 4.3. Initial rates of naphthalene C–H phenylation catalyzed by **5b**.

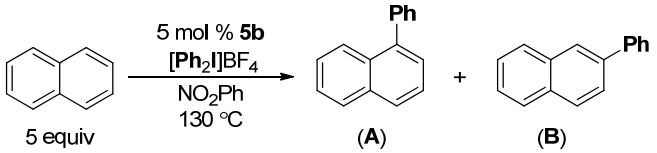

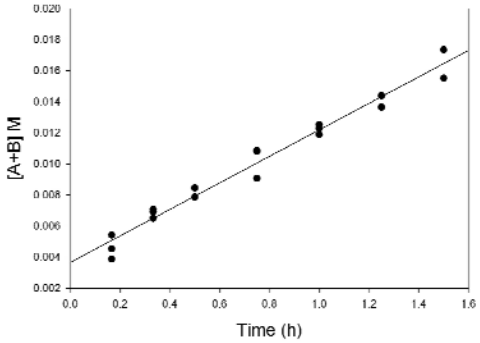

Conditions: Catalyst **5b** (2.0 mg, 3.68 μmol, 5 mol %), naphthalene (47.1 mg, 0.368 mmol, 5 equiv), $[Ph_2I]BF_4$ (27.1 mg, 0.0735 mmol, 1 equiv) in nitrobenzene (0.75 mL). Yield and selectivity were determined by GC analysis. The data was plotted using Sigma Plot 10 and fit to the function f=*y0*+*a**x; *a* = $8.5*10^{-3} \pm 0.4*10^{-3}$, *y0* = $3.7*10^{-3} \pm 0.3*10^{-3}$, $R^2 = 0.9725$.

Figure 4.4. Initial rates of naphthalene-d_8 C–H phenylation catalyzed by **5b**.

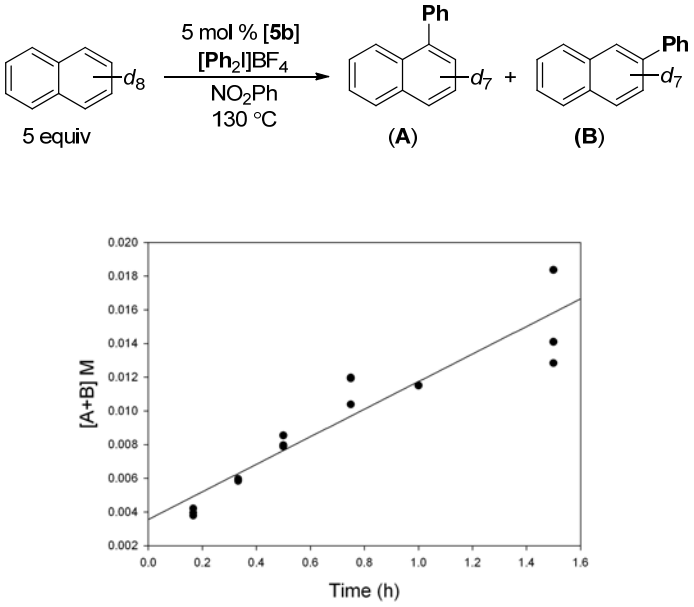

Conditions: Catalyst **5b** (2.0 mg, 3.68 μmol, 5 mol %), naphthalene-d_8 (50.1 mg, 0.368 mmol, 5 equiv), $[Ph_2I]BF_4$ (27.1 mg, 0.0735 mmol, 1 equiv) in nitrobenzene (0.75 mL). Yield and selectivity were determined by GC analysis. The data was plotted using Sigma Plot 10 and fit to the function f=*y0*+*a**x; $a = 8.2*10^{-3} \pm 0.8*10^{-3}$, $y0 = 3.6*10^{-3} \pm 0.7*10^{-3}$, $R^2 = 0.8752$.

A competition experiment between naphthalene and naphthalene-d_8 was also conducted. The ratio of phenylated products was determined by comparing the ratio of the intensities of the two parent ion peaks (204 and 211 for **A** and **A-*d*$_7$**) to a calibration curve (Figures 4.5 and 4.6). The calibration curve was generated using known quantities of **A** and **A-*d*$_7$**. On the basis of this data, the competition KIE (k_H/k_D) was determined to be 1.07 ± 0.03. This value is significantly smaller than is typical for Pd-catalyzed C–H arylation reactions that involve palladation at Pd^{II} centers (general range = 1.8-5.5).[56,57,58] However, the observed value is similar to that reported for the Pd-catalyzed carboamination of alkenes with benzene (competition k_H/k_D = 1.1). Michael and coworkers proposed that this small isotope effect resulted from π-coordination of benzene to a Pd^{IV} intermediate prior to C–H bond-breaking (Scheme 4.2).[59]

Figure 4.5 Representative mass spectrum of observed ratio **A** (m/z = 204) and **A-*d*$_7$** (m/z = 211).

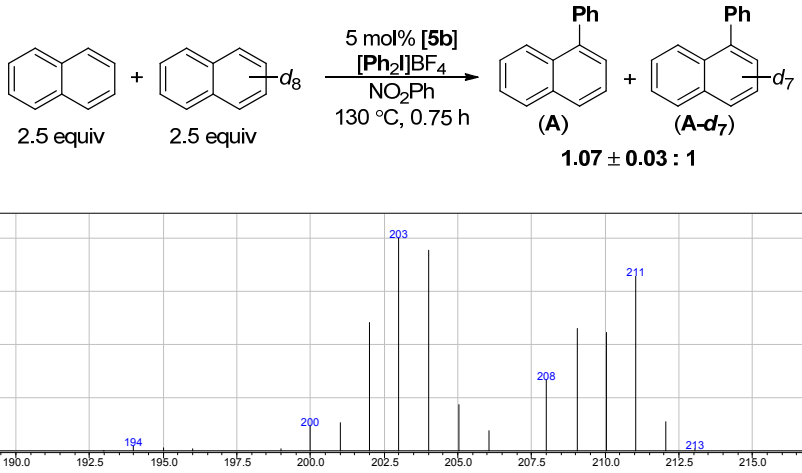

Figure 4.6. Calibration curve for **A** : **A-*d*$_7$**.

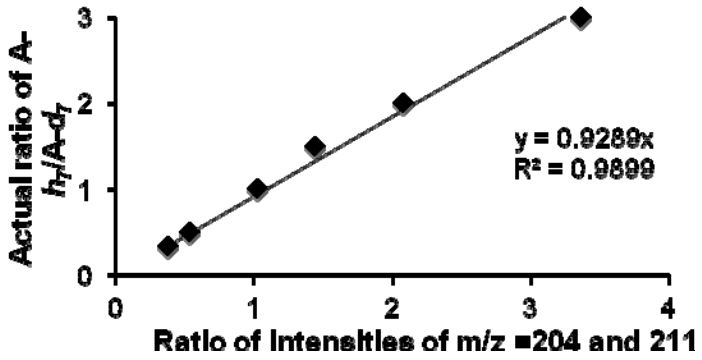

Scheme 4.2. Michael's Pd-catalyzed carboamination of alkenes with arenes, where the selectivity determining step is formation of a π-complex.[59]

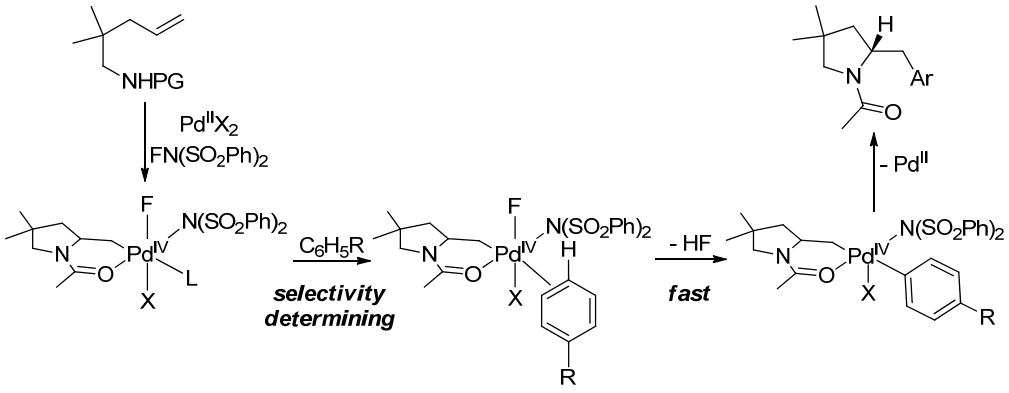

Finally, we established the kinetic order of C–H arylation in both $[Ph_2I]BF_4$ and naphthalene. The order in naphthalene was determined by studying the initial rate of each transformation at differing concentrations of naphthalene. Representative initial rates data is shown in Figure 4.2. This transformation is 0 order with respect to naphthalene, which provides further evidence against rate determining C–H bond cleavage (Figure 4.6).

Figure 4.6. Initial rates versus [naphthalene].

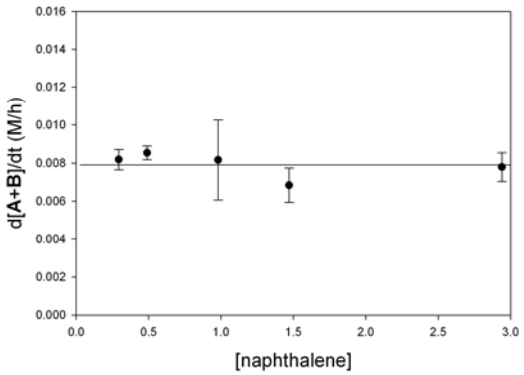

The data was plotted using Sigma Plot 10 and fit to the function f=*a**x^*b*; *a* = $7.9*10^{-3} \pm 0.3*10^{-3}$, *b* = $5.0*10^{-10} \pm 0.05$, where *b* is the order in [naphthalene].

Likewise, the order in $[Ph_2I]BF_4$ was determined by studying the initial rate of each transformation at differing concentrations of $[Ph_2I]BF_4$ (Figure 4.7). A 1st order dependence on $[Ph_2I]BF_4$ was observed, indicating that the arylating reagent is involved in the turnover-limiting step of the catalytic cycle.

Figure 4.7. Initial rate versus [(Ph_2I)BF_4].

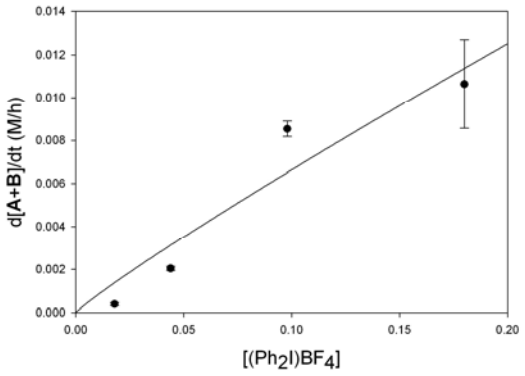

The data was plotted using Sigma Plot 10 and fit to the function f=*a**x^*b*; *a* = 0.05 ± 0.03, *b* = 0.9 ± 0.3, where *b* is the order in [Ph_2I]BF_4.

Collectively, these observations are consistent with the $Pd^{II/IV}$ mechanism shown in Figure 4.8. This pathway involves: (*i*) rate-determining oxidation of Pd^{II} catalyst **I** with [Ph_2I]BF_4 to form Pd^{IV} intermediate **II**,[60] (*ii*) π-coordination of naphthalene to Pd^{IV} to generate **III**, (*iii*) palladation to produce **IV**, and (*iv*) C–C bond-forming reductive elimination to release the product. We propose that π-coordination to Pd^{IV} is the chemoselectivity-determining step. This is consistent with the competition KIE (1.07 ± 0.03), which is very similar to that seen by Michael for an analogous mechanism.[59] In addition, this provides a compelling explanation for the unusually high chemoselectivity, as naphthalene is well known to form more stable metal π-complexes than benzene derivatives.[61]

Figure 4.8. Proposed mechanism for C–H arylation of naphthalene with $[Ph_2I]BF_4$

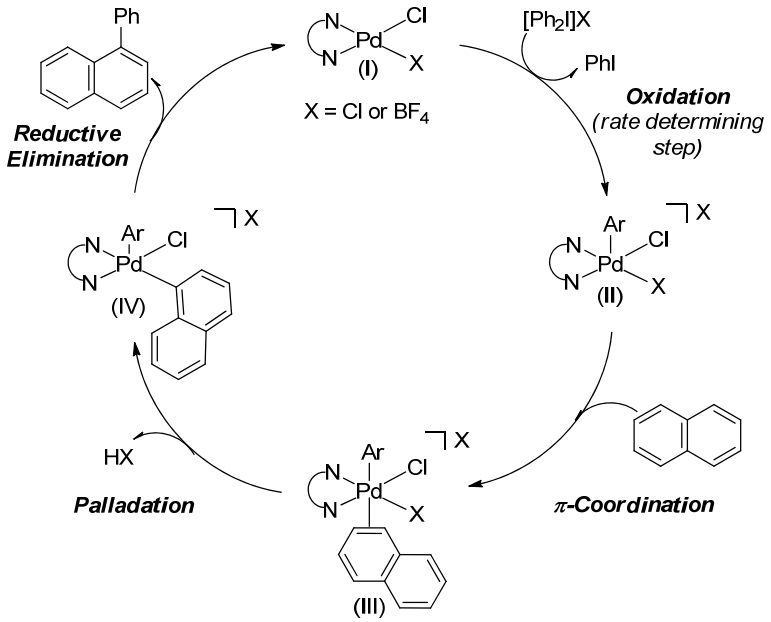

Preliminary stoichiometric studies provide further support for the mechanism in Figure 4.8. For example, no reaction was observed between catalyst **5b** and naphthalene when these two reagents were stirred at 130 ºC in NO_2Ph (Scheme 4.3).[62] In addition, the stoichiometric reaction between **5b** and $[Ph_2I]BF_4$ in the absence of naphthalene resulted in complete consumption of oxidant and concomitant formation of 1 equiv of PhCl and 1 equiv of PhI (Figure 4.9). This is consistent with the generation of Pd^{IV} intermediate **II** that undergoes C–Cl bond-forming reductive elimination in the absence of naphthalene.[63]

Scheme 4.3. Stoichiometric reaction of **5b** and naphthalene

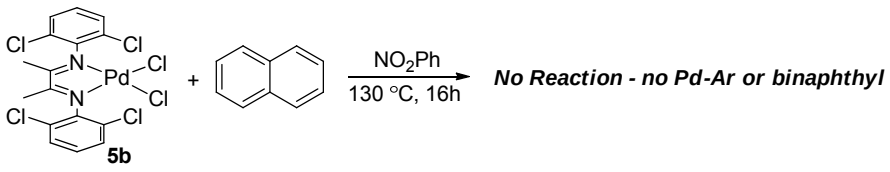

Figure 4.9. Stoichiometric reaction of **5b** and $[Ph_2I]BF_4$

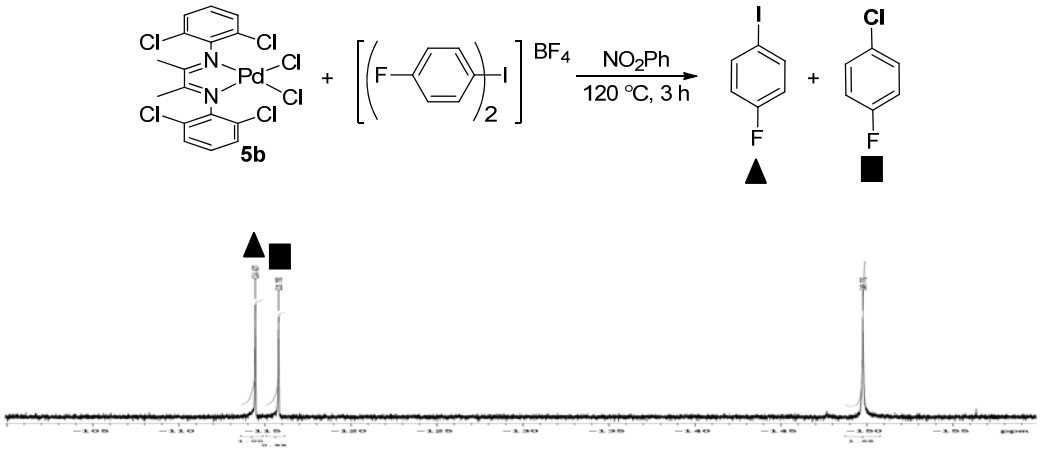

On the basis of this mechanism, we hypothesized that electron deficient diaryliodonium oxidants would be particularly effective, since they should accelerate the rate-determining oxidation step. Indeed, $[Ar_2I]BF_4$ reagents containing electron-deficient and neutral aryl substituents provided high yield and selectivity (Table 4.7, entries 1-5). In contrast, arylating agents containing electron rich aryl groups such as *p*-methoxyphenyl (Table 4.7, entry 7) and *ortho*-substituted aryl groups (Table 4.7, entry 6) performed poorly in this reaction. Again, these results are all consistent with the proposed mechanism.

Table 4.7. Oxidant scope for arylation of naphthalene with catalyst **5b**

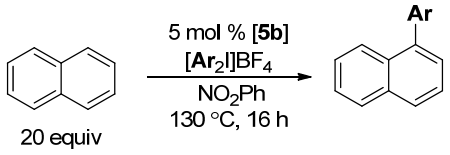

Entry	Ar	Yield[a]
1	C_6H_5	72%
2	*p*-$CH_3C_6H_4$	68%
3	*p*-BrC_6H_4	65%
4	*p*-$CF_3C_6H_4$	62%
5	*m*-$NO_2C_6H_4$	71%
6	*o*-$CH_3C_6H_4$	trace[b]
7	*p*-$MeOC_6H_4$	Nr

Conditions: Catalyst **5b** (19.3-24.5 μmol, 5 mol %), naphthalene (7.7-9.8 mmol, 20 equiv), $[Ar_2I]BF_4$ (0.39-0.49 mmol, 1 equiv) in NO_2Ph (98 mM in oxidant) for 16 h at 130 ºC. [a] Isolated yields. [b] Detected by GC-MS.

4.3 Applications

This work suggests, for the first time, that both reactivity and selectivity in Pd^{IV}-catalyzed C–H arylation can be tuned through modification of supporting ligand structure. A logical extension of these findings is to apply this strategy to develop solid supported catalysts for the direct arylation of arenes. Solid supported catalysts are desirable for industrial applications as they can be easily separated from the product stream.[64] Furthermore, the solid support could prevent decomposition and aggregation pathways leading to deactivated catalysts. Based on the investigations discussed above, design of the ligand linker to the solid support could be used to tune reactivity and selectivity.

In collaboration with Dr. Tae-Hong Park in Professor Adam Matzger's laboratory at the University of Michigan (Department of Chemistry), we sought to investigate the use of crystalline microporous coordination polymers (MCPs), and in particular the subset referred to as metal-organic frameworks (MOFs) as a

solid support for Pd-catalyzed C–H arylation. MOFs have shown extensive potential for use in applications such as gas storage,[65] chemical separations,[66] catalysis,[67] sensors,[68] and drug delivery.[69] These MCPs are constructed via the self-assembly of metal ions/clusters and organic linker under reaction conditions where relatively perfect single crystal growth is favorable. In the following discussion, Dr. Park and coworkers in the Matzger lab designed, synthesized, and characterized the novel heterogeneous catalyst. I then evaluated this new material's reactivity for the Pd-catalyzed arylation of naphthalene.

Coordination copolymerization (as in the use of mixed linkers) has presented tremendous opportunities to control functionality within the framework[70] and to build new materials with unparalleled surface areas.[71,72] Dr. Park recently developed a synthesis of a MOF uniquely functionalized with dangling carboxylate defects. Specifically, defects can be engineered into MOF-5 by the addition of a small amount of 1,3,5-tris(4-carboxyphenyl)benzene (H_3BTB) during synthesis. This leads to a new material nearly identical to MOF-5 albeit with octahedral morphology and a significant number of defect sites that functionalize the pores. For the rest of this chapter, this new material will be designated MOF-5(O_h).

Through a mechanism ascribed to the presence of uncoordinated carboxylate groups, MOF-5(O_h), adsorbs considerable quantities of palladium ions from a dilute $Pd(OAc)_2$ solution. When MOF-5(O_h) crystals were slowly shaken in a $Pd(OAc)_2$ solution (8.9 mM) in CH_2Cl_2 for 2 days, the colorless crystals became brown and the solution was visibly depleted in Pd. After adsorption in a fresh Pd solution for another 2 days, the crystals were washed with CH_2Cl_2 three times and immersed in CH_2Cl_2 for 2 days for which a fresh solvent was replenished three times to remove unbound Pd ions. The optical images of Pd ion adsorbed MOF-5(O_h), designated as Pd(II)@MOF-5(O_h), are shown in Figure 4.10.

Figure 4.10. Selective impregnation of Pd(II) ion in MOF-5(O_h). $Pd(OAc)_2$, CH_2Cl_2. For comparison, a deliberate mixtures of pristine MOF-5 or needle shaped UMCM-1 with MOF-5(O_h) crystals were tested.

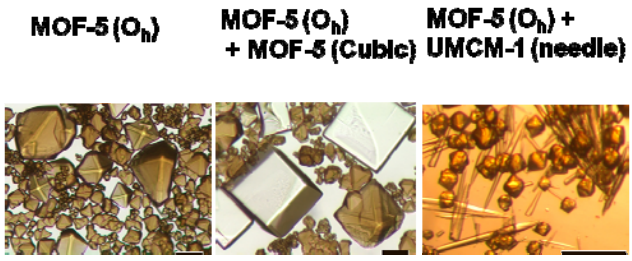

For comparison, the MOF-5(O_h) crystals were mixed with pure MOF-5 or UMCM-1 and then placed in a $Pd(OAc)_2$ solution. After 4 days, only MOF-5(O_h) became brown whereas MOF-5 (cubes) and UMCM-1 (needles) remained nearly colorless (Figure 4.10). Such selective impregnation suggests that the Pd adsorption is not significant in MOF-5[73] and UMCM-1, while, in contrast, the dangling carboxylate groups of MOF-5(O_h) extensively interact with $Pd(OAc)_2$. The Pd content of Pd(II)@MOF-5(O_h) was 2.3 wt % as determined by inductive coupled plasma-optical emission spectroscopy (ICP-OES). Overall, the above data strongly support the idea that BTB incorporates into the MOF-5 structure, giving rise to not only a morphology change but also to carboxylate functionality within the pores.

With this solid-supported Pd^{II} catalyst in hand, we next turned our attention to investigating its reactivity for the C–H phenylation of naphthalene. As shown in Table 4.2, entry 1, the use of 5 mol % of $Pd(OAc)_2$ as catalyst afforded low yield for this transformation. This is further exemplified by a time study of the reaction. As demonstrated in Figure 4.11, the $Pd(OAc)_2$-catalyzed C–H arylation of naphthalene in nitrobenzene at 120 ºC nearly terminated after 30 min, providing a total yield of 13% with 15:1 selectivity for the **A** versus **B** isomers. The solution begins to turn black within 5 min presumably signifying the aggregation and precipitation of Pd^0. Employing longer reaction times (17 h) only slightly improved yield and lowered selectivity (17%, 8:1, Figure 4.11). Collectively, the results

suggest that catalyst decomposition is fast under these conditions. We hypothesized that the MCP framework might serve to promote this transformation by slowing the relative rate of catalyst decomposition and/or by stabilizing Pd-intermediates during the catalytic cycle.

Gratifyingly, under otherwise identical conditions, the phenylation of naphthalene catalyzed by Pd(II)@MOF-5(O_h) (5 mol % of Pd) resulted in greatly increased yield (64%) of phenylated naphthalenes after 12 h. In contrast to the $Pd(OAc)_2$-catalyzed reaction, the yield of product steadily increased with time, indicating that Pd(II)@MOF-5(O_h) remains catalytically viable significantly longer than $Pd(OAc)_2$. Furthermore, the Pd(II)@MOF-5(O_h)-based catalyst provided significantly different site selectivity (3:1 ratio of **A** : **B** isomers) as compared to $Pd(OAc)_2$. This highlights the exciting promise of the MCP framework to modulate the selectivity of this and other transformations.[74]

Figure 4.11. Pd-catalyzed direct phenylation of naphthalene using Pd(II)@MOF-5(O_h) (circles) and $Pd(OAc)_2$ (triangles) as a catalyst.

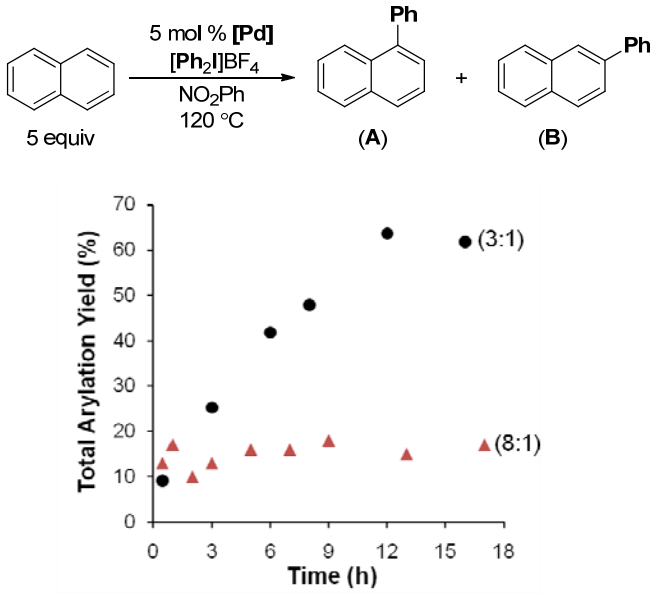

Conditions: The Pd loading of Pd(II)@MOF-5(O_h) is 2.3 wt % determined by ICP-OES, and yield and selectivity were determined by GC/MS using internal standard.The ratio of isomers (α:β) at the end of reaction is in the parenthesis

Next, potential loss of active Pd species from the crystals was tested. Pd(II)@MOF-5(O_h) crystals were removed from a catalytic reaction mixture by hot filtration after heating for 3 h. The isolated solution did not show any further catalytic activity under the same reaction conditions. In addition, nitrobenzene containing only Pd(II)@MOF-5(O_h) was heated for 3-16 h and the solid was then removed by hot filtration. Naphthalene and oxidant were added to the filtrate, and the mixture was heated for 12 h, giving only 2-8% of phenylated products. These results suggest that Pd catalyst diffusion out of the solid support is negligible.

PXRD studies of recovered solid from the reactions conducted by Dr. Park showed that the MOF-5(O_h) framework gradually degraded with reaction time, although Pd(II)@MOF-5(O_h) did not lose crystallinity under the same conditions when either of the reactants was not present in the solution (Figure 4.12). After 12 h, the crystallinity of the MCP completely disappeared and the arylation also terminated. A TEM study also conducted by Dr. Park and coworkers of solid collected from the reaction showed that ~20 nm Pd nanoparticles were spread over a non-crystalline solid which led to broad Pd metal reflections in the PXRD pattern at 40.2 and 46.5°. Such MCP decomposition suggests that defect inclusion in more robust MCP crystals will be useful in producing significantly improved catalysts for direct C–H arylation. Additionally, only modest site selectivity was observed for the Pd(II)@MOF-5(O_h)-catalyzed naphthalene arylation. Exploring the influence of pore size/shape on selectivity is another exciting future direction.

Figure 4.12. Characterization of Pd(II)@MOF-5(O_h) during and after catalysis. (a) PXRD study of solid obtained from filtration of the reaction mixture of the Pd(II)@MOF-5(O_h)-catalyzed phenylation of naphthalene in nitrobenzene at 120 °C. (b) TEM image of solid obtained from the 12 h reaction mixture (scale bar: 100 nm).

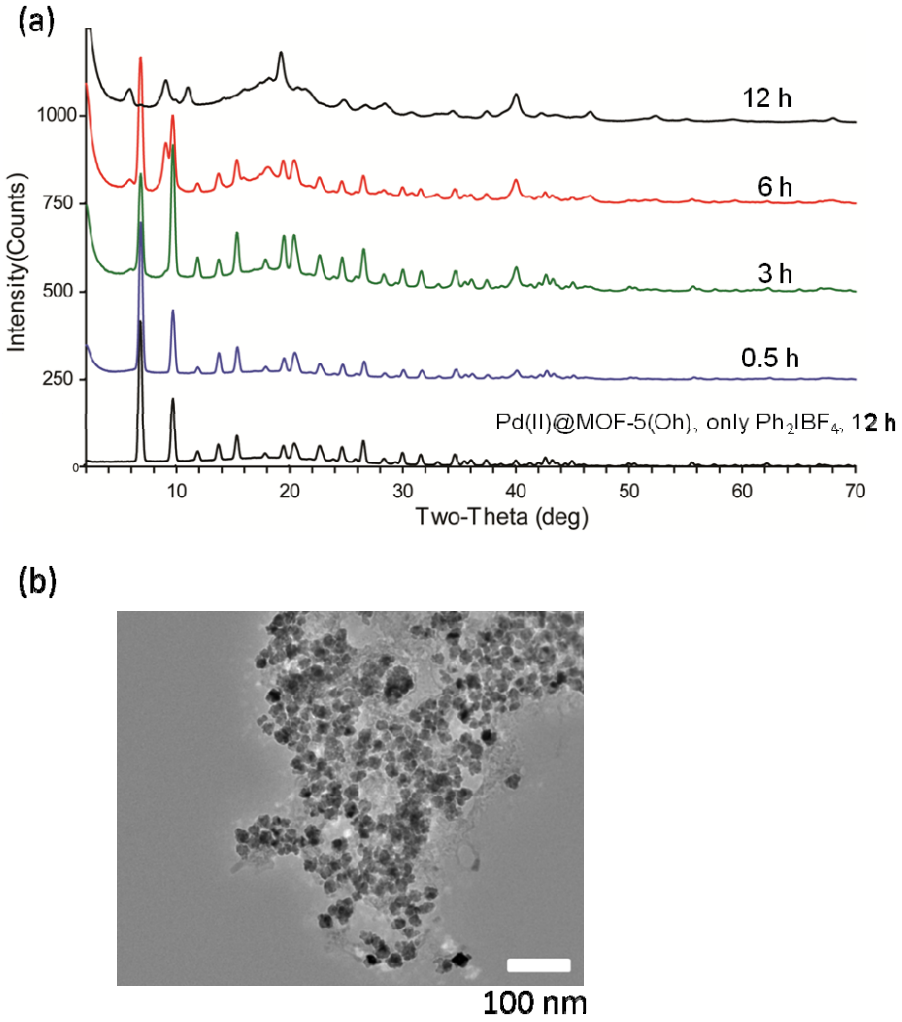

4.4 Conclusions

In conclusion, we have developed the first high yielding site- and chemoselective process for the C–H arylation of naphthalene. Under our optimized reaction conditions, preliminary mechanistic data is consistent with a $Pd^{II/IV}$ catalytic cycle involving naphthalene π-coordination and subsequent

palladation. This work adds to a small but growing body of literature implicating C–H activation at high oxidation state Pd centers in catalysis.[24,59,75,76] It also suggests, for the first time, that both reactivity and selectivity in Pd^{IV}-mediated C–H arylation can be tuned through modification of supporting ligand structure.

Additionally, this strategy was applied in the development of a heterogeneous Pd-catalyst for C–H arylation of naphthalene. This catalyst demonstrates significantly improved yield and catalyst longevity versus homogeneous $Pd(OAc)_2$ as well as different selectivity. We anticipate that this novel synthetic approach can be further applied to different MCPs with different dangling linkers that could be used to tune both reactivity and selectivity as was demonstrated in the homogeneous system.

4.5 Experimental

General: ^{1}H and ^{13}C NMR spectra were recorded on Varian Inova 500 or 400 MHz NMR spectrometers with the residual solvent peak as the internal reference. Chemical shifts are reported in parts per million (ppm) (δ). Multiplicities are reported as follows: br (broad resonance), s (singlet), d (doublet), t (triplet), app t (apparent triplet), q (quartet), and m (multiplet). Coupling constants (*J*) are reported in Hz. Infrared (IR) spectroscopy was performed on a Perkin Elmer FTIR, and peaks are reported in cm^{-1}. Elemental analyses were performed by Atlantic Microlab, Inc., Norcross, Georgia. Naphthalene was purchased from Fisher Scientific and nitrobenzene was purchased from Acros and used without further purification. $[Ph_2I]BF_4$[77] and $[Ar_2I]BF_4$[78] were prepared according to previously reported procedures and matched reported characterization.[79] dtbpyPdCl_2 (**2**)[80] and phenPdCl_2 (**3**)[81] were synthesized by adaptation of published procedures. All reactions were conducted on the bench top (without exclusion of ambient air/moisture) unless otherwise noted. Arylation reactions were analyzed on a Shimadzu GC-MS-QP2010 Plus equipped with a Shimadzu SHRXI-5MS column. Calibration curves were prepared for phenylnaphthalene,

biphenyl, 1,1-binaphthyl, and chlorobenzene relative to a hexadecane internal standard for determination of yields and selectivities.

General Procedure for Tables 2-4. Reactions were prepared in 4 mL screw cap vials. Each vial was charged with $[Ph_2I]BF_4$ (27.1 mg, 0.0735 mmol, 1 equiv), arene substrate (0.368 mmol total, 5 equiv), Pd catalyst (3.68 μmol, 5 mol %) and nitrobenzene (0.75 mL). The vials were fitted with Teflon-lined caps, stirred at the appropriate temperature in a preheated aluminum block for 16 h, and then cooled to room temperature. Hexadecane (22 μL, 0.0735mmol) was added to the vials as an internal standard. The reaction mixture was filtered through a Celite plug, and the plug was washed with ethyl acetate. The filtrate was diluted to approximately 10 mL and analyzed by GCMS. Yields and selectivities were determined by comparison to calibration curves.

General Procedure for Table 5. Reactions were prepared in 20 mL screw cap vials. Each vial was charged with $[Ar_2I]BF_4$ (0.39-0.49 mmol, 1 equiv), naphthalene (7.7-9.8 mmol, 20 equiv), Pd catalyst (19.3-24.5 μmol, 5 mol %) and nitrobenzene (3.9-5 mL, 98 mM in oxidant). The vials were fitted with Teflon-lined caps, stirred at 130 °C in a preheated aluminum block for 16 h, and then cooled to room temperature. The reaction mixture was transferred to a small round bottom flask and the nitrobenzene, naphthalene, and volatile iodoarenes were distilled away under vacuum at 50 °C. The remaining residue was then purified by flash column chromatography using Biotage Isolera gradient flash column chromatography (benzene (12-100%) : hexane).

*General Kinetics Information***.** The reaction kinetics were measured using the method of initial rates. In each experiment, the appearance of products (**A**+**B**) was monitored to ~10% conversion by GCMS. Each experiment was run in duplicate, and all kinetic orders represent an average of these two runs. Sigma Plot 10 was used to fit the data and determine both initial rates and orders.

Discussion of Kinetics Procedure. The catalysts used for kinetic experiments were stored on the bench top in 20 mL scintillation vials with Teflon-lined caps

from 24 h to 2 weeks before use. Kinetic experiments were run in two dram vials sealed with Teflon-lined caps. Each data point represents a reaction in an individual vial. When the reaction between catalyst **5b**, $[Ph_2I]BF_4$, and naphthalene was run directly, the kinetics showed a distinct induction period during which Ph–Cl was generated (prior to the formation of significant quantities of phenylnaphthalene). To eliminate the induction period, the catalyst was preinitiated by stirring with 1 equiv of oxidant in nitrobenzene at 130 °C (see below for full procedure). This pre-initiation of the catalyst led to clean initial rates kinetics.

Kinetics Procedure. Catalyst **5b** (1 equiv) and $[Ph_2I]BF_4$ (1 equiv) were dissolved in nitrobenzene to make a 24.2 mM solution, and the resulting mixture was heated to 130 ºC. After 3 h, all of the oxidant had been consumed and 1 equiv each of phenyl iodide and phenyl chloride were observed, signifying complete initiation. This solution was allowed to cool to room temperature and then used immediately. Each vial was then charged with oxidant, substrate, and nitrobenzene, and the pre-initiated solutions of catalyst were added to give a total volume of 0.75 mL. Each vial was heated in a preheated aluminum block for the required time and then immediately quenched by placing in an ice bath. Hexadecane (22 µL, 0.0735mmol) was added to the vials as an internal standard. The reaction mixture was filtered through a Celite plug, and the plug was rinsed with ethyl acetate. The filtrate was diluted to approximately 10 mL and analyzed by GCMS.

Kinetic Isotope Effect. The KIE was determined by comparing the initial reaction rate with naphthalene (Figure S1) to the initial reaction rate with naphthalene-d_8 (Figure S2). Both reactions were conducted using the standard kinetics procedure above, using arene substrate (0.368 mmol, 5 equiv), $[Ph_2I]BF_4$ (0.0735 mmol, 1 equiv), and **5b** (3.68 µmol, 5 mol %, added as a pre-initiated solution). These experiments provided a KIE of 1.0 ± 0.1.

Competition Isotope Effect. Naphthalene (23.6 mg, 0.184 mmol, 2.5 equiv), naphthalene-d_8 (25.0 mg, 0.184 mmol, 2.5 equiv), and $[Ph_2I]BF_4$ (27.1 mg, 0.0735 mmol, 1 equiv) were combined in a 4 mL vial and dissolved in nitrobenzene (0.60 mL). A pre-initiated solution of catalyst **5b** in nitrobenzene (0.15 mL of a 24.2 mM solution) was then added. The reaction was stirred at 130 ºC for 45 min (to 14.2 ± 0.7 % yield of phenylnaphthalene). The resulting mixture was filtered through a Celite plug, and the plug was rinsed with ethyl acetate. The filtrate was diluted to approximately 10 mL and analyzed by GCMS (Figure S3). The ratio of products was determined by comparing the ratio of the intensities of the two parent ion peaks (204 and 211 for **A** and **A-*d*$_7$**) to a calibration curve (Figures S4 and S5). The calibration curve was generated using known quantities of **A** and **A-*d*$_7$**. On the basis of this data, the competition KIE (k_H/k_D) was determined to be 1.07 ± 0.03.

General Procedure for Pd(II)@MOF-5(O_h)-catalyzed phenylation of naphthalene.

Reactions were prepared in 4 mL screw cap vials. Each vial was charged with $[Ph_2I]BF_4$ (27.1 mg, 0.0735 mmol, 1 equiv), naphthalene (47.1 mg, 0.368 mmol, 5 equiv), Pd(II)@MOF-5 (17.0 mg, 3.68 μmol Pd, 5 mol % Pd) and nitrobenzene (0.75 mL). The Pd content within Pd(II)@MOF-5(O_h) was 2.3 wt % determined by ICP-OES. The vials were fitted with Teflon-lined caps and slowly shaken at 120 °C in a preheated aluminum block for an appropriate time, and then cooled to room temperature. Hexadecane (22 μL, 0.0735mmol) was added to the vials as an internal standard. The reaction mixture was filtered through a Celite plug, and the plug was washed with ethyl acetate. The filtrate was diluted to approximately 10 mL and analyzed by GCMS. Yields and selectivities were determined by comparison to calibration curves.

4.6 Characterization

*General procedure for synthesis of compounds **S1-S6**:*

The diimine ligands were prepared according to literature procedure.[82,83] The appropriate aniline and 2,3-butanedione were dissolved in methanol. Formic acid (1-6 drops) was added, and the reaction was allowed to stand unstirred until crystals began to form (typically overnight). The reaction mixture was then stirred overnight. The precipitate was collected on a fritted filter, washed with methanol and dried under vacuum.

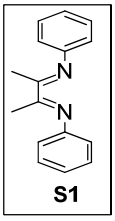

S1

The general procedure was followed using aniline (2.1 mL, 23 mmol, Aldrich), 2,3-butanedione (0.6 mL, 6.8 mmol, TCI), and methanol (10 mL). Compound **S1** was obtained as a pale yellow solid (422 mg, 26% yield). ^{1}H NMR (400 MHz, C_6D_6): δ 7.15 (t, *J* = 8 Hz, 4H), 6.93 (t, *J* = 8 Hz, 2H), 6.72 (d, *J* = 8 Hz, 4H), 2.10 (s, 6H). ^{13}C NMR (100 MHz, C_6D_6): δ 168.62, 152.00, 129.62, 124.36, 119.50, 15.61.

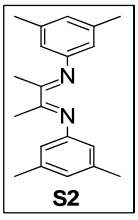

S2

The general procedure was followed using 3,5-dimethylaniline (1.0 mL, 8 mmol, Acros), 2,3-butanedione (0.21 mL, 2.4 mmol, TCI), and methanol (15 mL). Compound **S2** was obtained as a yellow solid (437 mg, 62% yield). ^{1}H NMR (400 MHz, C_6D_6): δ 6.64 (s, 2H), 6.46 (s, 4H), 2.23 (s, 6H), 2.17 (s, 12H). ^{13}C NMR (100 MHz, C_6D_6): δ 168.38, 152.29, 139.05, 126.00, 117.20, 21.77, 15.72.

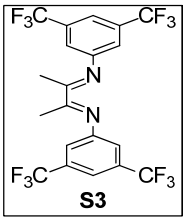

S3

The general procedure was followed using 3,5-ditrifluoromethylaniline (2.6 mL, 16.6 mmol, Matrix Scientific), 2,3-butanedione (0.76 mL, 8.7 mmol, TCI), and methanol (1 mL). Compound **S3** was obtained as a pale yellow solid (1.678 g, 38% yield). ^{1}H NMR (400 MHz, C_6D_6): δ 7.58 (s, 2H), 6.98 (s, 4H), 1.61 (s, 6H). ^{13}C NMR (100 MHz, C_6D_6): δ 169.97, 152.39, 133.24 (q, ^{2}J = 33 Hz), 124.1 (q, J = 273 Hz), 119.55, 118.21, 15.40. ^{19}F NMR (376 MHz, C_6D_6): δ 62.67 (s).

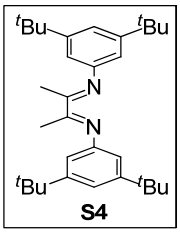

S4

The general procedure was followed using 3,5-di-*tert*-butylaniline (0.499 g, 2.4 mmol, TCI), 2,3-butanedione (0.11 mL, 1.3 mmol, TCI), and methanol (8 mL). Compound **S4** was obtained as a pale yellow solid (477 mg, 80%). ^{1}H NMR (400 MHz, acetone-d_6): δ 7.25 (s, 2H), 6.67 (s, 4H), 2.12 (s, 6H), 1.34 (s, 36H). ^{13}C NMR (100 MHz, acetone-d_6): δ 167.58, 151.37, 150.77, 117.39, 130.06, 34.58, 30.83, 14.41.

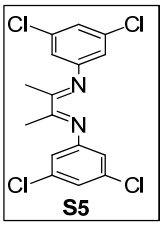

S5

The general procedure was followed using 3,5-dichloroaniline (2.7 g, 16.6 mmol, Aldrich), 2,3-butanedione (0.76 mL, 8.7 mmol, TCI), and methanol (1 mL). Compound **S5** was obtained as a light gray solid (1.948 g, 62% yield). ^{1}H NMR (400 MHz, C_6D_6): δ 6.94 (s, 2H), 6.46 (s, 4H), 1.69 (s, 6H). ^{13}C NMR (100 MHz, C_6D_6): δ 169.71, 153.53, 136.38, 124.69, 118.07, 15.71.

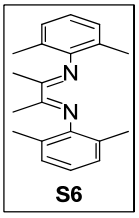

S6

The general procedure was followed using 2,6-dimethylaniline (1.6 mL, 13 mmol, Aldrich), 2,3-butanedione (0.56 mL, 6.4 mmol, TCI), and methanol (4 mL). Compound **S6** was obtained as a yellow solid (1.267 g, 67% yield). ^{1}H NMR (400 MHz, C_6D_6): δ 7.03 (d, *J* = 7.2 Hz, 4H), 6.95 (t, *J* = 7.2 Hz, 2H), 2.00 (s, 6H), 1.97 (s, 12H). ^{13}C NMR (100 MHz, C_6D_6): δ 168.45, 149.46, 128.74, 125.06, 123.96, 18.26, 16.06.

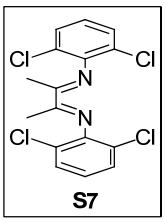

S7

Diimine ligand **S7** was synthesized on a 17.3 mmol scale according to a procedure reported by Chen.[4] However, in lieu of column chromatography, the crude yellow solid was purified by dissolving in a minimal quantity of methylene

chloride and then allowing the solvent to slowly evaporate overnight, which afforded large yellow crystals. The crystals were collected on a fritted filter and washed with hexanes (4 x 2 mL) to afford **S7** as a yellow crystalline solid (566.1 mg, 9% yield). ^{1}H NMR (400 MHz, C_6D_6): δ 6.96 (d, *J* = 8.0 Hz, 4H), 6.35 (t, *J* = 8.0 Hz, 2H), 2.16 (s, 6H). ^{13}C NMR (100 MHz, C_6D_6): δ 171.98, 146.03, 128.70, 125.16, 124.37, 17.20.

*General Procedure for synthesis of complexes **1**, **4a-d**, **5a,b**, and **10**:*

$PdCl_2$ was dissolved in acetonitrile, and the resulting suspension was heated at reflux until a clear, orange solution formed (indicative of $(MeCN)_2PdCl_2$). The appropriate diimine ligand was then added, and the reaction mixture was heated at reflux for 4-12 h. The reaction was cooled to room temperature, and the orange precipitate was collected on a fritted filter, washed with acetonitrile and ether, and dried under vacuum. ^{13}C NMR spectral data is not reported for any of the dichloride complexes due to their extremely low solubility.

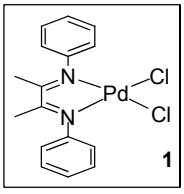

1

The general procedure was followed using $PdCl_2$ (88.7 mg, 0.5 mmol, Pressure), diimine ligand **S1** (118.16 mg, 0.5 mmol), and MeCN (10 mL). Complex **1** was obtained as a bright orange solid (161.4 mg, 78% yield). ^{1}H NMR (500 MHz, acetone-d_6): δ 7.44 (app t, *J* = 8 Hz, 4H), 7.33 (t, *J* = 8 Hz, 2H), 7.09 (d, *J* = 8 Hz, 4H), 2.29 (s, 6H). The purity of all samples of complex **1** used for catalysis was confirmed by elemental analysis. Anal. Calcd. for $C_{16}H_{16}Cl_2N_2Pd$: C, 46.46; H, 3.90; N, 6.77; Found: C, 46.26; H, 3.69; N, 6.79.

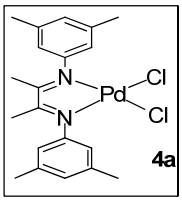

The general procedure was followed using $PdCl_2$ (88.7 mg, 0.5 mmol, Pressure), diimine ligand **S2** (146.21 mg, 0.5 mmol), and MeCN (10 mL). Complex **4a** was obtained as a bright orange solid (212.3 mg, 90% yield). NMR characterization of this complex was not possible due to low solubility. The purity of all samples of complex **4a** used for catalysis was confirmed by elemental analysis. Anal. Calcd. for $C_{20}H_{24}Cl_2N_2Pd$: C, 51.14; H, 5.15; N, 5.96; Found: C, 50.88; H, 5.06; N, 6.17.

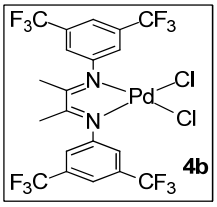

The general procedure was followed using $PdCl_2$ (88.7 mg, 0.5 mmol, Pressure), diimine ligand **S3** (254.15 mg, 0.5 mmol), and MeCN (10 mL). Complex **4b** was obtained as a bright orange solid (281.9 mg, 82% yield). ^{1}H NMR (400 MHz, acetone-d_6): δ 8.09 (s, 2H), 7.81 (s, 4H), 2.52 (s, 6H). ^{19}F NMR (376 MHz, acetone-d_6): δ 63.42 (s). The purity of all samples of complex **4b** used for catalysis was confirmed by elemental analysis. Anal. Calcd. for $C_{20}H_{12}Cl_2F_{12}N_2Pd$: C, 35.04; H, 1.76; N, 4.09; Found: C, 35.09; H, 1.67; N, 4.12.

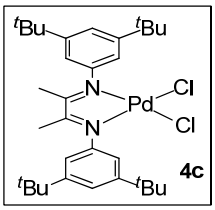

The general procedure was followed using $PdCl_2$ (19.5 mg, 0.11 mmol, Pressure), diimine ligand **S4** (49.6 mg, 0.11 mmol), and MeCN (2 mL). Complex **4c** was obtained as a bright orange solid (49.0 mg, 70% yield). ^{1}H NMR (400

MHz, acetone-d_6): δ 7.44 (s, 2H), 6.99 (s, 4H), 2.31 (s, 6H), 1.35 (s, 36H). The purity of all samples of complex **4c** used for catalysis was confirmed by elemental analysis. Anal. Calcd. for $C_{32}H_{48}Cl_2N_2Pd$: C, 60.24; H, 7.58; N, 4.39; Found: C, 59.58; H, 7.70; N, 4.88.

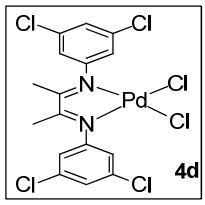

The general procedure was followed using $PdCl_2$ (53.9 mg, 0.304 mmol, Pressure), diimine ligand **S5** (113.7 mg, 0.304 mmol), and MeCN (5 mL). Complex **4d** was obtained as a bright orange solid (130.8 mg, 78% yield). NMR characterization was not possible due to insolubility. The purity of all samples of complex **4d** used for catalysis was confirmed by elemental analysis. Anal. Calcd. for Anal. Calcd. for $C_{16}H_{12}Cl_6N_2Pd$: C, 34.85; H, 2.19; N, 5.08; Found: C, 34.94; H, 2.09; N, 5.35.

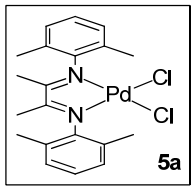

The general procedure was followed using $PdCl_2$ (145.9 mg, 0.823 mmol, Pressure), diimine ligand **S6** (240.7 mg, 0.823 mmol), and MeCN (10 mL). Complex **5a** was obtained as a bright orange solid (345.8 mg, 89% yield). NMR characterization was not possible due to insolubility. The purity of all samples of complex **5a** used for catalysis was confirmed by elemental analysis. Anal. Calcd. for $C_{20}H_{24}Cl_2N_2Pd$: C, 51.14; H, 5.15; N, 5.96; Found: C, 51.09; H, 5.05; N, 5.90.

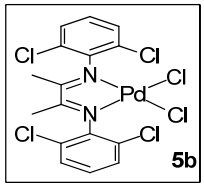

The general procedure was followed using $PdCl_2$ (145.9 mg, 0.823 mmol, Pressure), diimine ligand **S7** (307.8 mg, 0.823 mmol) and MeCN (10 mL). Complex **5b** was obtained as a bright orange solid (384.4 mg, 85% yield). ^{1}H NMR (400 MHz, CD_3CN): δ 7.55 (d, *J* = 8 Hz, 4H), 7.40 (t, *J* = 8 Hz, 2H), 2.20 (s, 6H). The purity of all samples of complex **5b** used for catalysis was confirmed by elemental analysis. Anal. Calcd. for $C_{16}H_{12}Cl_6N_2Pd$: C, 34.85; H, 2.19; N, 5.08; Found: C, 34.57; H, 2.00; N, 4.98.

*General procedure for synthesis of complexes **S8-S10:***

Complexes of general structure (diimine)$Pt(Me)_2$ were prepared using a procedure analogous to that reported by Bercaw.[82] An oven dried Schlenk flask under N_2 was charged with $[Me_2Pt(SMe_2)]_2$ and 2.5 equiv of the appropriate diimine. The flask was then cooled to –78 °C. Dry toluene was added, and the reaction was stirred for 3 d while warming to room temperature. Once per day, the headspace was evacuated to remove dimethylsulfide. After three days, the toluene was removed under vacuum. Petroleum ether was added and to afford a precipitate, which was collected by filtration and dried under vacuum.

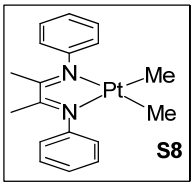

S8

The general procedure was followed using $[Me_2Pt(SMe_2)]_2$[84] (40 mg, 0.0696 mmol), diimine **S1** (41.1 mg, 0.174 mmol, 2.5 equiv), and dry toluene (4 mL). The solution turned dark purple upon reaching room temperature. Complex **S8** was obtained as a purple solid (41.5 mg, 65% yield). ^{1}H NMR (400 MHz, CD_2Cl_2): δ 7.50 (app t, *J* = 7.4 Hz, 4H), 7.30 (t, *J* = 7.4 Hz, 2H), 7.02 (d, *J* = 7.6 Hz 6H), 1.42 (s, 6H), 0.94 (s, J_{Pt-H} = 87 Hz, 6H). ^{13}C NMR (100 MHz, CD_2Cl_2): δ 171.29, 148.30, 129.23, 126.61, 122.27, 21.27, –13.4.

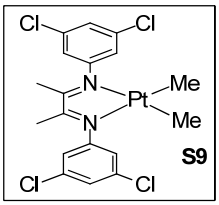

The general procedure was followed using $[Me_2Pt(SMe_2)]_2$ (40 mg, 0.0696 mmol), diimine **S5** (65.1 mg, 0.174 mmol, 2.5 equiv), and dry toluene (4 mL). The solution turned magenta upon reaching room temperature. Complex **S9** was obtained as a magenta solid (66.2 mg, 79% yield). ^{1}H NMR (400 MHz, CD_2Cl_2): δ 7.35 (s, 2H), 6.99 (s, 4H), 1.36 (s, 6H), 1.16 (s, $J_{Pt\text{-}H}$ = 87 Hz, 6H).

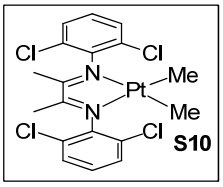

The general procedure was followed using $[Me_2Pt(SMe_2)]_2$ (40 mg, 0.0696 mmol), diimine **S7** (65.1 mg, 0.174 mmol, 2.5 equiv), and dry toluene (4 mL). The solution turned dark green upon reaching room temperature. Complex **S10** was obtained as a blue-green solid (71 mg, 69% yield). ^{1}H NMR (400 MHz, CD_2Cl_2): δ 7.55 (d, J = 8 Hz, 4H), 7.25 (t, J = 8 Hz, 2H), 1.16 (s, 6H), 1.14 (s, $J_{Pt\text{-}H}$ = 88 Hz, 6H). ^{13}C NMR (100 MHz, CD_2Cl_2): δ 172.39, 142.62, 128.14, 127.47, 127.26, 20.83, –15.63.

*General Procedure for synthesis of complexes **6**, **7d**, and **8b**:*

Under N_2, an oven dried Schlenk flask was charged with complex **S8**, **S9**, or **S10** (0.015 mmol) and trifluoroethanol (2 mL). HBF_4 (2 μL) was added. CO was bubbled through the solution for approximately 10 min. The reaction was then stirred under 1 atm of CO for 24 h. The solvent was removed under vacuum with the solution maintained at –10 C. The resulting sticky residue was triturated with

petroleum ether (1.5 mL), and the resulting solids were collected and dried under vacuum.

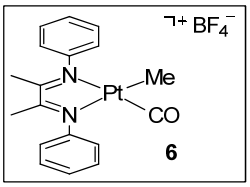

6

Complex **6** was obtained as a brown solid (5.3 mg, 63% yield) ^{1}H NMR (400 MHz, CD_2Cl_2): δ 7.59 (m, 4 H), 7.44 (m, 2H), 7.32 (d, J = 8 Hz, 2H), 7.14 (d, J = 8 Hz, 2H), 2.43 (s, 3H), 2.31 (s, 3H), 0.715 (s, $J_{Pt\text{-}H}$ = 34 Hz, 3H). ^{13}C NMR (100 MHz, CD_2Cl_2): δ 190.19, 177.64, 163.24, 147.85, 143.16, 130.67, 130.38, 129.38, 129.20, 122.65, 121.42, 22.55, 20.64, –10.53. ^{19}F NMR (376 MHz, CD_2Cl_2): δ –150.06 (s). IR (CH_2Cl_2): ν_{CO} = 2106.9 cm^{-1}.

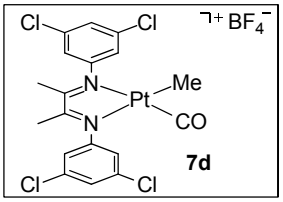

7d

Complex **7d** was obtained as a red solid (5.2 mg, 50% yield). ^{1}H NMR (500 MHz, CD_2Cl_2): δ 7.37 (s, 1H), 7.34 (s, 1H), 7.18 (s, 2H), 7.04 (s, 2H), 2.36 (s, 3H), 2.21 (s, 3H), 0.687 (s, $J_{Pt\text{-}H}$ = 34 Hz, 3H). ^{13}C NMR (100 MHz, CD_2Cl_2): δ 190.82, 178.94, 169.75, 148.79, 144.18, 137.18, 136.94, 129.61, 129.49, 121.39, 119.99, 22.81, 20.93, –10.22. ^{19}F NMR (376 MHz, CD_2Cl_2): δ –149.43 (s). IR (CH_2Cl_2): ν_{CO} = 2109.9 cm^{-1}.

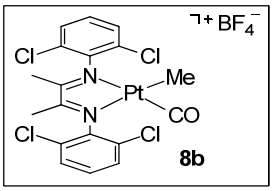

8b

Complex **8b** was obtained as a dark blue solid (6.1 mg, 58% yield). ^{1}H NMR (400 MHz, CD_2Cl_2): δ 7.37 (s, 1 H), 7.66 (m, 4H), 7.47 (m, 2H), 2.58 (s, 3H), 2.40 (s, 3H), 0.762 (s, $J_{Pt\text{-}H}$ = 34 Hz, 3H). ^{13}C NMR (100 MHz, CD_2Cl_2): δ 192.31, 181.35, 161.74, 141.48, 137.00, 131.76, 131.32, 130.07, 129.83, 128.66, 127.28, 22.58, 21.43, –11.34. ^{19}F NMR (376 MHz, CD_2Cl_2): δ –151.63 (s). IR (CH_2Cl_2): ν_{CO} = 2116.3 cm^{-1}.

Arylation Reactions:

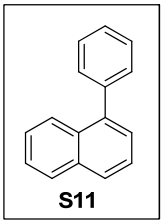
S11

The general procedure was followed using $[Ph_2I]BF_4$ (180.1 mg, 0.490 mmol, 1 equiv), naphthalene (1.245 g, 9.79 mmol, 20 equiv), Pd catalyst **5b** (24.5 μmol, 5 mol %) and nitrobenzene (5 mL) and stirring for 16 h. Compound **S11** was obtained as a yellow oil (72.2 mg, 72% yield). NMR data was consistent with the literature.[85] ^{1}H NMR (400 MHz, $CDCl_3$): δ 7.90-7.87 (m, 2H), 7.86-7.84 (m, 1H), 7.53-7.44 (m, 6H), 7.43-7.39 (m, 3H).

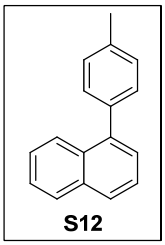

S12

The general procedure was followed using [*p*-Tol_2I]BF_4 (193.8 mg, 0.490 mmol, 1 equiv), naphthalene (1.245 g, 9.79 mmol, 20 equiv), Pd catalyst **5b** (24.5 µmol, 5 mol %) and nitrobenzene (5 mL) and stirring for 16 h. Compound **S12** was obtained as a yellow oil (72.5 mg, 68% yield). NMR data was consistent with the literature.[86] ^{1}H NMR (400 MHz, $CDCl_3$): δ 7.89 (app t, 2 H), 7.82 (d, J = 8 Hz, 1H), 7.45-7.51 (m, 2H), 7.42-7.37 (m, 4H), 7.29 (d, J = 8 Hz), 2.44 (s, 3H)

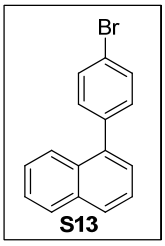

S13

The general procedure was followed using [*p*-$BrPh_2I$]BF_4 (214.8 mg, 0.490 mmol, 1 equiv), naphthalene (1.245 g, 9.79 mmol, 20 equiv), Pd catalyst **5b** (24.5 µmol, 5 mol %) and nitrobenzene (5 mL) and stirring for 16 h. Compound **S13** was obtained as a yellow oil (90.4 mg, 65% yield). NMR data was consistent with the literature.[85] ^{1}H NMR (400 MHz, $CDCl_3$): δ 7.90-7.81 (m, 3H), 7.60 (d, *J* = 8 Hz, 2H), 7.50-7.34 (m, 6H).

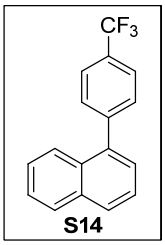

S14

The general procedure was followed using [*p*-CF_3Ph_2I]BF_4 (204.2 mg, 0.490 mmol, 1 equiv), naphthalene (1.245 g, 9.79 mmol, 20 equiv), Pd catalyst **5b** (24.5

μmol, 5 mol %) and nitrobenzene (5 mL) and stirring for 16 h. Compound **S14** was obtained as a yellow oil (82.5 mg, 62% yield). NMR data was consistent with the literature.[87] ^{1}H NMR (400 MHz, $CDCl_3$): δ 7.90 (app t, *J* = 8Hz, 2H), 7.79 (d, *J* = 8Hz, 1H), 7.74 (d, *J* = 8Hz, 2H), 7.60 (d, *J* = 8Hz, 2H), 7.55-7.39 (m, 4H)

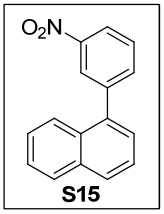

S15

The general procedure was followed using [*m*-NO_2Ph_2I]BF_4 (183.7 mg, 0.401 mmol, 1 equiv), naphthalene (1.02g, 8.02 mmol total, 20 equiv), Pd catalyst **5b** (11.0 mg, 20 μmol, 5 mol %) and nitrobenzene (4.1 mL) and stirring for 16 h. Compound **S15** was obtained as a yellow oil (70.5 mg, 71% yield). NMR data was consistent with the literature.[85] ^{1}H NMR (500 MHz, $CDCl_3$): δ 8.37 (s, 1H), 8.29 (d, *J* = 8 Hz, 1H), 7.93 (t, *J* = 7 Hz, 2H), 7.83-7.81 (m, 1H), 7.75 (d, *J* = 9 Hz, 1H), 7.66 (t, *J* = 8 Hz, 1H), 7.56-7.51 (m, 2H), 7.48-7.42 (m, 2H)

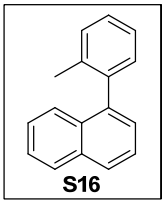
S16

The general procedure was followed using [*o*-$MePh_2I$]BF_4 (153.0 mg, 0.386 mmol, 1 equiv), naphthalene (990.75 mg, 7.73 mmol total, 20 equiv), Pd catalyst **5b** (10.7 mg, 19.3 μmol, 5 mol %) and nitrobenzene (3.9 mL) and stirring for 16 h. Compound **S16** was obtained as a clear oil (trace).

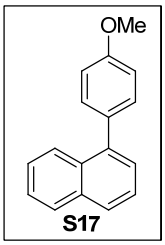

S17

The general procedure was followed using [*p*-OMePh$_2$I]BF$_4$ (171.6 mg, 0.401 mmol, 1 equiv), naphthalene (1.02 g, 8.02 mmol, 20 equiv), Pd catalyst **5b** (11.0 mg, 20 μmol, 5 mol %) and nitrobenzene (4.1 mL) and stirring for 16 h. Compound **S17** was not observed under the reaction conditions.

Synthesis of MOF-5(O_h) and impregnation of palladium

H_2BDC (0.300 g 1.81 mmol), H_3BTB (0.0794 g, 0.181 mmol), and $Zn(NO_3)_2 \cdot 6H_2O$ (1.50 g, 5.04 mmol) were dissolved in DEF (50 mL). The mixture was heated at 100 °C for 24 h. The mother liquor was decanted and the crystals were washed with DMF three times and CH_2Cl_2 twice. The MOF-5(O_h) crystals were immersed in a solution of $Pd(OAc)_2$ (25.0 mg, 0.111 mmol) in 12.5 mL CH_2Cl_2 (8.91 mM) and the mixture was slowly shaken using a shaker for 2 d. Then a fresh $Pd(OAc)_2$ solution was replenished and the mixture was shaken for another 2 d. The solution was decanted and the crystals were washed with CH_2Cl_2 three times and immersed in CH_2Cl_2 for 2 days during which fresh CH_2Cl_2 was replenished three times to afford brown Pd(II)@MOF-5(O_h) crystals. For reduction of Pd, Pd(II)@MOF-5(O_h) was immersed in DMF (5.0 mL). The solution of $NaBH_4$ (30.0 mg, 0.0793 mmol) in DMF (10 mL) was added and the mixture was shaken for 2 h. After the solution was decanted, the black crystals were washed with DMF three times and immersed in CH_2Cl_2 for 24 h during which fresh CH_2Cl_2 was replenished three times. The crystals were dried under vacuum at room temperature for 20 h (yield 370 mg).

4.7 References

[1.] Hassan, J.; Sevignon, M.; Gozzi, C.; Schulz, E.; Lemaire, M. *Chem. Rev*. **2002**, *102*, 1359.

[2.] Chiusoli, G. P.; Catellani, M.; Costa, M.; Motti, E.; Ca', N. D.; Maestri, G. *Coord. Chem. Rev*. **2010**, *254*, 456.

[3.] McGlacken, G. P.; Bateman, L. *Chem. Soc. Rev.* **2009**, *38*, 2447.

[4.] Alberico, D.; Scott, M. E.; Lautens, M. *Chem. Rev*. **2007**, *107*, 174.

[5.] Daugulis, O.; Do, H. Q.; Shabashov, D. *Acc. Chem. Res*. **2009**, *42*, 1074.

[6.] Lyons, T. W.; Sanford, M. S. *Chem. Rev*. **2010**, *110*, 1147.

[7.] Sun, C. L.; Li, B. J.; Shi, Z. J. *Chem. Commun*. **2010**, *46*, 677.

[8.] Chen, X.; Engle, K. M.; Wang, D.-H.; Yu, J.-Q. *Angew. Chem. Int. Ed.* **2009**, *48*, 5094.

[9.] Muñiz, K. *Angew. Chem. Int. Ed.* **2009***, 48,* 9412.

[10.] Shi, F.; Larock, R. C. *Top. Curr. Chem.* **2010**, *292*, 123.

[11.] Campeau, L. C.; Fagnou, K. *Chem. Commun*. **2006**, 1253.

[12.] Beck, E. M.; Gaunt, M. J. *Top. Curr. Chem.* **2010**, *292*, 85.

[13.] Ackermann, L.; Vicente, R.; Kapdi, A. R. *Angew. Chem. Int. Ed.* **2009**, *48*, 9792.

[14.] Bandini, M.; Eichholzer, A. *Angew. Chem. Int. Ed.* **2009**, *28*, 9608.

[15.] Rossi, R.; Bellina, F. Tetrahedron **2009**, 65, 10269.

[16.] Lewis, J. C.; Bergman, R. G.; Ellman, J. A. *Acc. Chem. Res.* **2008**, *41*, 1013.

[17.] Zhao, X.; Yeung, C. S.; Dong, V. M. *J. Am. Chem. Soc.* **2010**, *132*, 5837.

[18.] Brasche, G.; Garcia-Fortanet, J.; Buchwald, S. L. *Org. Lett.* **2008**, *10*, 2207.

[19.] Li, B. H.; Tian, S. L.; Fang, Z.; Shi, Z. J. *Angew. Chem. Int. Ed.* **2008**, *47*, 1115.

[20.] Hull, K.; Sanford, M. S. *J. Am. Chem. Soc*. **2007**, *129*, 11904.

[21.] Li, R.; Jiang, L.; Lu, W. *Organometallics* **2006**, *25*, 5973.

[22.] Kobayashi, O.; Uraguchi, D.; Yamakawa, T. *Org. Lett.* **2009**, *11*, 2679.

[23.] Qin, C.; Jiang, L.; Lu, W. *J. Org. Chem*. **2008**, *73*, 7424.

[24.] Kawai, H.; Kobayshi, Y.; Oi, S.; Inoue, Y. *Chem. Commun*. **2008**, 1464.

[25.] Slagt, v. F.; de Vries, A. H. M.; de Vries, J. G.; Kellogg, R. M. *Org. Process Res. Dev.* **2010**, *14*, 30.

[26.] Norsikian, S.; Chang, C.-W. *Curr. Org. Synth.* **2009**, *6*, 264.

[27.] Wuertz, S.; Glorius, F. *Acc. Chem. Res.* **2008**, *41*, 1523.

[28.] Hartwig, J. F. *Acc. Chem. Res.* **2008**, *41*, 1534.

[29.] Martin, R.; Buchwald, S. L. *Acc. Chem. Res.* **2008**, *41*, 1461.

[30.] Tietze, L. F.; Ila, H.; Bell, H. *Chem. Rev.* **2004**, *104*, 3453.

[31.] Oxidant/solvent controlled site selectivity in Pd-catalyzed indole C–H functionalization: Potavathri, S.; Dumas, A. S.; Dwight, T. A.; Naumiec, G. R.; Hammann, J. M.; DeBoef, B. *Tetrahedron Lett.* **2008**, *49*, 4050.

[32.] Oxidant/solvent controlled site selectivity in Pd-catalyzed indole C–H functionalization: Grimster, N. P.; Gauntlett, C.; Godfrey, C. R. A.; Gaunt, M. J. *Angew. Chem. Int. Ed.* **2005**, *44*, 3125.

[33.] Catalyst-controlled selectivity in Pd-catalyzed arene olefination: Zhang, Y.-H.; Shi, B.-F.; Yu, J.-Q. *J. Am. Chem. Soc.* **2009**, *131*, 5072.

[34.] Catalyst-controlled selectivity in Pd-catalyzed arene carboxylation: Jintoku, T.; Taniguci, H.; Fujiwara, Y. *Chem. Lett.* **1987**, 1159.

[35.] Catalyst controlled selectivity/reactivity in ligand-directed C–H functionalization: Engle, K. M.; Wang, D.-H.; Yu, J.-Q *J. Am. Chem. Soc.* **2010***, 132*, 14137.

[36.] Hickman, A. J.; Sanford, M. S. *ACS Catalysis* **2011**, *1*, 170.

[37.] Wagner, A. M.; Sanford, M. S. *Org. Lett.* **2011**, *13*, 288.

[38.] Xiao, B.; Fu, Y.; Xu, J.; Gong, T.-J.; Dai, J.-J.; Yi, J.; Liu, L. *J. Am. Chem. Soc*. **2010**, *132*, 468.

[39.] Phipps, R. J.; Gaunt, M. J. *Science* **2009**, *323*, 1593.

[40.] Deprez, N. R.; Sanford, M. S. *J. Am. Chem. Soc.* **2009**, *131*, 11234.

[41.] Deprez, N. R.; Kalyani, D.; Krause, A.; Sanford, M. S. *J. Am. Chem. Soc.* **2006**, *128*, 4972.

[42.] Daugulis, O.; Zaitsev, V. G. *Angew. Chem. Int. Ed*. **2005**, *44*, 4046.

[43.] phen: Shibahara, F.; Yamaguchi, E.; Murai, T. *Chem. Commun*. **2010**, *46*, 2471.

[44.] bpy: Hickman, A. J.; Villalobos, J. M.; Sanford, M. S. *Organometallics* **2009**, *28*, 5316.

[45.] diimines: Lersch, M.; Tilset, M. *Chem. Rev.* **2005**, *105*, 2471.

[46.] Zhong, H. A.; Labinger, J. A.; Bercaw, J. E. *J. Am. Chem. Soc.* **2002**, *124*, 1378.

[47.] Hanhan, M. E. *Appl. Organomet. Chem.* **2008**, *22*, 270.

[48.] Helldorfer, M.; Milius, W.; Alt, H. G. *J. Organomet. Chem.* **2003**, *197*, 1.

[49.] Several reports suggest that *ortho*-Cl-aryldiimines may be a 'privileged' ligand class for group 10 metal catalysis. For example, *ortho*-Cl diimine complexes show extremely high activity for benzene H/D exchange (Pt, ref. [44]), Heck and Suzuki coupling (Pd, ref. [47]) and olefin polymerization (Ni, ref. [48]).

[50.] The related Pd carbonyl complexes were not explored due to their instability. For example, see: Carfagna, C.; Gatti, G.; Martini, D.; Pettinari, C. *Organometallics* **2001**, *20*, 2175-2182.

[51.] Bugarin, A.; Connell, B. T. *Organometallics* **2008**, *27*, 4357.

[52.] Modest GC yields were obtained with other electron-rich aromatic substrates in the absence of naphthalene. For example, 1-methoxynapthalene gave 73% yield (three isomeric products, 26 : 7 : 1 ratio), anisole provided 30% yield (three isomeric products, 4 : 3 : 1), and veratrole reacted in 61% yield (two isomeric products, 43 : 1 ratio).

[53.] Gotta, M. F.; Mayr, H. *J. Org. Chem*. **1998**, *63*, 9769.

[54.] Mayr, H.; Patz, M. *Angew. Chem. Int. Ed*. **1994**, *33*, 938.

[55.] Shul'pin, G. B.; Nizova, G. V.; Nikitaev, A. T. *J. Organomet. Chem.* **1984**, *276*, 115.

[56.] Chiong, H. A.; Pham, Q.; Daugulis, O. *J. Am. Chem. Soc.* **2007**, *129*, 9879.

[57.] Shi, Z. J.; Li, B.; Wan, X.; Cheng, J.; Fang, Z.; Cao, B.; Qin, C.; Wang, Y. *Angew. Chem., Int. Ed.* **2007**, *46*, 5554.

[58.] Lafrance, M.; Fagnou, K. *J. Am. Chem. Soc.* **2006**, *128*, 16496.

[59.] Sibbald, P. A.; Rosewall, C. F.; Swartz, R. D.; Michael, F. E. *J. Am. Chem. Soc.* **2009**, *131*, 15945.

[60.] Canty, A. J.; Patel, J.; Rodemann, T.; Ryan, J. H.; Skelton, B. W.; White, A. H. *Organometallics* **2004**, *23*, 3466.

[61.] Belt, S. T.; Dong, L.; Duckett, S. B.; Jones, W. D.; Partridge, M. G.; Perutz, R. N. *Chem. Commun.* **1991**, 266.

[62.] Naphthalene dimerization was not detected by GCMS; furthermore, no H/D exchange was observed in presence of CD_3CO_2D.

[63.] The origin of the observed regioselectivity remains the subject of detailed investigations. However, we preliminarily propose that the selectivity for **A** may be due to the highly electrophilic nature of the Pd^{IV} center, which leads to facile palladation at the most nucleophilic carbon. Additionally, the octahedral environment of the Pd^{IV} center is likely more sensitive to steric effects during both C–H cleavage and reductive elimination. These results suggest a promising new direction of study for complementary reactivity at Pd^{II} and Pd^{IV} centers.

[64.] Sherrington, D. C.; Kybett, A. P. Supported Catalysts and Their Applications; Royal Society of Chemistry: Cambridge, 2001.

[65.] (a) Millward, A. R.; Yaghi, O. M. *J. Am. Chem. Soc.* **2005**, *127*, 17998. (b) Wong-Foy, A. G.; Matzger, A. J.; Yaghi, O. M. *J. Am. Chem. Soc.* **2006**, *128*, 3494. (c) Caskey, S. R.; Wong-Foy, A. G.; Matzger, A. J. *J. Am. Chem. Soc.* **2008**, *130*, 10870.

[66.] (a) Cychosz, K. A.; Ahmad, R.; Matzger, A. J. *Chem. Sci.* **2010**, *1*, 293. (b) Ahmad, R.; Wong-Foy, A. G.; Matzger, A. J. *Langmuir* **2009**, *25*, 11977.

[67.] (a) Lee, J.; Farha, O. K.; Roberts, J.; Scheidt, K. A.; Nguyen, S. T.; Hupp, J. T. *Chem. Soc. Rev.* **2009**, *38*, 1450. (b) Ma, L.; Abney, C.; Lin, W. *Chem. Soc. Rev.* **2009**, *38*, 1248.

[68.] Xie, Z.; Ma, L.; deKrafft, K. E.; Jin, A.; Lin, W. *J. Am. Chem. Soc.* **2009**, *132*, 922.

[69.] (a) An, J.; Geib, S. J.; Rosi, N. L. *J. Am. Chem. Soc.* **2009**, *131*, 8376. (b) Horcajada, P.; et al. *Nat. Mater.* **2010**, *9*, 172.

[70.] (a) Koh, K.; Wong-Foy, A. G.; Matzger, A. J. *Chem. Commun.* **2009**, 6162. (b) Park, T.-H.; Koh, K.; Wong-Foy, A. G.; Matzger, A. J. *Cryst. Growth Des.* **2011,** *11*, 2059.

[71.] (a) Koh, K.; Wong-Foy, A. G.; Matzger, A. J. *Angew. Chem. Int. Ed.* **2008**, *47*, 677. (b) Koh, K.; Wong-Foy, A. G.; Matzger, A. J. *J. Am. Chem. Soc*. **2009**, *131*, 4184. (c) Koh, K.; Wong-Foy, A. G.; Matzger, A. J. *J. Am. Chem. Soc*. **2010**, *132*, 15005.

[72.] Furukawa, H.; Ko, N.; Go, Y. B.; Aratani, N.; Choi, S. B.; Choi, E.; Yazaydin, A. O.; Snurr, R. Q.; O'Keeffe, M.; Kim, J.; Yaghi, O. M. *Science* **2010**, *329*, 424.

[73.] Kleist, W.; Maciejewski, M.; Baiker, A. *Thermochim. Acta* **2010**, *132*, 14382.

[74.] (a) Only a small background reaction was observed in the presence of unmetalated MOF-5(O_h) (resulting in 7% yield, 5:1 selectivity after 16 h). (b) The presence of MOF-5 crystals under a homogeneous catalyst reaction with $Pd(OAc)_2$ only slightly improved the yield (21%) with a parallel selectivity (8:1) after 16 h.

[75.] Hull, K. L.; Lanni, E. L.; Sanford, M. S. *J. Am. Chem. Soc.* **2006**, *128*, 14047.

[76.] Pilarski, L. T.; Selander, N.; Bose, D.; Szabo, K. J. *Org. Lett.* **2009**, *11*, 5518.

[77.] Ochiai, M.; Toyonari, M.; Nagaoka, T.; Chen, D.-W.; Kida, M. *Tet. Lett.* **1997**, *38*, 6709.

[78.] Bielawski, M.; Aili, D.; Olofsson, B. *J. Org. Chem.* **2008**, *73*, 4602.

[79.] Deprez, N. R.; Sanford, M. S. *J. Am. Chem. Soc.* **2006**, *128*, 4972.

[80.] Garcia, M. P.; Millan, J. L.; Esteruelas, M. A.; Oro, L. A. *Polyhedron* **1987**, *6*, 1427.

[81.] Mei, G.; Huang, K.; Chen, L. *Fenxi Ceshi Xuebao* **2008**, *27*, 113.

[82.] Zhong, H. A.; Labinger, J. A.; Bercaw, J. E. *J. Am. Chem. Soc*. **2002**, *124*, 1378.

[83.] Johansson, L.; Ryan, O. B.; Tilset, M. *J Am. Chem. Soc.* **1999**, *121*, 1974.

[84.] Hill, G. S.; Irwin, M. J.; Levy, C. J.; Rendina, L. M.; Puddephatt, R. J. *Inorg. Synth.* **1998**, *32*, 149.

[85.] Wang, L.; Lu, W. *Org. Lett*. **2009**, *11,* 1079.

[86.] Viswanathan, G. S.; Wang, M.; Li, C.-J. *Angew. Chem. Int. Ed.* **2002**, *41*, 2138.

[87.] Denmark, S. E.; Smith, R. C.; Chang, W.-T. T.; Muhuhi,J. M. *J. Am. Chem. Soc.* **2009**, *131*, 3104.

Chapter 5: Pt-Catalyzed Site-Selective C–H Arylation

5.1 Introduction

As described in Chapter 4, we have developed the first high yielding site- and chemoselective process for the C–H arylation of naphthalene (Scheme 5.1).[1] Using bidentate diimine ligands, the reactivity and selectivity of the reaction could be tuned. However, two important limitations of this system persisted with all ligands examined. First, the Pd-catalyzed reaction was always more selective for 1-aryl-naphthalene versus 2-aryl-naphthalene. Second, the reaction suffered from limited arene substrate scope. Only highly electron-rich substrates such as dimethoxybenzenes could be arylated with good yield and selectivity (Figure 5.1).

Scheme 5.1 Pd-catalyzed arylation of naphthalene

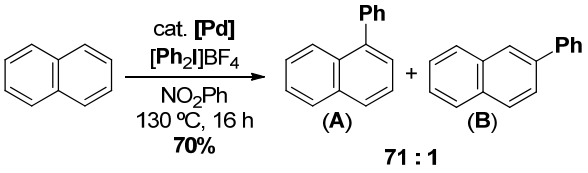

Figure 5.1. Limited arene substrate scope for Pd-catalyzed arylation

Under our optimized reaction conditions for Pd-catalyzed arylation, preliminary mechanistic data is consistent with a $Pd^{II/IV}$ catalytic cycle proceeding via rate-determining oxidation followed by naphthalene π-coordination and subsequent palladation (Figure 4.8). We propose that the origin of the observed selectivity for **A** may be due to the highly electrophilic nature of the Pd^{IV} center, which leads to facile palladation at the most nucleophilic carbon. Furthermore, the required π-

complex formation may explain the low yields obtained with electron neutral or deficient arene substrates.

We sought to a design a system that would be both more general for a wider range of arenes and demonstrate opposite selectivity (preference for the **B** isomer) in the arylation of naphthalene. Although there are many ways to imagine achieving these goals, we initially focused our efforts on the development of an analogous Pt-catalyzed C–H arylation reaction.

Notable differences in the reactivity of Pt and Pd C–H activation catalysts have been reported in the literature, previously. For example, Pt-catalysts have been shown to demonstrate a wider scope of reactivity for C–H activation including electron-deficient arenes,[2] alkanes,[3] and even methane,[3a-c,4] whereas only a few specialized Pd-catalysts exhibit similar scope.[5] One reason for the observed difference in activity may be a difference in the mechanism of C–H activation. Although an electrophilic mechanism is typically postulated for Pd catalysts,[6] oxidative addition of the C–H bond to form a metal hydride has been proposed and even observed in some cases with Pt-catalysts.[7,8]

Another possible explanation for this difference in reactivity is that Pt C–H activation catalysts are kinetically more active than their palladium analogs. To probe this hypothesis, we synthesized a series of Pt- (**1a**-**5a**) and Pd- (**1b**-**5b**) dichloride catalysts with various bidentate nitrogen ligands. These catalysts and the commercially available salts Na_2PtCl_4 and Na_2PdCl_4 were then evaluated using the H/D exchange assay described in Chapter 2. As shown in Figures 5.2 and 5.3, the Pt-catalysts consistently gave higher turnover numbers (TONs) than their Pd counterparts in both CF_3CO_2D and CD_3CO_2D under standard conditions. Measurements at shorter time points showed a similar trend, suggesting that the lower TONs of Pd catalysts are not the result of an increased rate of decomposition.

Figure 5.2 Pt- and Pd-catalyzed H/D exchange between C_6H_6 and CF_3CO_2D after 24 h.

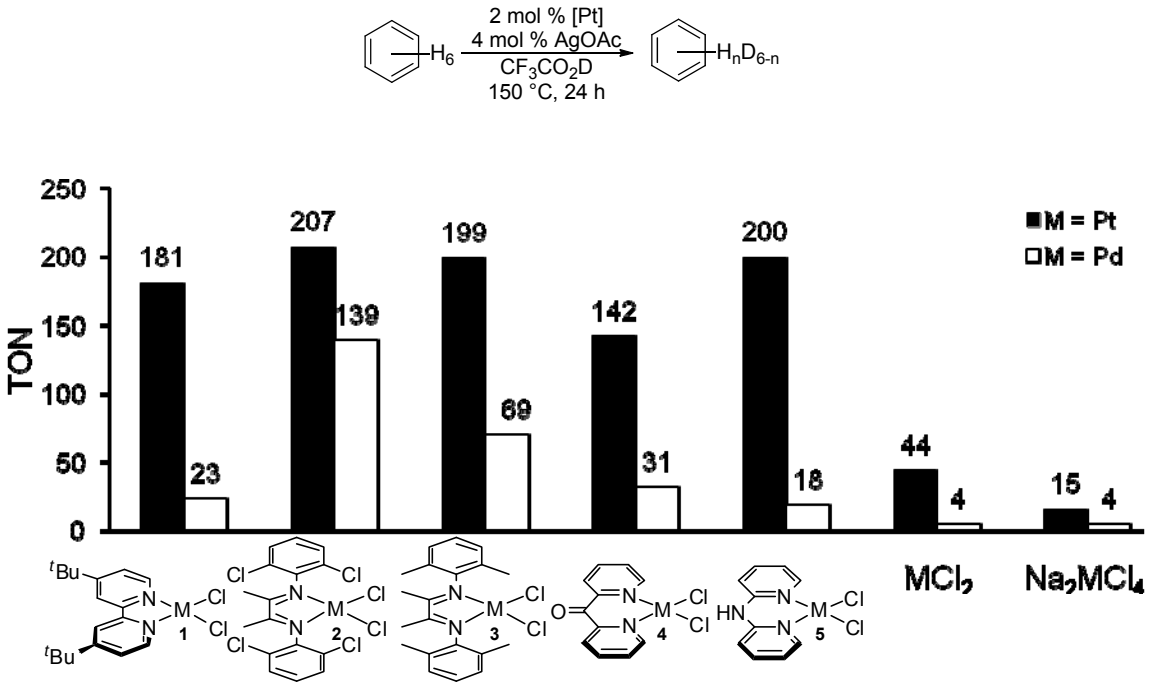

Conditions: M^{II} catalyst (2 mol %, 5 μmol), benzene (23.2 μL, 0.26 mmol), AgOAc (2 equiv, 1.7 mg, 10 μmol) in CF_3CO_2D (0.5 mL, 6.5 mmol, 25 equiv relative to benzene) at 150 ºC for 24 h. Reported as TON.

Figure 5.3 Pt- and Pd-catalyzed H/D exchange between C_6H_6 and CD_3CO_2D after 24 h.

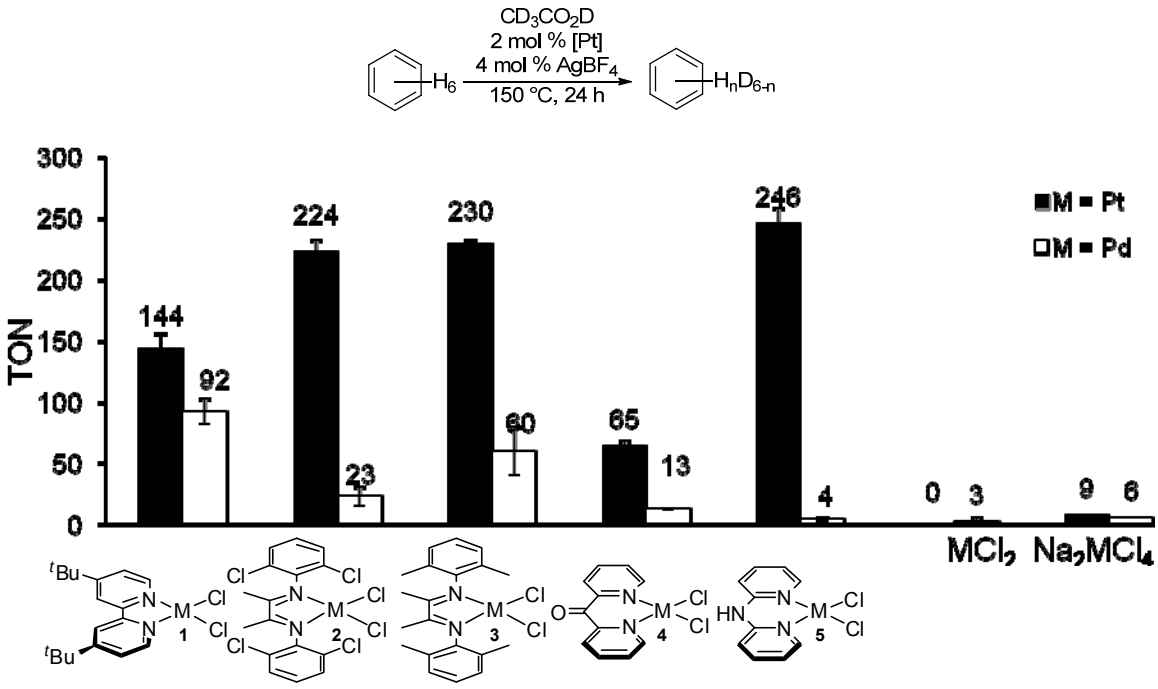

Conditions: Pt^{II} catalyst (2 mol %, 5 μmol), benzene (23.2 μL, 0.26 mmol), $AgBF_4$ (1.9 mg, 10 μmol) in CD_3CO_2D (0.37 mL, 6.5 mmol, 25 equiv relative to benzene) at 150 ºC.

Furthermore, we hypothesized that a Pt-catalyst might lead to different rate limiting step as a result of fundamental differences in the nature of Pd and Pt. Pt is a third row transition metal and therefore is more easily oxidized than its second-row congener Pd.[9] As a result high-valent organometallic Pt complexes are expected to be more stable than their Pd analogs.[10] Although oxidation was the rate-limiting step in the Pd-catalyzed reaction, this would be unlikely for a Pt-catalyzed reaction. Instead reductive elimination is more likely to be rate-limiting.

Indeed, the anticipated slow rates of C–C bond-forming reductive elimination are likely to be the greatest challenge in developing a Pt-catalyzed C–H arylation reaction. It is conceivable that the organo-Pt^{IV} intermediate may be so stable that catalytic turnover is either not observed or is prohibitively slow. There are very few examples of carbon–carbon bond formation from Pt in the literature. In

particular complexes with bidentate nitrogen ligands are generally resistant to C–C reductive elimination.[11] A key stoichiometric example of C–C reductive elimination from Pt^{IV} was reported by Goldberg and coworkers, who achieved C–C coupling to form ethane from a five-coordinate nitrogen ligated Pt^{IV} trimethyl complex.[12] Additionally, a recent example by Albert and coworkers reported the formation of a seven-membered platinacycle, which they propose is formed via carbon–carbon bond forming reductive elimination from Pt^{IV} and subsequent C–H activation/cyclometalation.[13]

Finally, Pt salts have been shown to exhibit β-selectivity for the C–H activation of naphthalene. For example, Pt salts have been used to catalyze site-selective H/D exchange reaction between naphthalene and acidic deuterium sources. Garnett and Hodges reported that 0.02 M K_2PtCl_4 in a mixture of CD_3CO_2D and D_2O and 1 equiv of HCl at 130°C resulted in 38.2% deuterium incorporation at the α-postions of naphthalene and 90.0% deuterium incorporation at the β-positons (Table 5.1).[14] Furthermore, at 80 °C exclusive deuteration at the β-positions was observed.

Table 5.1. Na_2PtCl_4-catalyzed H/D exchange between naphthalene and D_2O[14]

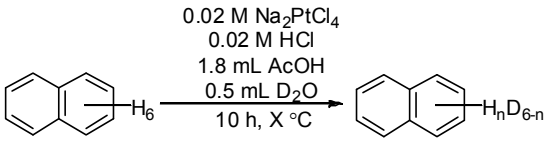

Temperature	%D	
	α	β
130 °C	38.2	90.0
80 °C	0.0	exclusive

In a separate example, Shul'pin and coworkers demonstrated the stoichiometric C–H activation of naphthalene by K_2PtCl_6 in a mixture of trifluoroacetic acid and water at reflux.[15,16] The Pt^{IV}–naphthyl complex was isolated by chromatography over silica treated with ammonia, and an X-ray

crystal structure was obtained. The structure demonstrated exclusive formation of the β C–H activated complex (Figure 5.4). Together these two examples suggest that Pt in both the +2 and +4 oxidation states exhibits a preference for C–H activation of the β-position of naphthalene, the opposite of what was observed in our Pd-catalyzed arylation reaction.

Figure 5.4. Shul'pin and coworkers' stoichiometric β C–H activation of naphthalene with K_2PtCl_6

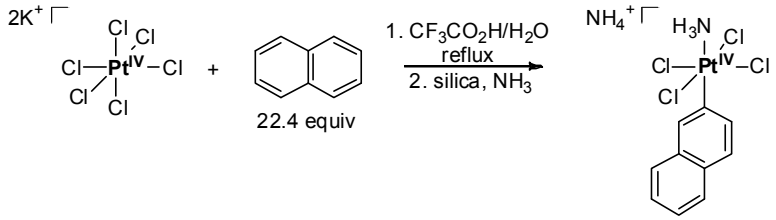

All of these factors suggest that a Pt-catalyzed arylation reaction analogous to the Pd reaction discussed in Chapter 4, could potentially proceed by a different mechanism and/or rate-determining step with different site-selectivity. In addition, the development of a catalytic carbon–carbon bond forming reaction from a Pt^{IV} center would be a novel contribution to the broader field of organometallic chemistry. Herein we will present our preliminary findings in the development of a Pt-catalyzed C–H arylation reaction and directly compare the reactivity of Pt and Pd for this transformation. Recommendations for ongoing development of this work are also presented.

5.2 Results

Our first attempt at Pt-catalyzed C–H arylation was to replace the best-performing Pd catalyst **2b** with its Pt analog **2a** under our optimized reaction conditions. Disappointingly, only 1% yield of phenylnaphthalene was observed with catalyst **2a**. (Table 5.2, entry 2). We hypothesized that the low yield might be due to slow reductive elimination from the diimine-ligated complex. Therefore, we next evaluated the reactivity of commercially available Pt salts Na_2PtCl_4 and

K_2PtCl_4, but less than 5% yield was observed with both catalysts (entries 3 and 4).

Table 5.2 Catalyst effects in the phenylation of naphthalene with $[Ph_2I]BF_4$

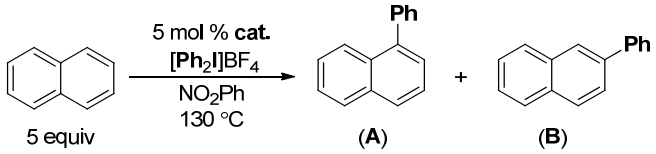

`Entry	Catalyst	Yield	A : B
1	**2b**	70%	71 : 1
2	**2a**	1%	6 : 1
3	Na_2PtCl_4	4%	7 : 1
4	K_2PtCl_4	3%	6 : 1

Conditions: Catalyst (3.68 μmol, 5 mol %), naphthalene (47.1 mg, 0.368 mmol, 5 equiv), Ph_2IBF_4 (27.1 mg, 0.0735 mmol, 1 equiv) in NO_2Ph (0.75 mL) at 130 ºC for 16 h. Yield and selectivity determined by GC.

We next chose to modify the reaction conditions based on the procedure reported by Shul'pin and coworkers for the stoichiometric C–H activation of naphthalene by Pt^{IV} (Figure 5.4). An excess of naphthalene was stirred with $[Ph_2I]BF_4$ in a mixture of trifluoroacetic acid and water at 100 °C for 16 h in the presence of 10 mol % of a Pt catalyst. Negligible arylated product was observed with bidentate nitrogen ligated Pt catalysts **1a** and **2a** or with $(DMSO)PtCl_2$ (Table 5.3, entries 1-3). In contrast, we were pleased to find that the use of commercially available K_2PtCl_4 resulted in 17% yield and a 1 : 14 ratio of **A** : **B** (Table 5.4, entry 4).

Table 5.3. Pt-catalyzed phenylation of naphthalene with $[Ph_2I]BF_4$

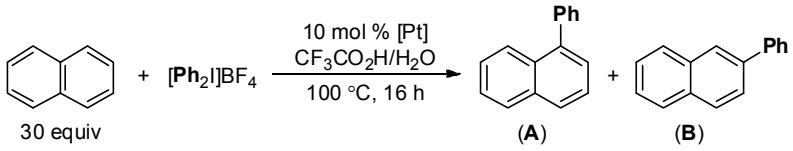

`Entry	Catalyst	% Yield	A : B
1	**1a**	1	nd
2	**2a**	1	nd
3	$(DMSO)_2PtCl_2$	3	1 : 4
4	K_2PtCl_4	17	1 : 14

Conditions: Catalyst (0.93 μmol, 10 mol %), naphthalene (358 mg, 2.7 mmol, 30 equiv), $[Ph_2I]BF_4$ (34.2 mg, 0.093 mmol, 1 equiv) in CF_3CO_2H (0.50 mL) and H_2O (0.15 mL) at 100 ºC for 16 h. Calibrated yield and selectivity determined by GC.

Encouraged by this result, we sought to optimize the reaction conditions in order to increase both yield and selectivity for isomer **B**. We first examined a variety of solvents that are typically used in C–H functionalization reactions. The highest yields and selectivities were observed with fluorinated solvents like trifluoroacetic acid, trifluoroethanol, and hexafluoroisopropanol (HFIP) (Table 5.4, entry 1-4). Going forward we chose to optimize in trifluoroethanol as it is considerably less corrosive than trifluoroacetic acid and less expensive than hexafluoroisopropanol.

Table 5.4. Solvent study for the Pt-catalyzed phenylation of naphthalene

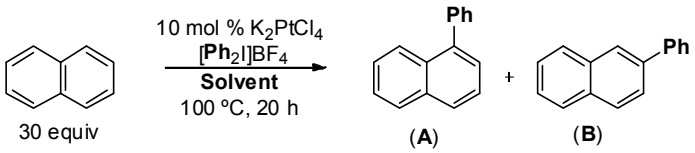

`Entry	Solvent	% Yield	A : B
1	TFA/H_2O	17 ± 1	1 : 14
2	TFA	22 ± 9	1 : 11
3	TFE	17 ± 6	1 : 8
4	HFIP[a]	23	1 : 9
5	AcOH	7	1 : 7
6	DCE	8	1 : 8
7	NO_2Ph	14	1 : 1.5
8	NO_2CH_3	2	1 : 4
9	MeOH	2	1 : 3

Conditions: K_2PtCl_4 (3.9 mg, 0.93 μmol, 10 mol %), naphthalene (358 mg, 2.7 mmol, 30 equiv), [Ph_2I]BF_4 (34.2 mg, 0.093 mmol, 1 equiv) in the designated solvent (0.65 mL) at 100 ºC for 16 h. Calibrated yield and selectivity determined by GC. Standard deviations are reported for reactions repeated at least three times. [a] HFIP = hexafluoroisopropanol

Next, we examined the impact of the diphenyl iodonium oxidant counterion. Previous work in our lab by Dr. Nicholas Deprez revealed a correlation between the rate of C–H arylation and the counterion, which suggests that the counterion may impact solubility and/or reactivity of the oxidant.[17] A variety of oxidants with different counterions were synthesized by stirring a biphasic solution of [Ph_2I]Cl and the desired NaX salt.[17] Relatively non-coordinating counterions such as tetrafluoroborate, triflate, and perchlorate gave comparable yields and selectivities (Table 5.5, entries 1-3). Coordinating, nucleophilic counterions such as chloride, benzoate, and *p*-methoxybenzoate resulted in diminished yields. Excitingly, use of fluorinated carboxylate ligands pentafluorobenzoate and

trifluoroacetate resulted in both increased yield (34 and 40%, respectively) and selectivity (**A** : **B**, 1 : 16 and 1 : 13, respectively) (Table 5.5, entries 7 and 8).

Table 5.5. Oxidant counterion effects in the Pt-catalyzed phenylation of naphthalene

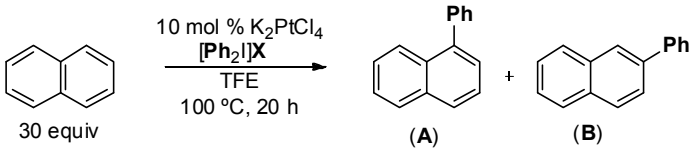

`Entry	Oxidant	% Yield	A : B
1	$[Ph_2I]BF_4$	17 ± 6	1 : 8
2	$[Ph_2I]OTf$	24	1 : 10
3	$[Ph_2I]ClO_4$	20	1 : 11
4	$[Ph_2I]Cl$	12	1 : 9
5	$[Ph_2I]CO_2Ph$	9	1 : 11
6	$[Ph_2I]$(*p*OMePh)	10	1 : 10
7	$[Ph_2I]CO_2C_6F_5$	34 ± 6	1 : 16
8	$[Ph_2I]CO_2CF_3$	40 ± 1	1 : 13

Conditions: K_2PtCl_4 (3.9 mg, 0.93 μmol, 10 mol %), naphthalene (358 mg, 2.7 mmol, 30 equiv), $[Ph_2I]X$ (0.093 mmol, 1 equiv) in trifluoroethanol (0.65 mL) at 100 ºC for 16 h. Calibrated yield and selectivity determined by GC. Standard deviations are reported for reactions repeated at least three times.

Additional efforts to increase the yield and selectivity of the transformation included examination of co-solvents, temperature, concentration, equivalents of reagents, catalyst loading, catalyst counterion, X-type ligands, and added bases/silver salts. Although, only minimal increases in yield have been observed so far, there are still many more avenues that could be pursued to potentially optimize the reaction.

Based on the current conditions, we turned our attention to assessing our original two goals: (1) to develop a Pt-catalyzed arylation reaction with complementary selectivity to Pd-catalyzed methods and (2) to develop a C–H

arylation reaction with wider arene substrate scope than previously observed. Although the Pt-catalyzed reaction does selectively form the **B** isomer as hoped, the reaction conditions developed are significantly modified from the original Pd-catalyzed method discussed in Chapter 4. Therefore, we sought to directly compare the reactivity of analogous Pt- and Pd-catalysts under our optimized reaction conditions. As shown in Table 5.6, use of commercially available sodium and potassium salts of tetrachloroplatinate results in > 1 : 10 selectivity for the **B** isomer of phenyl-naphthalene (entry 1 and 2). In contrast, use of commercial sodium tetrachloropalladate under the exact same conditions results in 65 % yield of phenyl–naphthalene with a 25 : 1 preference for the **A** isomer (Table 5.6, entry 3).

Table 5.6. Direct comparison of Pt- and Pd-catalyzed naphthalene phenylation

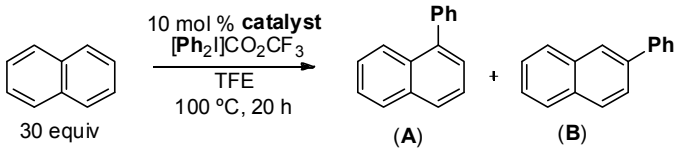

`Entry	Catalyst	% Yield	A : B
1	K_2PtCl_4	40 ± 1	1 : 13
2	Na_2PtCl_4	31	1 : 10
3	Na_2PdCl_4	65	25 : 1

Conditions: Catalyst (0.93 μmol, 10 mol %), naphthalene (358 mg, 2.7 mmol, 30 equiv), $[Ph_2I]CO_2CF_3$ (36.7 mg, 0.093 mmol, 1 equiv) in trifluoroethanol (0.65 mL) at 100 ºC for 16 h. Calibrated yield and selectivity determined by GC. Standard deviations are reported for reactions repeated at least three times.

We then turned our attention to examining the substrate scope of the reaction. Three substrates were chosen to assess reactivity: anisole (an electron-rich arene with an *ortho/para* directing group), *ortho*-xylenes (a moderately electron-rich arene with two similarly activated C–H bonds), and benzene (an electron neutral arene). Each substrate was subjected to the conditions optimized for naphthalene C–H arylation. As shown in Figure 5.5, modest yields were

observed for all three substrates. Notably, a single isomer was detected for both anisole arylation and *ortho*-xylene arylation.

Figure 5.5. Pt-catalyzed phenylation of arenes

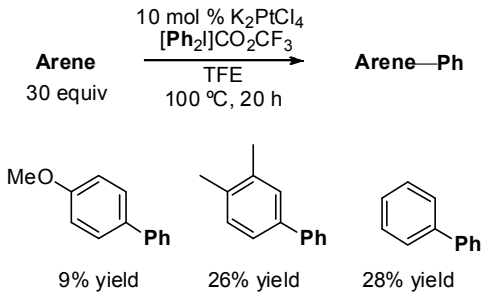

Conditions: K_2PtCl_4 (3.9 mg, 0.93 μmol, 10 mol %), arene (2.7 mmol, 30 equiv), $[Ph_2I]CO_2CF_3$ (36.7 mg, 0.093 mmol, 1 equiv) in trifluoroethanol (0.65 mL) at 100 ºC for 16 h. Calibrated yield and selectivity determined by GC.

Intriguingly, the yields for both substrates were significantly enhanced by slight modification of the reaction conditions (Scheme 5.2). In the case of anisole, changing the conditions to the $[Ph_2I]BF_4$ oxidant in a mixture of trifluoroethanol and trifluoroacetic acid gave 79 ± 8% yield of 4-phenylanisole as the sole observed isomer. This is a marked improvement over the Pd-catalyzed methodology discussed in Chapter 4, which gave 30% yield of phenylated anisole with *o:m:p* selectivity of 4 : 1 : 3 (Figure 5.1). Furthermore, the Pt-catalyzed methodology offers improvement over other recently published examples of anisole arylation in both yield and selectivity (Figure 5.6).[18,19,20] Monitoring the yield of the desired product with time showed that maximum yield is achieved after approximately 12 h (Figure 5.7). Common byproducts including biphenyl, bis-anisole, and diarylated anisole were not observed by GC. Catalyst decomposition and unproductive oxidant consumption may explain the observed lack of full conversion. The observed turnover number at 10 mol % loading was approximately 8. Reducing the catalyst loading to 5 mol % K_2PtCl_4 resulted in 65 ± 4% yield of 4-phenylanisole and an increase in the observed turnover number

to 13. This result is consistent with a bimolecular (or higher order) decomposition pathway for the catalyst.

Scheme 5.2. Optimized Pt-catalyzed phenylation of arenes

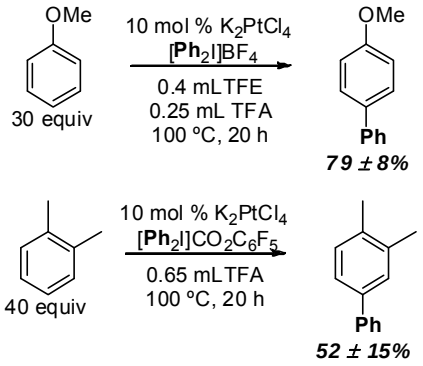

Conditions: Catalyst (0.93 μmol, 10 mol %), arene (2.7 mmol, 30 equiv), $[Ph_2I]X$ (0.093 mmol, 1 equiv) in the designated solvent (0.65 mL) at 100 °C for 20 h. Calibrated yield and selectivity determined by GC.

Figure 5.6. Literature precedent for metal-catalyzed C–H arylation of anisole

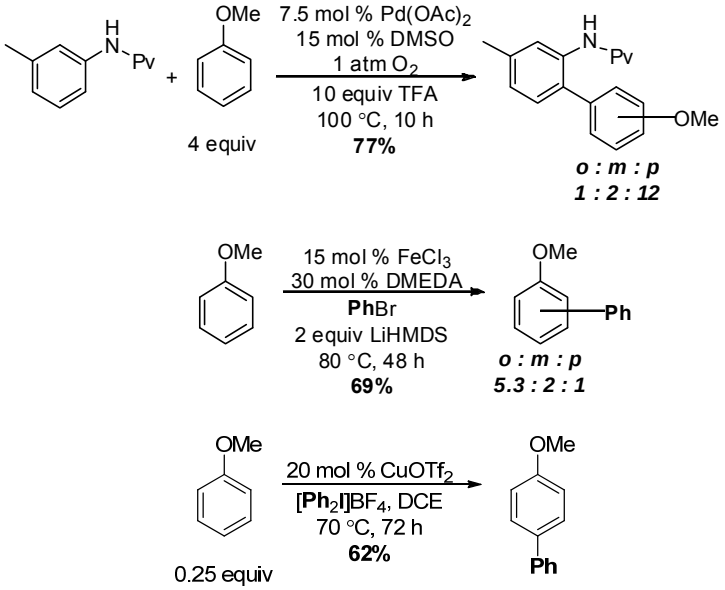

Figure 5.7. Time study of Pt-catalyzed C–H arylation of anisole

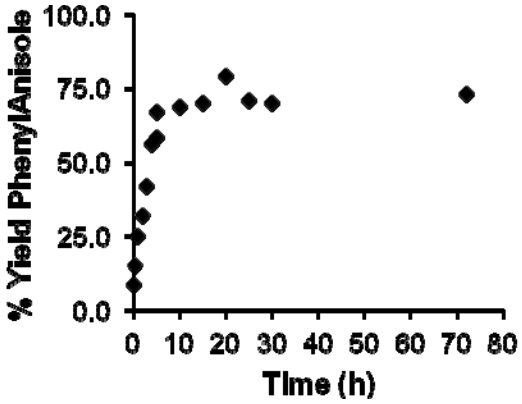

Conditions: Catalyst (0.93 μmol, 10 mol %), naphthalene (358 mg, 2.7 mmol, 30 equiv), $[Ph_2I]BF_4$ (34.2 mg, 0.093 mmol, 1 equiv) in trifluoroethanol (0.65 mL) at 100 ºC for 16 h. Calibrated yield and selectivity determined by GC.

5.3 Conclusions and Future Work

As predicted, use of a Pt-catalyst enabled the highly site-selective synthesis of 2-phenylnaphthalene **B** from naphthalene and diphenyliodonium salts. This methodology affords the opposite site-selectivity as was observed with previous Pd-catalyzed reactions. Additionally, a direct comparison of Na_2PtCl_4 and Na_2PdCl_4 under the optimized reaction conditions reveals a dramatic reversal in the observed selectivity. Furthermore, the methodology has been expanded to the arylation of anisole, *o*-xylenes, and benzene in good yield and with excellent site-selectivity. These promising preliminary results indicate that a robust and general Pt-catalyzed C–H arylation reaction is possible and should be pursued further.

A deeper understanding of the mechanism of Pt-catalyzed C–H arylation would be valuable to direct further optimization of the reaction yield and selectivity and to expand the substrate scope. Furthermore, this transformation provides a rare opportunity to directly compare the reactivity of Pt- and Pd-catalysts. Using this transformation as a framework, one could potentially elucidate inherent differences in the reactivity and mechanism of Pd- and Pt-catalyzed C–H

functionalization reactions that would be of broad interest to the field of metal-catalyzed C–H activation and functionalization.

Many mechanisms can be imagined for these Pt-catalyzed C–H arylation reactions. Importantly, it is conceivable that different mechanisms may be active for naphthalene versus anisole arylation, which may explain the necessary modifications to the reaction conditions. For the purposes of this discussion, a strategy for studying the mechanisms of Pd- and Pt-catalyzed naphthalene arylation will be addressed.

Two general classes of reactivity should be considered: C–H activation to yield an organo-Pt intermediate and electrophilic aromatic substitution (where Pt would act as a Lewis Acid). In the latter case, significant charge build-up is predicted. Therefore the kinetic product would be isomer **A**, where more resonance structures maintaining one aromatic ring are possible. On the other hand, the thermodynamic product should be isomer **B**, which lacks a ^{1,3} strain.

Notably, Gaunt and coworkers proposed that their $Cu(OTf)_2$ catalyzed C–H phenylation of anisole (Figure 5.6, bottom) likely occurs by a "Friedel-Crafts arylation" where the copper catalyst facilitates dissociation of the iodonium salt counterion.[20] Upon dissociation, the highly electrophilic arene can be attacked by the nucleophilic anisole coupling partner in an electrophilic aromatic substitution reaction. This mechanism is supported by the observed *para* selectivity and the presence of an uncatalyzed background reaction.

Intrigued by these observations, we subjected naphthalene to the conditions reported by Gaunt and coworkers using the copper triflate catalyst and $[Ph_2I]BF_4$. After 96 h, 37% yield of phenylnaphthalene was observed with a 6 : 1 selectivity for the **A** isomer, as expected for an electrophilic mechanism under kinetic control (Scheme 5.3). This result suggests that the Pt-catalyzed C–H arylation of naphthalene most likely does not proceed by a Friedel-Crafts arylation as a different isomer is obtained.

Scheme 5.3. Cu-catalyzed C–H arylation of naphthalene

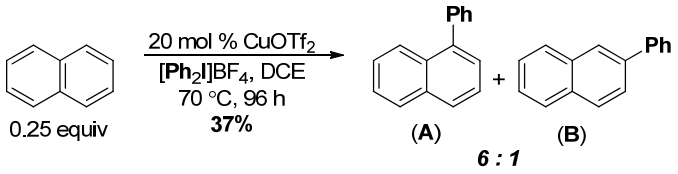

The likely alternative, C–H activation, can proceed by many different mechanisms. Changes in the order of the elementary steps (C–H activation, oxidation, and reductive elimination), the identity of the rate determining step, the mechanism of C–H activation (electrophilic deprotonation, Wheland intermediate, or oxidative addition), and the reversibility of the C–H activation step could all lead to different explanations of the observed selectivity. The three key questions to begin to understand the mechanism are (1) *What is the resting state of the catalyst?* (2) *What is the rate determining step of the reaction?* and (3) *Is C–H activation reversible?* Answering these questions for both the Pt- and Pd-catalyzed arylation reactions would also provide a useful comparison of the inherent reactivity of these catalysts and some understanding of the observed differences in selectivity.

To probe the resting state of the catalyst ^{19}F NMR could be used to monitor the course of the reaction. Use of a fluorine labeled oxidant, such as di(*para*-fluorophenyl)iodonium reagents, would provide an NMR handle to observe the resting state of the catalyst under the reaction conditions. Specifically, formation of a Pt- or Pd-aryl species should be detectable in this manner. If an organo-Pt species is observed, analysis by ^{195}Pt NMR may be used to determine the oxidation state of this species.

Next, the rate determining step of the reaction needs to be determined. Order studies in substrate, oxidant, and catalyst can be completed to determine the rate law of the reaction. Additionally, determination of the kinetic isotope effect can establish whether C–H bond breaking occurs at the rate determining step. Finally, conducting the reaction in CF_3CD_2OD and measuring the amount of

deuterium incorporation in both products and excess substrate would provide a means of determining if C–H activation is reversible.

Collectively, these investigations should provide good evidence to propose plausible mechanisms for the Pt- and Pd-catalyzed C–H arylation reaction. These studies should facilitate optimization of reaction yield and expansion of the substrate scope.

5.4 Experimental

General: ^{1}H and ^{13}C NMR spectra were recorded on Varian Inova 500 or 400 MHz NMR spectrometers with the residual solvent peak as the internal reference. Chemical shifts are reported in parts per million (ppm) (δ). Multiplicities are reported as follows: br (broad resonance), s (singlet), d (doublet), t (triplet), app t (apparent triplet), q (quartet), and m (multiplet). Coupling constants (*J*) are reported in Hz. Infrared (IR) spectroscopy was performed on a Perkin Elmer FTIR, and peaks are reported in cm^{-1}. Elemental analyses were performed by Atlantic Microlab, Inc., Norcross, Georgia. Naphthalene was purchased from Fisher Scientific and trifluoroethanol was purchased from Oakwood Products and used without further purification. K_2PtCl_4 and Na_2PdCl_4 were purchased from Pressure, and Na_2PtCl_4 monohydrate was purchased from Strem. $Pd(COD)Cl_2$,[21] $[Ph_2I]BF_4$,[22] $[Ph_2I]X$,[17] and $[Ar_2I]BF_4$[23] were prepared according to previously reported procedures and matched reported characterization.[24] Complexes **1b-5b** were synthesized by adaptation of a published procedure.[25] All reactions were conducted on the bench top (without exclusion of ambient air/moisture) unless otherwise noted. Calibration curves were prepared for phenylnaphthalene, biphenyl, and phenyl-anisole relative to a hexadecane internal standard for determination of yields and selectivities.

General Procedure for Table 5.2. Reactions were prepared in 4 mL screw cap vials. Each vial was charged with $[Ph_2I]BF_4$ (27.1 mg, 0.0735 mmol, 1 equiv), naphthalene (47.1 mg, 0.368 mmol, 5 equiv), catalyst (3.68 μmol, 5 mol %) and nitrobenzene (0.75 mL). The vials were fitted with Teflon-lined caps, stirred at 130 °C in a preheated aluminum block for 16 h, and then cooled to room temperature. Hexadecane (22 μL, 0.0735mmol) was added to the vials as an internal standard. The reaction mixture was filtered through a Celite plug, and the plug was washed with ethyl acetate. The filtrate was diluted to approximately 10 mL and analyzed by GC. Yields and selectivities were determined by comparison to calibration curves.

General Procedure for Tables 5.3-5.6. Reactions were prepared in 4 mL screw cap vials. Each vial was charged with $[Ph_2I]X$ (0.093 mmol, 1 equiv), arene substrate (2.7 mmol total, 5 equiv), catalyst (3.68 μmol, 5 mol %) and the designated solvent (0.65 mL). The vials were fitted with Teflon-lined caps, stirred at the appropriate temperature in a preheated aluminum block for 16-20 h, and then cooled to room temperature. Hexadecane (27 μL, 0.093mmol) was added to the vials as an internal standard. The reaction mixture was filtered through a Celite plug, and the plug was washed with ethyl acetate. The filtrate was diluted to approximately 10 mL and analyzed by GC. Yields and selectivities were determined by comparison to calibration curves.

5.5 Characterization

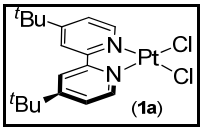

(**1a**)

Complex **1a** was prepared from 4,4'-di-*tert*-butylbipyridine (Aldrich) and *cis*-$(Me_2SO)_2Pt(Cl)_2$[26] using the procedure of Vicente and coworkers.[27] The ^1H NMR spectrum of **1a** matched that reported in the literature. In addition, the purity of samples of **1a** used for catalysis was confirmed by elemental analysis. Anal.

calcd. for $C_{18}H_{24}Cl_2N_2Pt$: C, 40.46; H, 4.53; N, 5.24; Found: C, 40.34; H, 4.51; N, 5.17.

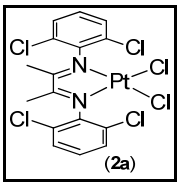

(**2a**)

Complex 2**a** was prepared from the diimine ligand[28] (115 mg, 0.31 mmol) and *cis*-$(Me_2SO)_2Pt(Cl)_2$[44] (100 mg, 0.24 mmol) in acetone (10 mL). The reaction mixture was heated to 70 ºC for 4 h. During heating, the mixture changed color from yellow to red, and a reddish-brown precipitate was observed. The reaction was filtered while still hot, and the reddish-brown precipitate was collected and dried under vacuum to afford **2a** (32.9 mg, 22% yield). ^{1}H NMR (400 MHz, DMF-d_7): δ 7.73 (d, J = 8 Hz, 4H), 7.55 (t, J = 8 Hz, 2H), 2.02 (s, 6H). ^{13}C NMR (100 MHz, DMF-d_7): δ 182.83, 140.42, 130.63, 128.84, 128.76, 20.08. The purity of samples of **2a** used for catalysis was confirmed by elemental analysis. Anal. calcd. for $C_{16}H_{12}Cl_6N_2Pt$: C, 30.02; H, 1.89; N, 4.38; Found: C, 30.00; H, 1.83; N, 4.33.

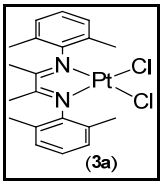

(**3a**)

Complex **3a** was prepared from the diimine ligand[29] and $[Pt_2Cl_4(C_2H_4)_2]$ (105 mg, 0.18 mmol, Strem). Zeise's dimer was suspended in tetrahydrofuran (7 mL) in a 20 mL scintillation vial. Slowly, the diimine ligand (114.0 mg, 0.39 mmol) was added to the reaction with constant stirring. The clear yellow liquid turned murky brown with the addition of the diimine and the reaction was allowed to stir overnight yielding a brown solid (154.3 mg, 77%). ^{1}H NMR (400 MHz, DMSO-d_6): δ 7.18 (s, 6H), 2.12 (s, 12H), 1.75 (s, 6H). The purity of samples of complex

3a used for catalysis was confirmed by elemental analysis. Anal. Calcd. for $C_{20}H_{24}Cl_2N_2Pt$: C, 43.02; H, 4.33; N, 5.02; Found: C, 42.97; H, 4.37; N, 4.86.

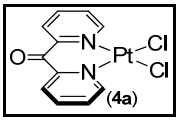

Complex **4a** was prepared from *cis*-$(Me_2SO)_2Pt(Cl)_2$[44] (36 mg, 0.11 mmol, 1.0 equiv) in CH_3OH (13 mL) under an inert atmosphere. This solution was heated to 60 ºC, and then 2,2'-dipyridyl ketone (Aldrich) (20 mg, 0.11 mmol, 1.0 equiv) was added. The reaction was refluxed overnight and then cooled to room temperature. The volume was reduced to 2 mL, resulting in the precipitation of a light yellow solid. The precipitate was collected, washed with Et_2O (3 x 5 mL), and dried under vacuum to afford **4a** as a yellow solid (25 mg, 51% yield). ^1H NMR (500 MHz, DMSO-d_6): δ 9.13 (m, 1H), 8.38 (m, 1H), 8.16 (m, 1H), 7.88 (m, 1H). ^{13}C NMR (100 MHz, DMSO-d_6): δ 185.92, 153.90, 149.85, 141.63, 130.02, 127.30. IR (KBr pellet, cm^{-1}): 1681 (s). The purity of samples of **4a** used for catalysis was confirmed by elemental analysis. Anal. calcd. for $C_{11}H_8Cl_2N_2OPt$: C, 29.35; H, 1.79; N, 6.22; Found: C, 29.15; H, 1.92; N, 6.22.

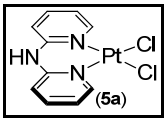

Complex **5a** was prepared from 2,2'-dipyridyl amine (Aldrich) and *cis*-$(Me_2SO)_2Pt(Cl)_2$[44] following the procedure of Tu and coworkers.[30] ^1H NMR (400 MHz, DMSO-d_6): δ 11.07 (s, 1H), 8.78 (m, 2H), 7.97 (m, 2H), 7.27 (m, 1H), 7.11 (m, 1H). ^{13}C NMR (100 MHz, DMSO-d_6) δ 150.59, 150.14, 141.04, 119.58, 114.29. The purity of samples of **5a** used for catalysis was confirmed by elemental analysis. Anal. calcd. for $C_{10}H_9Cl_2N_3Pt$: C, 27.67; H, 2.07; N, 9.61; Found: C, 27.72; H, 2.10; N, 9.79.

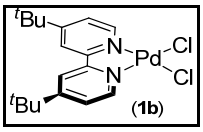

(**1b**)

Complex **1b** was prepared from $Pd(COD)Cl_2$ (285.5 mg, 1 mmol) and the 4,4'–di-*tert*-butyl-2,2'-dipyridyl ligand (268.4 mg, 1 mmol) in acetone (20 mL). 4,4'–di-*tert*-butyl-2,2'-dipyridyl ligand was dissolved in acetone and then the palladium starting material was added. The mixture was stirred overnight to afford an orange precipitate, which was collected on a fritted filter, washed with acetone, and dried under vacuum (381.8 mg, 86% yield). ^{1}H NMR (400 MHz, DMSO-d_6): δ 9.01 (d, J = 6Hz, 2H), 8.59 (s, 2H), 7.81 (d, J = 6Hz, 2H), 1.41 (s, 18H).

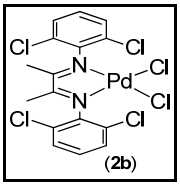

(**2b**)

Complex **2b** was prepared from $PdCl_2$ (145.9 mg, 0.823 mmol, Pressure) and the diimine ligand (307.8 mg, 0.823 mmol) in MeCN (10 mL). Palladium was dissolved in acetonitrile, and the resulting suspension was heated at reflux until a clear, orange solution formed (indicative of $(MeCN)_2PdCl_2$). The diimine ligand was then added, and the reaction mixture was heated at reflux for 4-12 h. The reaction was cooled to room temperature, and the orange precipitate was collected on a fritted filter, washed with acetonitrile and ether, and dried under vacuum (384.4 mg, 85% yield). ^{1}H NMR (400 MHz, CD_3CN): δ 7.55 (d, J = 8 Hz, 4H), 7.40 (t, J = 8 Hz, 2H), 2.20 (s, 6H). The purity of all samples of complex **2b** used for catalysis was confirmed by elemental analysis. Anal. Calcd. for $C_{16}H_{12}Cl_6N_2Pd$: C, 34.85; H, 2.19; N, 5.08; Found: C, 34.57; H, 2.00; N, 4.98.

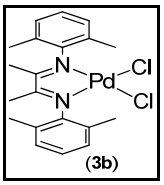

(3b)

Complex **3b** was prepared from $PdCl_2$ (145.9 mg, 0.823 mmol, Pressure) and the diimine ligand (240.7 mg, 0.823 mmol) in MeCN (10 mL). Palladium was dissolved in acetonitrile, and the resulting suspension was heated at reflux until a clear, orange solution formed (indicative of $(MeCN)_2PdCl_2$). The diimine ligand was then added, and the reaction mixture was heated at reflux for 4-12 h. The reaction was cooled to room temperature, and the orange precipitate was collected on a fritted filter, washed with acetonitrile and ether, and dried under vacuum (345.8 mg, 89% yield). NMR characterization was not possible due to insolubility. The purity of all samples of complex **3b** used for catalysis was confirmed by elemental analysis. Anal. Calcd. for $C_{20}H_{24}Cl_2N_2Pd$: C, 51.14; H, 5.15; N, 5.96; Found: C, 51.09; H, 5.05; N, 5.90.

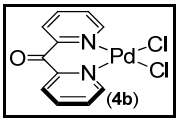

(4b)

Complex **4b** was prepared from $Pd(COD)Cl_2$ (285.5 mg, 1 mmol) and dipyridylketone (184.19 mg, 1 mmol) in acetone (20 mL). Dipyridylketone was dissolved in acetone and then the palladium starting material was added. The mixture was stirred for 12 hours to afford an orange precipitate, which was collected on a fritted filter, washed with acetone, and dried under vacuum (283.7 mg, 78% yield). ^{1}H NMR (400 MHz, DMSO-d_6): δ 9.08 (d, J = 4.8 Hz, 2H), 8.36 (app t, J = 8 Hz, 2H), 8.17 (d, J = 8 Hz, 2H), 7.91 (m, 2H).

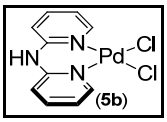

Complex **5b** was prepared from $Pd(COD)Cl_2$ (285 mg, 1 mmol) and dipyridylamine (171.2 mg, 1 mmol) in acetone (20 mL). Dipyridylamine was dissolved in acetone and then the palladium starting material was added. The mixture was stirred overnight to afford a yellow precipitate, which was collected on a fritted filter, washed with acetone, and dried under vacuum (233.6 mg, 67% yield). ^{1}H NMR (400 MHz, DMSO-d_6): δ 11.11 (s, 1H), 8.59 (m, 2H), 7.96 (m, 2H), 7.27 (m, 2H), 7.14 (m, 2H).

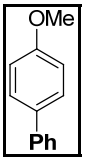

4-phenylanisole was prepared by combining anisole (1.8 mL, 16.3 mmol, 30 equiv), $[Ph_2I]BF_4$ (200 mg, 0.543 mmol, 1 equiv), K_2PtCl_4 (22.5 mg, 54.3 µmol, 10 mol %), in trifluoroethanol (2.3 mL) and trifluoroacetate (1.5 mL) in a 20 mL scintillation vial and stirring at 100 ºC for 20 h. The reaction was then cooled to room temperature and filtered over a plug of Celite. The Celite was then rinsed with 3 x 5 mL EtOAc. The acid was then quenched by addition of 3 x 5 mL saturated sodium carbonate to the filtrate. The organic layer was concentrated under vacuum to remove solvent, excess arene, and iodobenzene. The residual sticky solid was purified by gradiant column chromatography using the automated Biotage system (1% methylene chloride in hexanes to 8% methylene chloride in hexanes). The product was isolated as a clear oil (52 mg, 52% yield).

^{1}H NMR

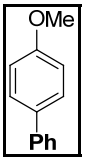

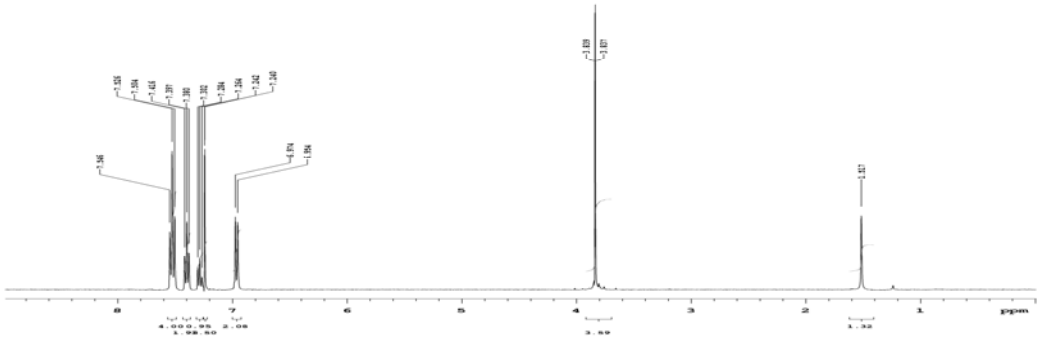

5.6 References

[1] Hickman, A. J.; Sanford, M. S. *ACS Catalysis* **2011**, *1*, 170.

[2] (a) Garnett, J. L.; Hodges, R. J. *Chem. Commun.* **1967**, 1001. (b) Garnett, J. L.; Hodges, R. J. *J. Am. Chem. Soc.* **1967**, *89*, 4546. (c) Shul'pin, G. B. *J. Organometallic Chem.* **1981**, *212*, 267. (d) Shul'pin, G. B.; Kitaigorodskii, A. N. *J. Organometallic Chem.* **1981**, *212*, 275. (d) Emmert, M. H.; Gary, J. B.; Villalobos, J. M.; Sanford, M. S. *Angew. Chem., Int. Ed.* **2010**, *49*, 5884.

[3] (a) Hodges, R. J.; Webster, D. E.; Wells, P. B. *Chem. Commun.* **1971**, 462. (b) Hodges, R. J.; Webster, D. E.; Wells, P. B. *J. Chem. Soc. A* **1971**, 3230. (c) Hodges, R. J.; Webster, D. E.; Wells, P. B. *J. C. S. Dalton* **1972**, 2571. (d) Goldshleger, N. G.; Shteinman, A. A.; Shilov, A. E.; Eskova, V. V. *Zh. Fiz. Khim.* **1972**, *46*, 1353. (e) Shilov, A. E.' Shteinman, A. A. *Coord. Chem. Rev.* **1977**, *24*, 97.

[4] (a) Periana, R. A.; Taube, D. J.; Gamble, S.; Taube, H.; Satoh, T.; Fujii, H. *Science* **1998**, *280*, 560. (b) Johansson, L.; Ryan, O. B.; Tilset, M. *J. Am. Chem. Soc.* **1999**, *121*, 1974. (c) Ahrens, S.; Strassner, T. *Inorg. Chim. Acta* **2006**, *259*, 4789.

[5] (a) Muehlhofer, M.; Strassner, T.; Herrmann, W. A. *Angew. Chem., Int. Ed.* **2002**, *41*, 1745. (b) Periana, R. A.; Mironov, O.; Taube, D.; Bhalla, G.' Jones, C.J. *Science* **2003**, *301*, 814. (c) Strassner, T.; Muehlhofer, M.; Zeller, A.; Herdtweck, E.; Herrmann, W. A. *J. Organometallic Chem.* **2004**, *619*, 1418.

[6] Gretz, E.; Oliver, T. F.; Sen, A. *J. Am. Chem. Soc.* **1987**, *109*, 8109.

[7] (a) Crabtree, R. H. *J. Organometallic Chem.* **2004**, *689*, 4083. (b) Lersch, M.; Tilset, M. *Chem. Rev.* **2005**, *105*, 2471.

[8] Wick, D. D.; Goldberg, K. I. *J. Am. Chem. Soc.* **1997**, *119*, 10235.

[9] Henry, P. M. Palladium catalyzed oxidation of hydrocarbons. Ugo, R., Ed. Reidel Publishing Company, Dordrecht: 1980.

[10] (a) Canty, A. J.; Denney, M. C.; van Koten, G.; Skelton, B. W.; White, A. H. *Organometallics* **2004**, *23*, 5432. (b) Crumpton-Bregel, D. M.; Goldberg, K. I. *J. Am. Chem. Soc.* **2003**, *125*, 9442.

[11] (a) Van Asselt, R.; Rijnberg, E.; Elsevier, C. *J. Organometallics* **1994**, *13*, 706. (b) Gschwind, R. M.; Schlecht, S. *J. Chem. Soc., Dalton Trans.* **1999**, 1891**.** (c) Rendina, L. M.; Puddephatt, R. *J. Chem. Rev.* **1997**, *97*, 1735.

[12] (a) Fekl, U.; Kaminsky, W.; Goldberg, K. I. *J. Am. Chem. Soc.* **2001**, *123*, 6423. (b) Fekl, U.; Goldberg, K. I. *J. Am. Chem. Soc.* **2002**, *124*, 6804.

[13] Albert, J.; Bosque, R.; Crespo, M.; Granell, J.; Rodri' guez, J.; Zafrilla, J. *Organometallics* **2010,** 29, 4619.

[14] Garnett, J. L.; Hodges, R. J. *Chem. Commun.* **1967**, 1001.

[15] Shul'pin, G. B.; Rozenberg, L. P.; Shibaeva, R. P.; Shilov, A. E. *Kinetika i Katalic* **1979**, *20*, 1570.

[16] Shul'pin, G. B. *J. Organomet. Chem.* **1981**, *212,* 267.

[17] Deprez, N. R. Development of and Mechanistic Insights into Palladium-Catalyzed C-H Arylation Reactions. Ph.D. Thesis, University of Michigan, Ann Arbor, MI, 2010.

[18] Brasche, G.; Garcia-Fortanet, J.; Buchwald, S. L. *Org. Lett.* **2008**, *10*, 2207.

[19] Liu, W., et al. *Angew. Chem. Int. Ed.* **2010**, *49*, 2004.

[20] Ciana, C.-L.; et al. *Angew. Chem. Int. Ed.* **2011**, *50*, 458.

[21] Drew, D.; Doyle, J. R. *Inorg. Synth.* **1990**, *28*, 346.

[22.] Ochiai, M.; Toyonari, M.; Nagaoka, T.; Chen, D.-W.; Kida, M. *Tet. Lett.* **1997**, *38*, 6709.

[23.] Bielawski, M.; Aili, D.; Olofsson, B. *J. Org. Chem.* **2008**, *73*, 4602.

[24.] Deprez, N. R.; Sanford, M. S. *J. Am. Chem. Soc.* **2006**, *128*, 4972.

[25.] Garcia, M. P.; Millan, J. L.; Esteruelas, M. A.; Oro, L. A. *Polyhedron* **1987**, *6*, 1427.

[26] Hill, G. S.; Irwin, M. J.; Levy, C. J.; Rendina, L. M.; Puddephatt, R. J. *Inorg. Synth.* **1998**, *32,* 149.

[27] Vicente, J.; Cazlez-Herrero, P.; Prez-Cadenas, M.; Jones, P. G.; Bautista, D. *Inorg. Chem.* **2007**, *46*, 4718.

[28] Gerdes, G.; Chen, P. *Organometallics*, **2003**, *22*, 2217.

[29] See Chapter 3 for preparation of the diimine ligand.

[30] Tu, C.; Wu, X.; Liu, Q.; Wang, X.; Xu, Q.; Guo, Z. *Inorg. Chim. Acta.*, **2004**, *357*, 95.

Chapter 6: Conclusions and Future Perspectives

The development of mild and selective methods for the functionalization of simple arene C–H bonds is an important challenge in organic chemistry. In this dissertation we have explored Pt- and Pd-catalyzed C–H functionalization as a means to achieve this goal. Specifically, we have developed catalysts that promote C–H activation and site-selective functionalization of arene C–H bonds in substrates that do not contain directing groups. Pt- and Pd-catalysts containing nitrogen donor ligands were evaluated using a catalytic H/D exchange assay to elucidate trends in reactivity. Highly active C–H activation catalysts were identified and studied for site-selective C–H arylation.

6.1 Studying C–H Activation

In the first half of this dissertation, we explored Pt-catalyzed H/D exchange between benzene and acidic deuterium sources as a metric for directly comparing the reactivity of different Pt C–H activation catalysts. In chapter 2, we presented the development of a systematic H/D exchange assay including rigorous evaluation of background uncatalyzed exchange and the impact of common additives.[1] Using this quick, first-pass assay, we then directly compared the reactivity of known Pt C–H activation catalysts to elucidate trends in reactivity. Intriguingly, the relative activity of the catalysts examined was found to vary substantially depending on the nature of the deuterium source. This result reveals the importance of comparing new catalysts in *several different assays* in order to fully evaluate their reactivity.

The conditions developed here have served as a valuable method to rapidly screen and benchmark new transition metal catalysts for C–H activation. In chapter 2, we discussed our study of Pt catalysts with quaternary nitrogen

ligands, which have previously been implicated in methane oxidation catalysis. Since these initial investigations, more robust Pt- and Pd-catalysts containing quaternary nitrogen ligands have been developed in the Sanford group. Their application in arene and alkane H/D exchange and oxidation reactions was recently reported using the H/D exchange assay as a valuable tool for catalyst design and optimization.[2] This assay has also been applied to the development of iridium C–H activation catalysts by the Ison group at North Carolina State.[3]

In yet another example of the utility of the H/D exchange assay, we reported the systematic study of the structure/activity relationship of diimine ligands for Pt-catalyzed C–H activation in chapter 3. A series of diimine ligands were synthesized to probe the effects of sterics, electronics, and halogen substitution. The analogous Pt dichloride complexes were then subjected to the H/D exchange conditions, and the initial rates of C–H activation were measured. This work demonstrated a remarkable relationship between diimine ligand substitution at the *N*-aryl group and catalyst activity for H/D exchange between C_6H_6 and RCO_2D. Our study identified that substitution in the 2 and 6 positions of the *N*-aryl group of the diimine ligand, especially incorporation of halogens in these positions, leads to significant increases in catalyst reactivity.

In the two years since publication, the H/D exchange assay that we have developed has already seen several exciting applications. The intent of the assay was to provide an operationally simple means to directly compare the reactivity of a given catalyst to complexes already known in the literature and to optimize reactivity within a given class of complexes. New ligand architectures for C–H activation are published regularly providing new opportunities to use our assay. For example, *N*-heterocyclic carbene ligands have been used in the development of methodology for Pd-catalyzed methane oxidation reactions.[4] The H/D exchange assay would likely be a useful tool in the design and optimization of such ligands to improve both catalyst longevity and TOF.

6.2 Developing Metal-Catalyzed C–H Functionalization Reactions

In the second half of this dissertation, we discuss our results to develop site-selective C–H functionalization reactions. Our approach was to use steric and electronic modification of ancillary ligands at the metal to modulate reactivity and dictate the preferred site of C–H activation. In chapter 4, we presented the first high yielding site- and chemoselective process for the C–H arylation of naphthalene. This work suggests, for the first time, that both reactivity and selectivity in Pd^{IV}-mediated C–H arylation can be tuned through modification of supporting ligand structure. This proof of principle suggests that other types of C-H functionalization reactions, such as halogenation, oxygenation, and trifluoromethylation, could be similarly affected by modification of supporting ligands. Furthermore, this concept potentially could be extended to the development of asymmetric C–H functionalization reactions.

Our studies also revealed preliminary mechanistic data consistent with a $Pd^{II/IV}$ catalytic cycle involving naphthalene π-coordination and subsequent palladation. This work added to a small but growing number of examples in the literature implicating C–H activation at high oxidation state Pd centers in catalysis.[24,59,5,6] Since publishing this work, our group has reported the first stoichiometric example of C–H activation at Pd^{IV}, which further supports the plausibility of our proposed mechanism.[7] Future efforts in this field should aim to understand the differences in reactivity and selectivity between C–H activation at Pd^{II} versus Pd^{IV}. Stoichiometric investigations of these transformations hopefully would provide valuable insights into the differences in reactivity that could inform the development of new complementary catalytic transformations.

Additionally, this chapter presented the development of a heterogeneous Pd-catalyst for C–H arylation of naphthalene. In collaboration with Dr. Tae-Hong Park in Professor Adam Matzger's laboratory at the University of Michigan (Department of Chemistry), we studied a new material nearly identical to MOF-5 albeit with octahedral morphology and a significant number of defect sites that functionalize the pores, enabling significant adsorption of $Pd(OAc)_2$. This catalyst

demonstrates improved yield and catalyst longevity versus homogeneous $Pd(OAc)_2$ as well as different selectivity. However, significant decomposition of the microporous coordination polymer (MCP) framework was observed. To improve the catalyst, this novel synthetic approach for defect inclusion should be expanded to more robust MCP crystals. Additionally, only modest site selectivity was observed for the Pd(II)@MOF-5(O_h)-catalyzed naphthalene arylation. We anticipate that by applying the synthetic approach to develop different MCPs with different dangling linkers both reactivity and selectivity of the C–H arylation reaction could be tuned. One specific future direction would be to explore the influence of pore size/shape on selectivity.

Finally, in chapter 5 we presented preliminary results on the development of an analogous Pt-catalyzed C–H arylation reaction. Our goals were to develop a reaction that would selectively form 2-phenyl-naphthalene (the opposite isomer of the Pd-catalyzed methodology) and that would exhibit a broader substrate (arene) scope. Based on literature precedent, we hypothesized that using a Pt catalyst could result in increased reactivity for a variety of substrates and different selectivity for naphthalene C–H activation. As presented in chapter 5, the use of commercially available platinum salts under modified reaction conditions affords a pathway to selective formation of 2-phenyl-naphthalene. Furthermore, the methodology has been expanded to the arylation of anisole, *o*-xylenes, and benzene in good yield and with excellent site-selectivity. These promising preliminary results indicate that a robust and general Pt-catalyzed C–H arylation reaction is possible and should be pursued further. A deeper understanding of the mechanism of Pt-catalyzed C–H arylation would be valuable to direct further optimization of the reaction yield and selectivity and to expand the substrate scope.

Additionally, a direct comparison of Na_2PtCl_4 and Na_2PdCl_4 under the optimized reaction conditions reveals a dramatic reversal in the observed selectivity. This transformation provides a rare opportunity to directly compare the reactivity of Pt- and Pd-catalysts. Using this transformation as a framework,

one could potentially elucidate inherent differences in the reactivity and mechanism of Pd- and Pt-catalyzed C–H functionalization reactions that would be of broad interest to the field of metal-catalyzed C–H activation and functionalization.

References

[1] Hickman, A. J.; Villalobos, J. M.; Sanford, M.S *Organometallics* **2009**, *28*, 5316-5322.

[2] Emmert, M. H.; Villalobos, J. M.; Gary, J. B.; Sanford, M. S. *Angew. Chem. Int. Ed.* **2010**, *49*, 5884-5886.

[3] Feng, Y.; Jiang, B.; Boyle, P. A.; Ison, E. A. *Organometallics* **2010**, *29*, 2857.

[4] (a) Muehlhofer, M.; Strassner, T.; Herrmann, W. A. *Angew. Chem., Int. Ed.* **2002**, *41*, 1745. (b) Strassner, T.; Muehlhofer, M.; Zeller, A.; Herdtweck, E.; Herrmann, W. A. *J. Organometallic Chem.* **2004**, *619*, 1418.

[5.] Hull, K. L.; Lanni, E. L.; Sanford, M. S. *J. Am. Chem. Soc.* **2006**, *128*, 14047.

[6.] Pilarski, L. T.; Selander, N.; Bose, D.; Szabo, K. J. *Org. Lett.* **2009**, *11*, 5518.

[7] Racowski, J. M.; Ball, N. D.; Sanford, M. S. *J. Am. Chem. Soc.* **2011**, ASAP. DOI: 10.1021/ja2051099